Persistence of river populations

Yasmine Samia

Thesis submitted to the Faculty of Graduate and Postdoctoral Studies in partial fulfillment
of the requirements for the degree of
Doctor of Philosophy in Mathematics [1]

Department of Mathematics and Statistics
Faculty of Science
University of Ottawa

[1]The Ph.D. program is a joint program with Carleton University, administered by the Ottawa-Carleton Institute of Mathematics and Statistics

Abstract

Streams and rivers are examples of vital ecosystems that frequently undergo various environmental and anthropogenic stresses. A core question in population ecology is whether a given population will persist under changing ecological conditions. This thesis consists of three papers and is devoted to the mathematical analysis of responses of river-dwelling species to population persistence threats. The first paper presents a stochastic approach to the 'drift paradox' problem, where the classical reaction-advection-diffusion model is replaced by a birth-death-emigration process. We explore the effects of temporally varying flow on the persistence probability and highlight the importance of the benthic stage for the persistence of stream organisms. The second paper addresses the problem of river network fragmentation through disconnecting structures such as dams. We construct a population matrix model that incorporates the spatial structure of the studied river network and compare structural connectivity to an indicator of population persistence. The third paper adapts the same basic matrix model to examine fish response to disturbances travelling downstream from upstream sites. The study of these three aspects of persistence challenges for river populations contributes to the cumulative effects assessment on river networks.

Acknowledgements

Within a year, I had two babies. No, not twins. The first is my little angel Yasmine, and the second is this thesis. Both came after some suffering and a long wait, and both are my lifetime achievements that couldn't have been accomplished without the support of a loving family and an understanding supervisor.

The very first thanks goes to my Ph.D. supervisor, Dr. Frithjof Lutscher, for all his encouragement, inspiration, flexibility and confidence in me. Working with you for the last seven years taught me that anyone can be a supervisor, but it takes a lot be a teacher. Thank you for all your guidance and help. I am truly grateful and proud to be one of your students, and I wish that one day my students will regard me with the same respect and admiration that I have for you.

I would like to thank Dr. Robert Smith? and Dr. Brett Stevens for insightful discussions and feedback throughout my studies. I am also grateful to the Faculty of Graduate and Postdoctoral Studies and the Department of Mathematics and Statistics at the University of Ottawa for their academic and financial support during my journey. I also wish to acknowledge the interest and the financial support of external funding agencies throughout my research. In particular, I am grateful for an Ontario Graduate Scholarship from the Province of Ontario and for an Alexander Graham Bell doctoral scholarship from the Natural Science and Engineering Research Council of Canada (NSERC).

I can't thank my parents enough, to whom I owe who I am today. You believed in me and were always my biggest fans. Thank you for all your devotion. I hope that with this work I can pay you back at least some of your sacrifices.

To my dear husband Nick, thank you for your continuous love and support of all my endeavours. You are my inspiration. Thank you for being in my life, for your patience and for your sense of humor. I couldn't be more blessed.

To my little angel, you are my life. One day, you will grow up and learn what your mom has written in these pages; you may even blame me for being completely absorbed by work these last few weeks, while you are only a few months old. Believe me, I couldn't wait to be done so I can enjoy some precious moments with you. Thank you for teaching me patience and unconditional love. Thank you for being the best part of every day.

What I have learned in this long mathematical modelling journey is that the world is made with a great perfection; the more we try to model, explore and explain phenomena, the more we realize that there is a miraculous touch governing all kinds of life on this planet. I thank this Creator for the uncountable questions that keep us scientists busy finding answers. Deep inside, I know that he is the answer, and I couldn't be more grateful for all the blessings I have.

Dedication

"Remember that wherever your heart is, there you will find your treasure."

- *Paulo Coelho, The Alchemist*

To mom, dad, Nick and Yasmine. You are my treasure.

Contents

List of Tables

Chapter 1

Introduction

Rivers are the arteries of our planet. Their immense historical, ecological and economic importance is undeniable. The great milestones of human history took place by the banks of rivers, along which many civilisations sprung up [38]. The world's first cities flourished in Mesopotamia, in the fertile plains of the Tigris and Euphrates, while the ancient Egyptian civilisation could not have blossomed without the Nile. Many early societies referred to rivers as 'mothers', just like the Yellow river was known in the ancient Chinese ages [32]. Through the ages, rivers continued to play a central role in sustaining societies, supplying resources such as irrigation, industrial and household water, multiple sources of food and hydro energy. The economic value of rivers and their ecosystems is noteworthy. By providing navigation routes, producing energy, transporting waste, attenuating the drastic effects of floods or pollution events, renewing the finite supply of water on continents and sustaining all life on land, the economic value of the services granted by freshwater ecosystems was estimated at an average 33 trillion dollars a year [14].

As much as nations worshipped the role of rivers, they also abused these ecosystems. With advancing technology, human development has brought with it pollution, fragmentation, degradation and overexploitation, threatening not only the geological aspect of river systems, but also the persistence of fish and aquatic populations living and dispersing in rivers. Throughout this thesis, we mathematically model and treat three aspects of an-

thropogenic disturbances on rivers and explore their effects on the persistence of particular aquatic organisms. In Chapter 2, we present a stochastic approach to the persistence problem in river reaches under variable environmental conditions. This work tackles in particular the variability of the water flow provoked by flow-regulating dams. In Chapter 3, we scale up to address the problem of persistence in river networks under fragmentation by dams and other disconnecting structures. In Chapter 4, we explore the effects of downstream transport of upstream conditions in river networks. In particular, we focus on transportable conditions that are harmful to fauna and flora such as the spread of chemical contaminants, organic matter from waste-water or any form of river pollution.

In the following, we give a brief introduction to each of these three parts of the thesis.

1.1 Population persistence and the 'drift paradox'

Streams and rivers are by nature advective environments, characterized by unidirectional water flow. This particular feature places some inhabiting aquatic organisms — especially those of reduced motility such as phytoplankton, insects and drifting invertebrates — under the risk of being washed downstream, into habitats where conditions are not suitable for growth or reproduction. While extinction seems inevitable in these circumstances, many species manage to persist for generations. The fundamental question of how a closed population can persist in advective environments is known as the 'drift paradox' [21] and was the focus of many recent modelling efforts [22, 25, 26, 28, 27, 34, 36, 43, 46]. Diffusion-mediated persistence in stream ecosystems was first explored by Speirs and Gurney [43]. Their hypothesis states that a sufficient amount of random movement in the right range can counter-balance the drift effect and lead to population persistence at a given location [46]. Using a reaction-advection-diffusion equation (see equation (1) in Chapter 2) to model the density of a population subject to flow, they derived a threshold for the flow speed above which the population cannot persist, while, below it, persistence is possible on a large enough domain. Their results encompass the necessary balance between advection, diffusion, domain size and population growth rate required for population persistence.

Extensions to Speirs and Gurney's model mainly consisted of including, distinct or jointly, a benthic stage and temporal variations. Pachepsky et al. [34] were the first to explore the effect of considering benthic population on the overall persistence. Their two-compartment model (see equation (3) in Chapter 2) consists of a benthos–drift system, and accounts for individuals who spend a part of their life residing on the benthos and not only in the drift. This consideration is especially important for aquatic insect larvae who spend a considerable proportion of their time resting on the benthos and move periodically by jumping into the flow and drifting downstream [1]. The authors showed that if the production rate on the benthos exceeds the rate at which individuals enter the drift at low population density, then the population can persist, independently of the flow speed or the domain size. Although most of the contributions assumed the water flow to be constant over time, it is not in reality. For instance, variations in flow speed can result from seasonality, weather conditions or anthropogenic disturbances such as hydroelectric dams. The effects of temporally periodic flow speed on persistence was studied by Lutscher and Seo [29] through the calculation of invasion speeds, for both the single and the two-compartment models. They find that, on one hand, the averages of parameters determine the invasion speeds for a single-compartment model; on the other hand, for a two-compartment model, the temporal variation can enhance population persistence.

Models inspired by the work of Speirs and Gurney are mostly deterministic, and their results, based on equilibrium analysis, confirm the presence of sharp thresholds, such as a critical flow speed and a critical domain size governing the extinction or persistence dynamics. Deterministic models do not address the effect of stochasticity on persistence. In particular, populations dispersing in advective media are subject to demographic and environmental stochasticity. Demographic stochasticity refers to the variability in the internal population dynamics, such as number of births and deaths, while environmental stochasticity refers to the unpredictability in external processes that occur independently of the population and affect the ecological dynamics. In stochastic models, one considers the probability of persistence, the expected residence time in a certain area or the expected time to extinction of a

population. Kolpas and Nisbet [22] formulated a first stochastic analogue to the integrodifferential equation developed in Lutscher et al. [28] for the dynamics of a stream population. Their simulations explored the effects of demographic stochasticity, both in reproduction and movement, on persistence times and probabilities. They found that thresholds resulting from deterministic models were replaced with a smooth and sometimes steep transition from essential persistence to essential extinction. Another stochastic contribution to evaluate persistence in stream environments is presented by Pasour and Ellner [36], who compared residence times of zooplankton in a given flow field by simulating individual trajectories but did not consider persistence of an entire population.

In the first part of the thesis, we use transport-based models for population dynamics in streams and rivers to derive extinction probabilities and expected times to extinction in a given reach. We consider demographic stochasticity in the form of a birth–death process and emigration from the stream reach. We also include environmental stochasticity in the form of temporal variation of the abiotic conditions; e.g., seasonal effects, floods or power dam operation. We begin with a single model of a drift population but later consider a population with a benthic stage as well. We use the mean residence time of the advection-diffusion equation to transition from a spatially explicit description to a spatially implicit birth–death process, in which individual washout from the domain appears as an additional death term. The mean residence time is simply given by the inverse of the dominant eigenvalue of the advection-diffusion operator [13]. We also present some explicit formulae for the probability of extinction for both the single and two-compartment models, as well as for constant and temporally variable parameters. We find that the probability of extinction in our stochastic model smoothes out the extinction threshold that a deterministic model predicts. Our results also highlight the importance of a benthic stage for population persistence. Furthermore, we find that temporal variation often decreases the persistence probability, and we focus on a few examples of how variation can increase population persistence.

Our approach on temporal variation illustrates, among other examples, the effects of flow-regulating dams that operate on a predefined schedule. Of course, this is only one of

many impacts of damming on river populations; in the following chapter, we consider river fragmentation by dams as obstacles to fish migration.

1.2 River networks under fragmentation

Fragmentation of rivers represents a serious threat to biodiversity and is likely to become more serious in the future, as human development continues to exhaust river ecosystems for a multitude of purposes. With the worldwide need of alternate sources of energy and the race to develop new recreational and tourist activities, fragmentation of river networks for mainly economic purposes is a fast growing ecological issue. Dams and road crossings are only a few examples of engineered infrastructures that disconnect river reaches, alter the serenity and impoverish the health of rivers ecosystem. Nowadays, only a third of the world's largest rivers remain free-flowing from source to mouth [47].

Unlike terrestrial networks, river systems exhibit a particular hierarchical arrangement of habitat branches, referred to as dendritic geometry [4, 18]. For a schematic representation, see Figure 2 of Chapter 3, page 41. By nature, and in the absence of any movement obstacles, the dendritic structure of these systems restricts the access of resident fish populations to other habitat patches [18]. In particular, there is only one path from any reach to any other reach. Hence, disconnections in rivers are particularly damaging. It is therefore impossible for individuals to avoid physical obstacles obstructing their dispersal pathways, because alternative routes are absent [20]. In addition, a dam can impose a mortality risk during fish transit through hydraulic turbines or over spillways [23] and so be even more detrimental to a fish population.

The extent to which habitat patches in a network remain linked, given all the degradation and external stressors that reduce the connections between them, is quantified using connectivity indices [3, 19, 39]. Connectivity indices for watersheds represent the ability of organisms to disperse throughout the river network. Hence they are well suited to assess the impacts of barriers to fish movement [31]. One of the recently elaborated indices is the Dendritic Index of Connectivity (DCI) [15]. Two variations of this index exist, each representing

a different life history of fish species (DCI_p for potadromous and DCI_d for diadromous), and both including habitat quality through the size of the multiple fragments formed by barriers. Overall, DCI is a network-scale measure of connectivity, specifically designed for freshwater systems and readily adapted to account for multiple barriers and their permeability; i.e., the movement probability of individuals between sections connected by the obstacles [15, 16, 20].

A downside of most the connectivity metrics is that they assume that a barrier completely blocks fish passage and separates a patch into two disjoint sections. In reality, this assumption is relatively pessimistic, since many barriers are somewhat passable [37]. For instance, nowadays most dams have fish passes (e.g., fish ladders) that allow partial passage of fish through them [23]. In addition to the physical attributes of the river, ecological dynamics and migration patterns of species should not be ignored but rather incorporated in these connectivity metrics [3].

For all the existing indices describing connectivity on a patch or on a landscape level, the intuitive common idea being promoted is that a higher connectivity index represents a better habitat quality for fish populations [15, 17, 35]. However, a complete evaluation of habitat suitability for fish populations in river networks requires more than just structural connectivity indices. In particular, population end-points describing persistence conditions should be considered and compared to connectivity metrics. In Chapter 3, we conduct a comparison between the dendritic connectivity index DCI_p and the asymptotic growth rate of a potadromous fish population. Specifically, we determine the key locations within a dendritic river network where fragmentation is detrimental for population persistence and compare with the connectivity index corresponding to placing a barrier at the same location.

To achieve our objectives, we use a discrete-time matrix model to represent changes of population densities on a yearly basis. Classic matrix population models, originated by Leslie [24], typically integrate population dynamics and population structure [5]. The particular flexibility of these models to account for numerous demographic aspects and their ability to assess the status of a population are what makes them a powerful mathematical tool in ecological modelling and population management [5, 6]. In the present work, we construct

an updating matrix that does not only include demographic processes of fish population but also accounts for the spatial structure of the dendritic network in question as well as the obstacles to fish movement. More importantly, we explain in detail how such a matrix can be constructed, numerically, for any dendritic topology. In particular, we formulate our results for two extremes of dendritic geometries that can be associated to real-world rivers: the simplest linear shape, comparable for example to the Nile, and the highly branched complete binary tree, which can represent, among others, the Amazon. Results for any randomly generated dendritic network are bounded by these two topologies.

Our approach highlights the effects of obstacle-induced mortality on fish populations, an aspect that was not tackled in previous contributions. Above all, our results untangle the interplay between habitat fragmentation and population persistence. While introducing a barrier to fish movement reduces connectivity, it can sometimes be beneficial for populations. This counterintuitive result suggests that this index cannot capture all effects of movement barriers on population dynamics. Hence structural connectivity indices should not entirely replace more detailed demographic models to understand questions of persistence and extinction.

1.3 Downstream transport of upstream effects

Flow regulation and fragmentation are not the only threats to fish populations in rivers. Water-mediated transport of physical, chemical or organic matter, such as run-off, contamination and sewage, puts river ecosystems in even more serious peril. River-pollution accidents worldwide make the news every now and then. In the U.S. state of Colorado alone, some 23,000 abandoned mines have polluted 2,300 kilometers of streams [2]. The most recent of these events occurred in August 2015, when toxic waste from a shuttered gold mine spilled into the Animas river in Colorado and tainted the water orange [33]. While consequences of river pollution on human activities and agricultural projects are indirect and controllable to a certain extent, they are definitely devastating to fish populations, contaminating habitats and drastically reducing the quality of fundamental vital conditions.

Since river ecosystems are controlled by the unidirectional downstream flow of water, organisms in downstream sites can be affected by processes occurring upstream, without having to migrate towards those headwater streams [20, 30]. This unidirectional water-mediated transport, together with the dendritic geometry, distinguishes rivers from other ecosystems. Hence the demographics for any population in river networks will not only depend on local river conditions but also on landscape influences and transportable upstream effects traveling downstream. Consequently, upstream reaches should be accorded a higher importance in ecological management of freshwater ecosystems [44].

More generally, the contribution of each reach to the overall ecosystem should be assessed. In the previous chapter, the importance of each connection in the dendritic network was evaluated using the connectivity index. In this chapter, on the contrary, we do not have a predefined measure that we can apply to river reaches. Rather, we systematically investigate the role of each habitat patch in the persistence of a potadromous fish species. Starting with a pristine river system, clear of any disturbances, we begin by introducing a negative disturbance to one patch at a time and explore its effects on the asymptotic population growth rate. By negative disturbance, we represent a condition that is unfavorable for fish populations and that leads to a decline in the local growth rate in the disturbed patch. Accordingly, we identify the patches where the change in quality affects the persistence of the population the most. Later on, we introduce two disturbances and evaluate their joint effect on the asymptotic growth through sensitivity analysis.

Spatially structured models for river populations typically consider travel between reaches in terms of individuals movement, whereas habitat quality is independent of movement and stays local [7, 8, 9, 15, 35]. Only one group of authors recently extended the use of matrix models to include ecotoxicological effects of contaminants on a specific riverine fish species [6, 10, 11, 12]. Their tactical model explores the effects of a specific contaminant (cadmium) on a particular fish species (brown trout) dispersing in a homogeneous dendritic river network (complete binary tree with 15 patches). While corresponding results take into account the age-class structure of the population, they are limited to a specific case. We note that

these are the only contributions we are aware of in the context of dendritic networks.

On the contrary, our model is more strategic. Even though it does not consider age classes or contaminants' concentration explicitly, it generalizes the disturbances concept to any random dendritic network, where local conditions for population growth are either homogeneous or heterogeneous throughout the network. Moreover, the effects of movement preferences of individuals is yet another aspect we examine. For instance, this bias in dispersal illustrates the potential motility of different age classes within the population. While adults are typically keen on swimming upstream against the drift, juveniles are usually driven downstream by the flow. Hence critical disturbance locations will depend upon these preferences.

Our results highlight in particular the importance of upstream reaches through the effect of downstream transport of negative upstream conditions and, at the same time, emphasize the value of buffer zones in watersheds, given their role in absorbing disturbances and impeding their downstream travel. With its flexibility to account for any spatial dendritic structure of rivers, movement preference, heterogeneity and downstream transport of effects, our novel approach provides a decision-making tool for management authorities and conservation ecology.

Chapter 2

Persistence probabilities for stream populations

This paper is published in Bulletin of Mathematical Biology [40];
Samia, Y. and Lutscher, F. Persistence probabilities for stream populations. *Bulletin of Mathematical Biology.* 74(7):1629-1650. 2012

The contribution by each author is as follows. The second author conceived and designed the study and critically edited the manuscript. The first author carried out the analysis and drafted the manuscript. Both authors gave their final approval for publication.

Persistence probabilities for stream populations

Yasmine Samia and Frithjof Lutscher
Department of Mathematics and Statistics
University of Ottawa
Ottawa, ON, K1N6N5, Canada

Abstract

Individuals in streams and rivers are constantly at risk of being washed downstream and thereby lost to their population. The possibility of diffusion-mediated persistence of populations in advective environments has been the focus of a multitude of recent modelling efforts. Most of these recent models are deterministic, and they predict the existence of a critical advection velocity, above which a population cannot persist. In this work, we present a stochastic approach to the persistence problem in streams and rivers. We use the dominant eigenvalue of the advection-diffusion operator to transition from a spatially explicit description to a spatially implicit birth-death process, in which individual washout from the domain appears as an additional death term. We find that the deterministic persistence threshold is replaced by a smooth transition from almost sure persistence to extinction as advection velocity increases. More interestingly, we explore how temporal variation in flow rate and other parameters affect the persistence probability. In line with general expectations, we find that temporal variation often decreases the persistence probability, and we focus on a few examples of how variation can increase population persistence.

Keywords

Drift paradox, persistence probability, birth-death process, spatially implicit model, temporal variation

1 Introduction

Streams and rivers are prime examples of so-called advective environments. Individuals in such an environment are subject to unidirectional flow that threatens to transport them downstream and, eventually, out of their suitable habitat. In stream ecology, the question of how a population can persist in an advective environment has been called the "drift paradox" (Hershey *et al.*, 1993). Inspired by the work of Speirs and Gurney (2001), this question has received much attention recently (Pachepsky *et al.*, 2005; Lutscher *et al.*, 2005, 2006; Pasour and Ellner, 2010; Kolpas and Nisbet, 2010; Lutscher *et al.*, 2010; Vasilyeva and Lutscher, 2011). The persistence question in an

advective environment also occurs in plug-flow reactors, modeling gut-dwelling bacteria (Ballyk and Smith, 1999; Boldin, 2007), sinking phytoplankton (Huisman *et al.*, 2002), benthic marine species along coastlines with dominant long-shore currents (Byers and Pringle, 2006; Pringle *et al.*, 2009), and even terrestrial species under the influence of climate change (Potapov and Lewis, 2004).

One of the main insights from all these models is that there is a critical threshold for the flow speed: as long as the flow speed is below the threshold, the population will persist whereas for flow speeds above the threshold, the population faces extinction. As most of these models are deterministic and their study is based on equilibrium analysis, such a sharp threshold is to be expected. However, population dynamics in nature are subject to a variety of stochastic events, so that sharp thresholds are not to be expected. Instead, one can ask for the probability of persistence, the expected residence time in a certain area, or the expected time to extinction of a population. We know of only two studies addressing these issues. Kolpas and Nisbet (2010) formulated and simulated a stochastic analogue of the integrodifferential equation from Lutscher *et al.* (2005) and studied persistence times and probabilities. Pasour and Ellner (2010) used a hydrodynamic simulation model to obtain realistic flow fields (e.g. exchange flow in a lake-embayment system) and then simulated individual zooplankton trajectories in that flow field, studying residence times.

In this work, we present an alternative approach to include stochasticity into a model for stream invertebrates. We consider a population in a single stream reach and formulate a birth-death-emigration process for the number of individuals there. We relate the emigration rate to physical quantities of the system via an advection-diffusion equation with appropriately chosen boundary conditions. We use the mean residence time of the advection-diffusion equation to transition from the spatially explicit movement description to the spatially implicit stochastic process. For the stochastic process, we can derive the persistence probability explicitly and study the effects of different parameters on the persistence probability. We also include temporal variation into our model and study its effects on persistence.

We begin with a brief overview of the two deterministic models whose stochastic analogues we study. We then present our models in Section 3. The derivation of the persistence probabilities is given in Section 4, whereas a detailed exploration of the influence of the different model parameters on persistence is presented in Section 5. We highlight our results in the discussion, where we also compare and contrast our approach with the two previous stochastic approaches.

2 Background on deterministic models

Speirs and Gurney (2001) were the first to explore the idea of diffusion-mediated persistence in stream ecosystems. Sufficient random movement of individuals, either active or as a result of eddies and other turbulent phenomena, can counterbalance unidirectional drift and allow a population to persist. Speirs and Gurney (2001) used the reaction-

advection-diffusion equation

$$u_t = Du_{\xi\xi} - qu_\xi + f(u) \tag{1}$$

to describe the density $u(t, \xi)$ of a population subject to an effective flow speed, q, and random diffusion coefficient, D. The reaction term, $f(u)$, describes birth and death of individuals. They studied this equation on a domain of length L with appropriate boundary conditions, which we will discuss in detail in Section 3.3. Among other things, they found that when the flow speed exceeds the threshold

$$q^* = 2\sqrt{Dr}, \qquad r = f'(0), \tag{2}$$

then the population cannot persist on an arbitrarily long domain, but for $q < q^*$ there is always a finite domain length $L = L(q)$, above which the population can persist.

Incidentally, the quantity q^* is also the "invasion speed" at which a population described by (1) with $q = 0$ expands its range, see e.g. Lewis *et al.* (2009) for more details on this connection. So, a population can persist in a long enough stretch of a river if the effective advection speed is slower than the population invasion speed.

Based on the observation that many stream insects have a benthic phase, during which they reside on the bottom of the stream rather than in the flowing water zone, Pachepsky *et al.* (2005) extended the model by Speirs and Gurney (2001) to include such a benthic phase. They denoted the population in the flowing water and benthic zone by $u(t, \xi)$ and $w(t, \xi)$, respectively, and studied the system

$$\begin{aligned} u_t &= Du_{\xi\xi} - qu_\xi - \sigma u + \tau w, \\ w_t &= f(w) + \sigma u - \tau w. \end{aligned} \tag{3}$$

In this system, parameters σ, τ denote the exchange rates between the benthic and flowing water zone. They found that if $\tau > r = f'(0)$, then the system behaves exactly like equation (1) with threshold value

$$q^* = 2\sqrt{Dr\frac{\sigma}{\tau - r}}. \tag{4}$$

However, if $\tau < r$, then the population can persist, independently of the flow speed and the domain length. The relationship between persistence and invasion speeds is exactly the same as for the single equation.

In a certain limit, as the exchange rates become large, one can derive a single integrodifferential equation from (3). The analysis of this equation was carried out by Lutscher *et al.* (2005), and corresponding results were obtained.

Temporal variation was introduced into models (1) and (3) by Lutscher and Seo (2011), and in the corresponding integrodifferential model by Jin and Lewis (2011). Lutscher and Seo (2011) analyzed invasion rates under periodic temporal variability and found that for the single equation model (1), the averages of the parameters over one period determine the invasion speed. In contrast, for the two-compartment model (3), temporal correlations between the parameters determine whether the population

spreads faster or slower than for averaged conditions. Jin and Lewis (2011) also find that the exact form of temporal variation and correlation between parameters determines persistence conditions, and not only the average parameter values.

Simulating the stochastic analogue of the integrodifferential equation, Kolpas and Nisbet (2010) found that stochasticity in population dynamics and movement parameters simply "smears" out the deterministic threshold (see e.g. their Figure 4). The probability of persistence at some large time smoothly decreases from 1 to 0 as the advection speed increases above the critical threshold. In the following, we formulate our spatially implicit stochastic model and then compare our results to those by Kolpas and Nisbet (2010).

3 Models

We formulate and analyze two spatially implicit, stochastic models, corresponding to the single drift compartment model (1) and the drift-benthos model (3), respectively. We consider a single reach of a stream, and model birth and death of individuals in that reach as well as emigration from the reach. We relate emigration from the reach to a mechanistic movement model via the dominant eigenvalue of the movement operator, based on some observations by Ballyk *et al.* (1998) and similar in spirit to the ideas by Strohm and Tyson (2011); Vasilyeva (2011), but in a stochastic setting.

3.1 Single compartment model

We consider a continuous-time Markov chain, where the number of individuals increases by one in the case of a birth event (with probability $\beta\Delta t$) and decreases by one if either a death occurs (with probability $\mu\Delta t$) or an individual emigrates from the reach (with probability $\varepsilon\Delta t$). Accordingly, the population remains unchanged with probability $1-(\beta+\mu+\varepsilon)\Delta t$, see Figure 1 for illustration. Since we want to explore the effects of temporal variation on the extinction probability, we allow all parameters to be functions of time, i.e. $\beta=\beta(t)$ and so on. In particular, we consider the case that all coefficient functions are periodic functions with some common period T. We drop the explicit time-dependence for simplicity of notation. If we denote the probability that there be n individuals in the reach at time t by $p_n(t)$, then we obtain the infinite system of differential equations (see e.g. Kot (2001))

$$\frac{dp_n}{dt}=\beta(n-1)p_{n-1}+(\mu+\varepsilon)(n+1)p_{n+1}-(\beta+\mu+\varepsilon)np_n. \tag{5}$$

These equations are complemented by the initial condition that there be n_0 individuals at time $t=0$, i.e. $p_{n_0}(0)=1$, and $p_n(0)=0$ for $n\neq n_0$. Our analysis of this first model will focus on the probability of persistence up to some time, i.e. on $1-p_0(t)$. Since the death and emigration probabilities appear only as a sum in this model, we could combine them into a single parameter, but we prefer to separate them because they describe different processes, and their respective effects will be analyzed later in more detail.

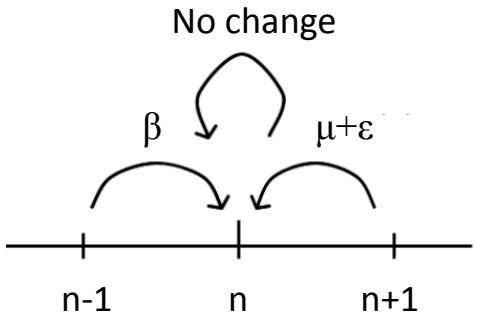

Figure 1: Transition probabilities in the Markov chain for the single compartment model. A birth is indicated by β, a death by μ, and emigration from the reach by ε.

The expected value, $N(t) = \sum np_n(t)$, of the process described in (5) satisfies the equation

$$\frac{dN}{dt} = (\beta(t) - \mu(t) - \varepsilon(t))N, \tag{6}$$

which is a spatially implicit analogue of the linearization at zero of model (1) with $f'(0) = r = \beta - \mu$. The equation for the expected value is closed since the original equation is linear. This fact substantially simplifies the analysis since no moment closure method is necessary.

3.2 Two compartment model

When we divide the population into a benthic and drift compartment as in Pachepsky *et al.* (2005), then a birth or death event increases or decreases the benthic population by one whereas an emigration event decreases the drift population by one. We limit birth-death events to the benthic compartment because the time spent in the drift is often short compared to the time spent on the benthos. The inclusion of these events is straightforward but comes at the price of lengthier calculations and additional parameters. Transitions from drift to benthic state and vice versa occur with probabilities $\sigma\Delta t$ and $\tau\Delta t$, respectively, see Figure 2 for illustration and Appendix 7.2 for details. As above, all parameters are allowed to be functions of time. The probability $p_{n,m}(t)$ that there be n individuals in the drift and m individuals on the benthos at time t satisfies the equation

$$\begin{aligned}\frac{dp_{n,m}}{dt} &= \varepsilon(n+1)p_{n+1,m} + \mu(m+1)p_{n,m+1} + \sigma(n+1)p_{n+1,m-1} + \beta(m-1)p_{n,m-1} \\ &\quad + \tau(m+1)p_{n-1,m+1} - [n(\sigma+\varepsilon) + m(\beta+\tau+\mu)]p_{n,m}\end{aligned} \tag{7}$$

As in the single-compartment model, we provide initial conditions for n_0 drift and m_0 benthic individuals as $p_{n_0,m_0}(0) = 1$ and $p_{n,m}(0) = 0$ otherwise. The probability of extinction at time t is $p_{0,0}(t)$.

The expected values of the marginal distributions for the drift and the benthic population,

$$N_d = \sum_n \sum_m n p_{n,m}, \qquad N_b = \sum_m \sum_n m p_{n,m}, \tag{8}$$

satisfy the linear system

$$\begin{aligned} \frac{dN_d}{dt} &= -(\sigma + \varepsilon) N_d + \tau N_b, \\ \frac{dN_b}{dt} &= (\beta - \mu - \tau) N_b + \sigma N_d, \end{aligned} \tag{9}$$

see Appendix 7.2 for details. As in the previous case, this system can be considered the linearization at zero of the spatially implicit analogue of model (3) with $f'(0) = r = \beta - \mu$.

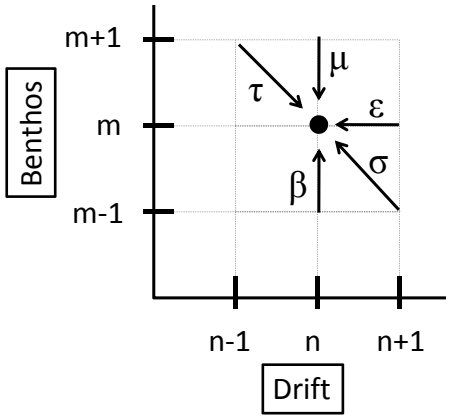

Figure 2: Transition probabilities in the two-compartment model. Exchange between benthos and drift occur at rates σ and τ, other parameters as in Figure 1.

3.3 Emigration

We use the dominant eigenvalue of the diffusion-advection operator that accounts for movement in (1) and (3) to describe the residence time within the stream reach. Then, assuming that residence time is exponentially distributed, we obtain the emigration rate parameter ε as the inverse of residence time. For deterministic models, the transition from a spatially explicit reaction-diffusion model to a spatially implicit ordinary differential equation model via the dominant eigenvalue of the movement operator has been used successfully to predict the dynamics of predator-prey systems (Strohm and Tyson, 2011) and competition systems of two and three species (Vasilyeva, 2011; Vasilyeva and Lutscher, 2012). In their stochastic model, Kolpas and Nisbet (2010) also used the dominant eigenvalue of the deterministic movement operator to estimate decay rates of the persistence probability.

We assume that individual movement due to diffusion ($D > 0$) and advection ($q \geq 0$) in the one-dimensional domain $[0, L]$ is modeled by the equation

$$\frac{\partial u}{\partial t} = D\frac{\partial^2 u}{\partial \xi^2} - q\frac{\partial u}{\partial \xi}, \tag{10}$$

for the probability density $u(t, \xi)$ of the location of an individual. Several different boundary conditions have been applied to advective systems (Ballyk *et al.*, 1998; Pachepsky *et al.*, 2005; Speirs and Gurney, 2001; Vasilyeva and Lutscher, 2011). In the simplest case, we consider hostile conditions upstream ($\xi = 0$) and downstream ($\xi = L$), i.e.

$$u(t, 0) = u(t, L) = 0. \tag{11}$$

There is a countable, unbounded sequence of eigenvalues $0 > -\lambda_1 > -\lambda_2 > \dots$ of (10). Separation of variables and application of the boundary conditions gives the explicit expression

$$\lambda_1 = \frac{q^2}{4D} + \frac{D\pi^2}{L^2}. \tag{12}$$

Following Ballyk *et al.* (1998), we conclude that $1/\lambda_1$ is the mean residence time of individuals in the domain. Hence, we choose the emigration rate parameter $\varepsilon = \lambda_1$ as the inverse of the mean residence time.

For more realistic boundary conditions, an explicit expression of the dominant eigenvalue is not available, but implicit expressions can be derived. The case of a no-flux boundary condition upstream and a hostile condition downstream as used by Speirs and Gurney (2001); Pachepsky *et al.* (2005), is captured by the conditions

$$\big(Du' - qu\big)_{|\xi=0} = 0, \qquad \text{and} \qquad u(L) = 0. \tag{13}$$

The dominant eigenvalue is given by

$$\lambda_1 = \frac{q^2}{4D} + D\nu^2, \tag{14}$$

where ν is the smallest positive solution of the equation $2D\nu = -q\tan(\nu L)$. In the case of Danckwerts conditions (Ballyk *et al.*, 1998; Vasilyeva and Lutscher, 2011), we have

$$\big(Du' - qu\big)_{|\xi=0} = 0, \qquad \text{and} \qquad u'(L) = 0. \tag{15}$$

Here, the downstream condition states that individuals leave the reach due to advection whereas diffusive fluxes into and out of the reach balance. The dominant eigenvalue is again given by (14), but this time with ν being the smallest positive solution of

$$\tan(\nu L) = \frac{4Dq\nu}{4D^2\nu^2 - q^2}. \tag{16}$$

We compare the different resulting values for the emigration rate in Figure 3. We see that the emigration rate is highest when both boundaries are hostile and lowest when no boundary is hostile.

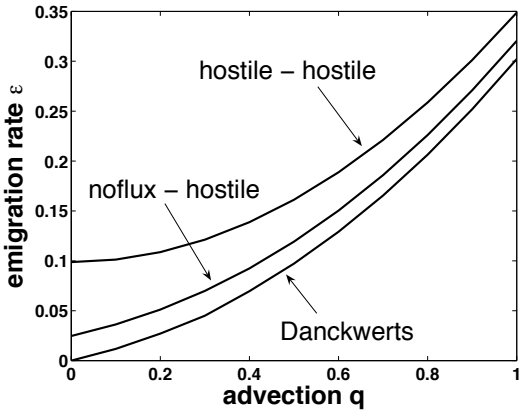

Figure 3: Emigration rates for different boundary conditions as a function of advection speed. The highest emigration rate occurs for hostile conditions upstream and downstream (top). With no-flux upstream condition and hostile downstream condition, we obtain the middle curve. For Danckwerts' conditions, the lowest emigration rate results. For $q = 0$, Danckwerts' conditions are simply no-flux conditions. Since no individuals leave the domain, the emigration rate is zero. Parameters are $L = 10, D = 1$.

4 Results

In this section, we first present some explicit formulae for the probability of extinction. Then we illustrate our results numerically, and we compare the effects of various sources of stochasticity on the extinction probability.

4.1 Extinction probability for the drift model

The standard approach to solving the set of equations (5) is to introduce the probability generating function and derive a partial differential equation for it. For constant parameters, this process is explained in detail in Kot (2001). The case where only ε depends on time was treated by Zaider and Minerbo (2000). The calculations in the general case are similar. For completeness, we give an outline in Appendix 7.1.

The expected number of individuals, starting with a single individual, is given by the solution of (6) with temporally varying parameters as

$$N(t) = \exp\left(\int_0^t (\beta(z) - \mu(z) - \varepsilon(z))dz\right). \tag{17}$$

With this solution, the extinction probability can be written as

$$p_0(t) = \left[1 - \frac{N(t)}{1 + N(t)\int_0^t \frac{\beta(z)dz}{N(z)}}\right]^{n_0}. \tag{18}$$

For constant coefficients, one obtains $N(t) = \exp[(\beta - \mu - \varepsilon)t]$, so that (18) simplifies to

$$p_0(t) = \left[1 - \frac{(\beta - \mu - \varepsilon)N(t)}{\beta N(t) - \mu - \varepsilon}\right]^{n_0}, \tag{19}$$

provided $\beta - \mu - \varepsilon \neq 0$. In that case, one also obtains an explicit expression for the asymptotic extinction probability as

$$\lim_{t\to\infty} p_0(t) = \left(\frac{\mu + \varepsilon}{\beta}\right)^{n_0}, \tag{20}$$

provided $\beta > \mu + \varepsilon$ and unity otherwise.

When all coefficient functions are periodic with period T, we can still simplify (18) somewhat to obtain

$$p_0(kT) = \left[1 - \frac{N(T)^k}{1 + TN(T)\frac{N(T)^k - 1}{N(T) - 1}\langle\frac{\beta}{N}\rangle}\right]^{n_0}. \tag{21}$$

Here, $\langle g\rangle = \int_0^T g(z)dz/T$ denotes the average of a function $g(z)$ between $z = 0$ and $z = T$. While the preceding formula may look more complicated than the general expression (18), the advantage of (21) is that only two quantities need to be calculated, namely the expected number of individuals after one period ($N(T)$) and the average of β/N over one period.

Also in this case, we can obtain the asymptotic extinction probability as

$$\lim_{k\to\infty} p_0(kT) = \left(1 - \frac{N(T) - 1}{N(T)T\langle\frac{\beta}{N}\rangle}\right)^{n_0}, \tag{22}$$

provided $N(T) > 1$ and the expression in brackets is positive.

We illustrate how the extinction probability depends on parameters and their temporal variation below. First, we derive some analogous formulae for the two-compartment model.

4.2 Extinction probability for the drift-benthos model

The analysis of equations (7) follows the same steps as for the single-compartment model, but is a lot more involved; in fact, no explicit formulas are available. One introduces the probability generating function $\Psi(t, x, y) = \sum_{n,m} p_{n,m}x^n y^m$. This function satisfies the first-order equation

$$\frac{\partial\Psi}{\partial t} + [(\sigma + \varepsilon)x - \sigma y - \varepsilon]\frac{\partial\Psi}{\partial x} + [(\beta + \tau + \mu)y - \beta y^2 - \tau x - \mu]\frac{\partial\Psi}{\partial y} = 0, \tag{23}$$

subject to the initial condition $\Psi(0, x, y) = x^{n_0}y^{m_0}$. The goal is to find the probability of extinction at time t, which is $\Psi(t, 0, 0)$. The solution $\Psi(t, x, y)$ is constant along the

characteristic curves given by $t(s) = s$ and

$$\begin{aligned} \frac{dx}{ds} &= (\sigma + \varepsilon)x - \sigma y - \varepsilon, \\ \frac{dy}{ds} &= (\tau + \beta + \mu)y - \beta y^2 - \tau x - \mu. \end{aligned} \tag{24}$$

Hence, to obtain $\Psi(t, 0, 0)$, we find (κ_1, κ_2) such that the solution of (24) with initial conditions $(x(0), y(0)) = (\kappa_1, \kappa_2)$ satisfies $(x(t), y(t)) = (0, 0)$. Then $\Psi(t, 0, 0) = \Psi(0, x(0), y(0)) = \kappa_1^{n_0}\kappa_2^{m_0}$ is the extinction probability. In the case of constant parameters, system (24) can be studied by phase-plane methods and the asymptotic extinction probability

$$\lim_{t\to\infty} \psi(t, 0, 0) = \min\left\{1, (x^*)^{n_0}(y^*)^{m_0}\right\}, \tag{25}$$

can be derived (Maler and Lutscher, 2010), where

$$y^* = \frac{\tau\varepsilon}{\beta(\sigma + \varepsilon)} + \frac{\mu}{\beta}, \qquad x^* = \frac{\sigma y^* + \varepsilon}{\sigma + \varepsilon}. \tag{26}$$

It is clear that $x^* < 1$ only if $y^* < 1$. An obvious necessary condition is $\beta > \mu$. Under this condition, the asymptotic extinction probability is less than one if and only if

$$\varepsilon < \frac{\sigma(\beta - \mu)}{\tau - \beta - \mu}, \qquad \tau > \beta - \mu, \tag{27}$$

whereas if $\tau < \beta - \mu$, then the asymptotic extinction probability is less than one for all values of ε. This switch between certain extinction and positive persistence probability reflects the results for the deterministic model by Pachepsky *et al.* (2005), reported in the introduction.

In general, an explicit expression for the extinction probability is not available for the two-compartment model, even in the case of constant coefficients. In the case of temporally varying coefficients, the system of characteristic curves (24) is a non-autonomous system, but the theory remains the same.

5 Numerical results

Since we are not modeling any particular species, we chose model parameters conveniently to illustrate results, in particular so that the various existence thresholds and their dependence on stochastic effects and variation can be observed. Throughout, we choose $L = 50$, and 50 individuals initially (split equally between drift and benthos where applicable). Unless otherwise noted we set $r = 2$.

5.1 Single compartment, no temporal variation

In the simplest case of a single drift compartment and temporally constant parameters, the extinction probability is given by (19): $p_0(t)$ is a decreasing function of birth rate β and initial population n_0, and an increasing function of death rate μ, emigration

rate ε and time. Figure 4 illustrates that (a) stochasticity serves to smooth out the deterministic persistence condition (labeled q^*), and that (b) for constant net growth rate $r = \beta - \mu$, persistence probability decreases for increasing β and μ. These analytical results completely match the simulation outcomes by Kolpas and Nisbet (2010). Since emigration and death occur only as a sum in our model, a high birth rate can also not compensate for a high emigration rate when their difference is held constant.

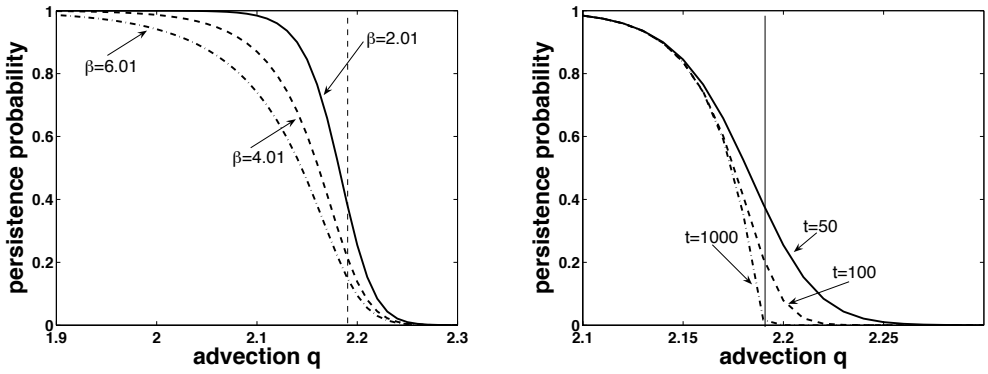

Figure 4: **Left:** Persistence probability as a function of advection speed in the single-compartment model. The deterministic persistence boundary, indicated by the dashed line, is simply smoothed out by stochasticity. The net growth rate $r = \beta - \mu = 2$ is held constant for different values of β; we chose $D = 0.6$, and time is $t = 50$. **Right:** The effect of time on the persistence probability. For larger times, the persistence probability in the stochastic model approaches the deterministic threshold. Parameters are $\beta = 2.01$ and the rest as above.

We mention without illustration that increased advection leads to decreased persistence and that, for different boundary conditions, persistence probability is highest for Danckwerts' conditions and lowest for hostile conditions, as expected from Figure 3. For small domains, the difference in boundary conditions can make the difference between asymptotic persistence or extinction, but for long domains, the difference in boundary conditions is negligible.

5.2 Two compartments, no temporal variation

The asymptotic extinction probability for a population divided into a benthic and a drift compartment with constant parameters is given by (25,26). The extinction probability is a decreasing function of β, n_0, m_0, and an increasing function of μ and ε. Whether it increases or decreases with σ, τ depends on the relative magnitude of μ and ε, the loss rates from the two compartments. Large values of σ (τ) correspond to short residence times in the drift (benthos) and hence to a smaller (larger) probability of wash-out.

For constant net growth rate, $r = \beta - \mu$, the persistence probability decreases when the values of β and μ are increased, just as in the single-compartment case. As τ

approaches r from above, the persistence probability increases. For $\tau \leq r$, formula (27) predicts a positive asymptotic persistence probability.

We consider the trade-off between diffusion and residence time in the drift. The (deterministic) critical advection speed (4) depends on the product $D\sigma$. A higher rate of random movement allows for a longer residence time in the drift. The persistence probability increases with D while holding $D\sigma$ constant, see Figure 5. In the limit of large exchange rates ($\tau = \kappa\sigma$ and $\sigma \to \infty$) the two-compartment model (3) can be approximated by the single-compartment model (1) with appropriately scaled parameters (Pachepsky *et al.*, 2005). The deterministic threshold (4) is a decreasing function of σ when $\tau = \kappa\sigma$. The same is true for the persistence probability, see Figure 5. In the limit $\sigma \to \infty$, the persistence probability approaches the corresponding curve from the single-compartment model; the two are indistinguishable on the given scale for $\sigma = 100$.

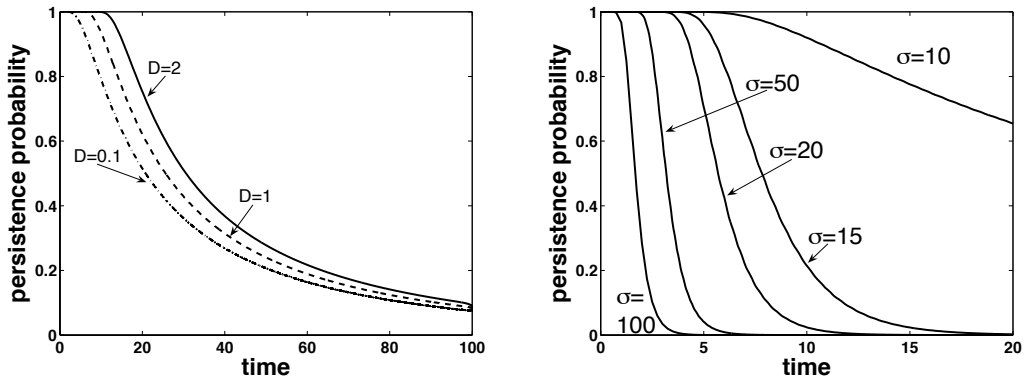

Figure 5: **Left:** Persistence probability as a function of time, for different values of D and σ, under the constraint that $D\sigma = 6$ =const., so that the deterministic threshold q^* is constant. The other parameters are $q = 7 > q^*$, $\beta = 2.01$, $\mu = 0.01$, and $\tau = 3$. **Right:** Persistence probability as a function of time, for different values of σ with fixed relationship $\tau = \sigma/3$. The other parameters are $q = 6, D = 0.6$ $\beta = 2.01$, and $\mu = 0.01$.

5.3 Single compartment, temporal variation

We begin investigating temporal variability by considering how the amplitude, the period and the initial phase of the flow speed change the persistence probability as compared to the case of constant average flow. We model flow speed as a piecewise constant, T-periodic function, alternating between low and high flow for the two halves of the period. Hence, the two flow speeds are $q^{\pm} = \bar{q} \pm \Delta q$, with mean flow $\bar{q}$ and amplitude Δq.

When $\bar{q} > q^*$ then the asymptotic persistence probability is zero. The two main insights are that (1) variation in flow speed decreases the persistence probability for intermediate and long times, and (2) variation in flow speed may increase the persistence probability for short times provided that the period is large and the system starts

in the low flow regime, see Figure 6. For a period of one time unit, the persistence probability for constant mean flow is higher than with variable flow, starting with low flow conditions, which in turn is higher than when starting with high flow conditions (left panel). A close inspection near $t = 0$ reveals that the solid line is actually above the dash-dot line for very small times. For a ten times larger period, variation in flow rates with initially low flow can increase the persistence probability for a short while, but will eventually also drop below the situation for constant flow. When the initial conditions are high flow, then the persistence probability will always be below the other two cases (right panel). For very short periods, $T \ll 1$, the initial conditions do not matter, i.e. the solid and dashed lines are indistinguishable (plot not shown).

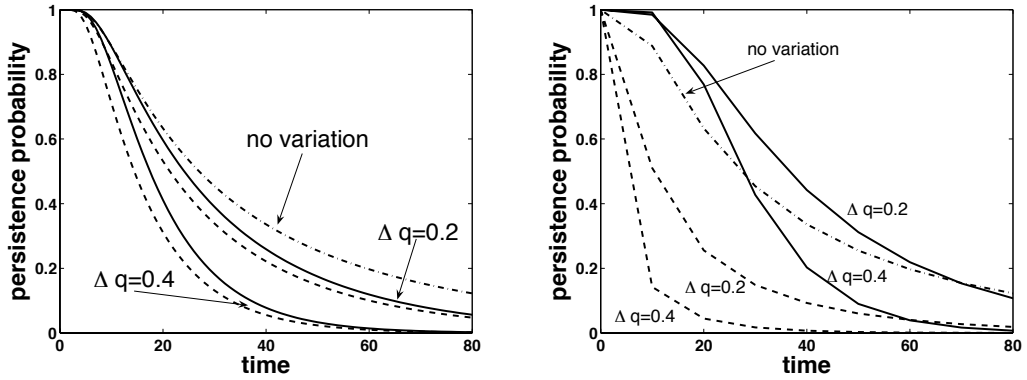

Figure 6: Persistence probability as a function of time, for different flow regimes. Constant mean flow of $\bar{q} = 2.2$ is labeled as "no variation" (dash-dot curve). The solid curves represent variable flow with the initial period being a low flow regime, whereas the dashed curves correspond to initially high flow regime. The plot on the left has short period $T = 1$, whereas the plot on the right has long period $T = 10$. The other parameters are $D = 0.6$ $\beta = 2.01$, and $\mu = 0.01$.

Temporal variation in flow speed can have significant beneficial effects in deterministic models (Lutscher and Seo, 2011), but is often associated with increased extinction risk in stochastic models (Schreiber, 2010). Persistence probability is a non-increasing function of time. If it drops during a high flow regime, it will not increase again thereafter. More importantly, we observe that flow speed and emigration rate are nonlinearly related; in fact, ε is a convex function of q, see (12). By Jensen's inequality, the average emigration rate in a variable environment is higher than the emigration rate at the averaged flow speed. This observation explains why the persistence probability decreases with variation, at least for long enough times.

When $\bar{q} < q^*$, the asymptotic persistence probability is positive, and a number of different phenomena can occur, particularly for large T. The asymptotic persistence probability with variation can be above the one for constant average conditions for small enough amplitude and for initial low flow regime. As the amplitude increases, the

asymptotic persistence probability drops below that for average conditions (left panel, Figure 7). The reason is that the persistence probability is a non-increasing function; high emigration during the high flow regimes cannot be compensated for during the low flow periods. This phenomenon of increased persistence occurs only at long periods, and that, as the period decreases, the difference between the initial conditions (high or low flow regime) disappears (right panel, Figure 7). The effect of initial conditions increases with period (plot not shown).

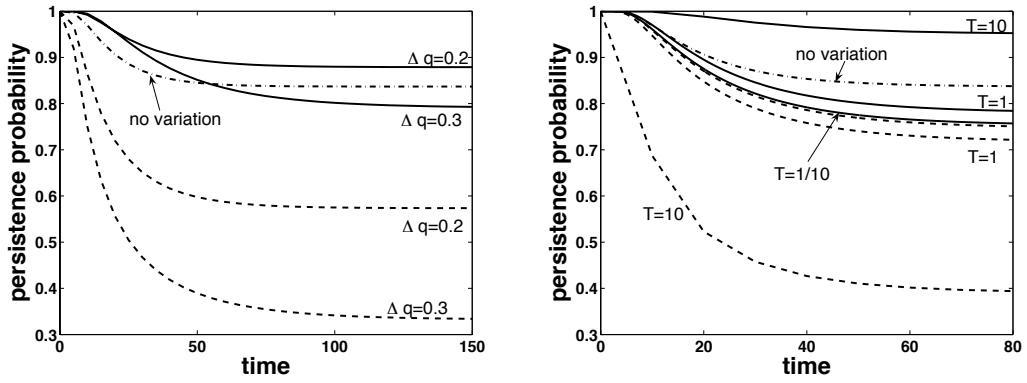

Figure 7: Persistence probability as a function of time, for different flow regimes. Constant mean flow of $\bar{q} = 2.15$ is labeled as "no variation" (dash-dot curve). The solid curves represent variable flow with the initial period being a low flow regime, whereas the dashed curves correspond to initially high flow regime. The plot on the left is for period $T = 5$, and two different values for the amplitude as indicated. The plot on the right is for fixed amplitude $\Delta q = 0.2$ with different periods as indicated. The other parameters are $D = 0.6$ $\beta = 2.01$, and $\mu = 0.01$.

Since variation in nature is often more gradual than just switching between two states, we also studied the persistence probability with a sinusoidally varying flow rate

$$q(t) = \bar{q} + \Delta q \sin\left(\frac{2\pi}{T}(t - \phi)\right). \tag{28}$$

The sinusoidal variation most closely imitates the piecewise constant flow rate when the phase shift ϕ is zero (high flow regime first) or half the period (low flow regime first). In both cases, we found same qualitative results as with piecewise flow.

We illustrate the effect of phase shift on the persistence probability when only the birth rate varies temporally. We define $\beta(t)$ by (28) with $\bar{q}$ and Δq replaced by $\bar{\beta}$ and $\Delta\beta$, respectively. Since the growth rate appears under the integral in (21), it is not obvious how its variation affects the persistence probability. When $\phi = 0$, growth conditions are good initially, and $N(t)$ increases until $T/2$. Greater amplitude ($\Delta\beta$) implies higher persistence probability. Vice versa, if $\phi = T/2$, growth conditions are initially bad, so that $N(t)$ decreases until $T/2$. Greater amplitude implies lower persistence probability.

For intermediate phase shifts, the value of $N(T/2)$ is the deciding factor. If $|\phi| < T/4$ then $N(T/2)$ is larger than it would be under averaged conditions, and therefore variation in growth rate increases persistence in this case. If $|\phi| > T/4$, the reverse effect occurs. Curiously, when $|\phi| = T/4$ so that $N(T/2)$ equals the value for averaged conditions, then variation in growth rate is mildly beneficial for small amplitude but detrimental for large amplitude, see Figure 8.

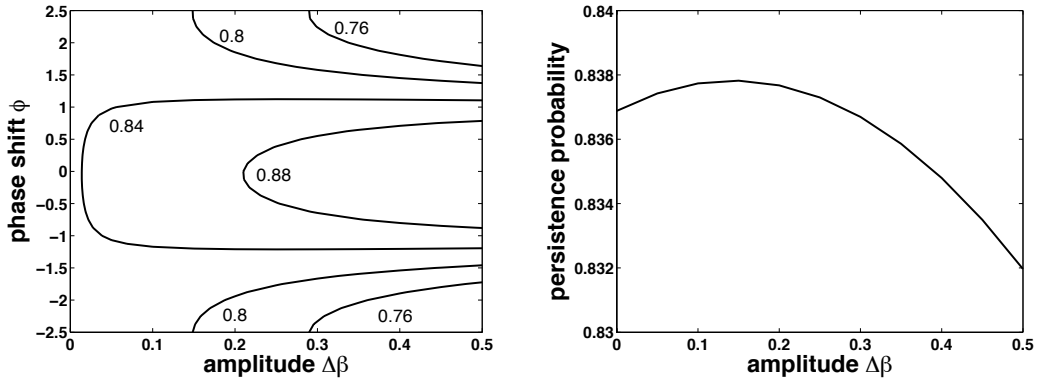

Figure 8: Persistence probability as a function of amplitude and phase shift for sinusoidally varying growth rate. The plot on the left shows contour lines of the persistence probability at time 250. The plot on the right shows the persistence probability for phase shift $\phi = T/4$. Parameters are $D = 0.6$ $q = 2.15$, $\bar{\beta} = 2.01$, and $\mu = 0.01$. The period is $T = 5$, and the persistence probability is calculated after $k = 50$ periods.

5.4 Two compartments, temporal variation

Here we consider how variation in physical effects (flow speed q) and behavior (jumping rate τ) affect persistence. The deterministic model (3) predicts unconditional persistence if $\tau < r$, and has critical flow speed q^* if $\tau > r$. With constant parameters, the stochastic model shows smooth transitions for these critical values. We vary each parameter according to (28) with appropriate parameter names. Unless otherwise noted, parameters are $\beta = 2.01, \mu = 0.01, D = 0.6, T = 5$, but we checked our results for a wide range of parameters.

Varying flow. When $\tau = \bar{\tau} < r$, then the asymptotic persistence probability is essentially unity for constant parameters, and the same holds true for variable flow speeds. While persistence declines slightly as Δq increases, extinction probabilities are negligibly small for all parameter values we tried (e.g. $\tau = \sigma = 1.5$ and $\bar{q} = 4, \Delta q \leq 4$ gave $p_0 = 10^{-7} \sim 10^{-5}$, plots not shown). As expected, the persistence probability is higher when the system starts in a low flow period and lower when the system starts with high flow.

When $\tau = \bar{\tau} > r$, and flow speeds vary with $\bar{q} < q^*$, then the persistence probability is expected to decrease (increase) as Δq increases when the initial regime is high (low)

flow. Indeed, we see this pattern when τ, σ are both large, and also when τ is only slightly above r and σ is very small. Surprisingly the persistence probability can increase with increasing variation in flow speed even with initial high-flow period, for intermediate values of σ, see Figure 9. Large values of Δq mean high emigration during the high flow regime (detrimental) and low emigration during the low flow regime (beneficial). In all previous examples, the negative effect outweighed the positive effect on persistence probability, but here, the beneficial effect of low flow periods shows. This effect only occurs in the two-compartment model where individuals can escape emigration during high flow period if they happen to be on the benthos. For the observation in Figure 9, we speculate that some resonance phenomenon occurs, whereby individuals manage to be in the drift mostly during low flow conditions and on the benthos during high flow conditions. Note that τ is constant here, i.e. there is no behavioral response to high flow.

When $\tau = \bar{\tau} > r$, and flow speeds vary with $\bar{q} > q^*$, extinction is certain for constant average conditions. Variation in flow rates can increase the persistence probability for intermediate times, and even lead to asymptotic population persistence, especially for an initially low-flow regime (Figure 10).

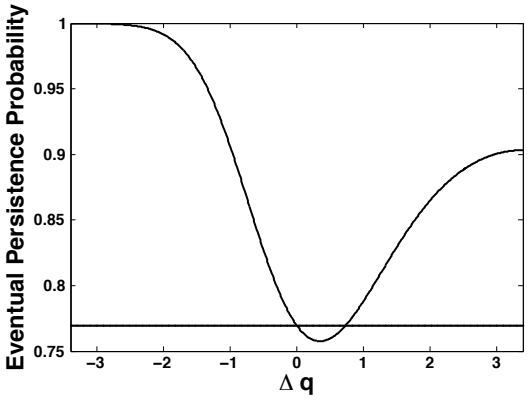

Figure 9: The asymptotic persistence probability has a minimum at intermediate flow amplitudes. Positive effects of low flow periods override negative effects of high flow periods for large variation. Note that positive values of Δq correspond to high initial flow regime and negative values to low initial flow regime. The horizontal line corresponds to constant parameter values. Parameters are $q = 3.4$, $\sigma = 1.5$, and $\tau = 2.5$.

Varying jumps. Zooplankton migrate in the water column on a daily basis: some prefer daylight and migrate up accordingly, others migrate downwards during the day to avoid predators (Pasour and Ellner, 2010). When $\tau(t) < r$, then there is no critical flow speed according to (4), and the asymptotic persistence probability is near unity, similar to the constant case (plot not shown). When $\bar{\tau} < r$ but $\bar{\tau} + \Delta\tau > r$ the persistence probability decreases for increasing (temporally constant) flow speeds, but this decrease is only marginal. For example, a ten-fold increase in flow speed would

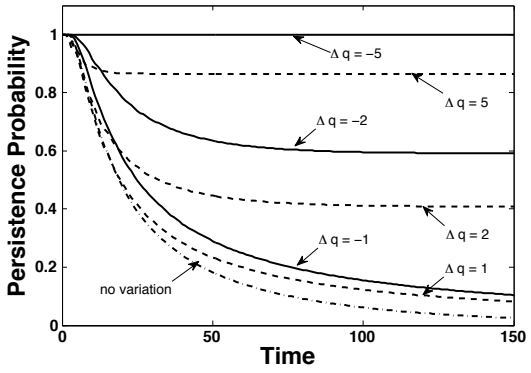

Figure 10: Persistence probability can increase with flow variation. Solid lines correspond to low initial flow regime ($\Delta q < 0$); dashed lines are high initial flow regime ($\Delta q > 0$). All lines are above the constant case (dash-dot). Parameters are $\bar{q} = 5$, $\sigma = 2.5$, and $\tau = 2.5$.

drop the asymptotic persistence probability only from 99% to 94%, all else being equal. ($\bar{\tau} = 1.5, \Delta\tau = 1, \sigma = 1.5, \bar{q} \in [5, 50]$, plots not shown). We conclude that even though $\Delta\tau$ has some impact on persistence, the determining factor is still the average condition $\bar{\tau} < r$.

When $\bar{\tau} > r$, then there is a critical speed q^* for averaged conditions. When $q = \bar{q} < q^*$, then the persistence probability decreases with variation in τ, if the initial regime is large τ, and increases if the initial condition is small τ. Small values of τ mean that individuals remain on the benthos and, thus, are not being washed away with the flow. Again, the order of events is crucial.

When $\bar{\tau} > r$ and $q = \bar{q} > q^*$, extinction is inevitable for constant τ and for small $\Delta\tau$. However, large variation in τ can increase the persistence probability significantly. In particular, if individuals can choose not to jump at all for some time, this can lead to essential persistence. The combination of short residence time in the drift compartment ($1/\sigma$) combined with the long residence time on the benthos during the periods of small τ, allows individuals to reproduce fast enough to avoid washout, see Figure 11.

Varying both. Flow rates and jumping behavior can interact in various ways. For example, one physical effect of high flow speeds is scouring of the benthic community, which we can model by increasing jumping rates. Conversely, behavioral responses to high emigration risk during high flow periods could include lowering the jumping rate. To emulate the effect of scouring, we let q and τ vary in phase; out-of-phase variation simulates the behavioral response to avoid washout if individuals can sense flow speeds. (Rather than varying the phase, ϕ in (28), we use Δq and $\Delta\tau$ of the same sign for in-phase variation and of opposite signs for out-of-phase variation.)

Intuition would suggest that scouring decreases the persistence probability whereas individual behavior to avoid washout can increase it. Results depend on parameter values, and, again, much on the initial phase. We choose $\bar{\tau} > r$ and $\bar{q} < q^*$. An

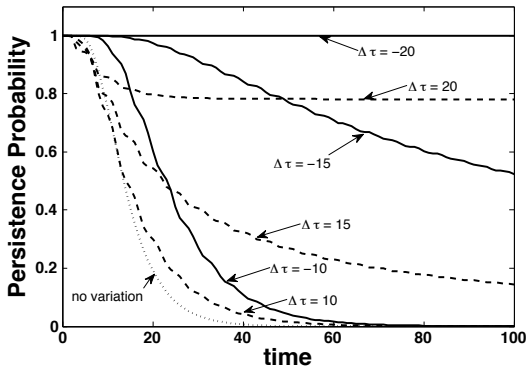

Figure 11: The persistence probability can increase dramatically when jumping rate τ varies. Parameters are $q = 2.5$, $\sigma = 20$, $\bar{\tau} = 20$.

initially high flow regime combined with scouring decreases the persistence probability as compared to constant parameters. An initially low flow regime combined with scouring gives a highly favorable initial phase, so that the persistence probability exceeds that of the constant parameter case. The persistence probability in an initially high flow regime can be increased by appropriate behavior, see Figure 12. When the flow regime is low initially, then behavior can have a negative effect on the persistence probability, but only for small $\Delta q, \Delta\tau$; for large enough variation, the persistence probability will increase above the constant coefficient case.

When $\bar{\tau}$ and σ are both large, and $\bar{q} > q^*$, then variation in τ seems to play a minor role. Even large variation in τ cannot overrule the effect that initially high flow leads to a decreased persistence probability (compared to average conditions) and initially low flow can give a higher persistence probability. These results are already present for the single-compartment model, and since the two compartment model may be approximated by a single-compartment model for large values of τ, σ, we see that the effect of variation in flow speed are stronger than the effects of variation in τ.

6 Discussion

Streams and rivers are vital ecosystems; many recent modeling efforts are geared towards a mechanistic understanding of population persistence and extinction in running waters, e.g. (Speirs and Gurney, 2001; Pachepsky *et al.*, 2005; Ryabov and Blasius, 2008). Almost all of these models are deterministic, and they typically find critical thresholds in parameter values that guarantee population persistence. In the first stochastic simulation model for stream populations, Kolpas and Nisbet (2010) found that these deterministic thresholds are replaced with a smooth and sometimes steep transition from essential persistence to essential extinction. Pasour and Ellner (2010) compared residence times of zooplankton in a given flow field by simulating individual trajectories, but did not consider persistence of an entire population. In contrast to these two spatially explicit

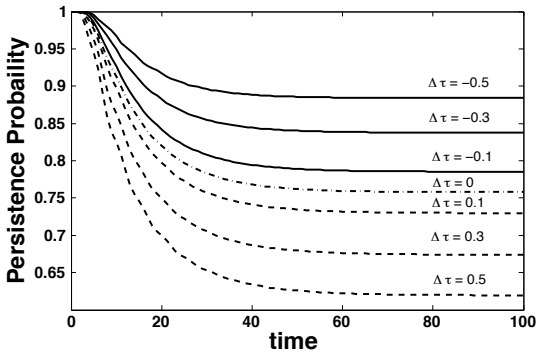

Figure 12: With initially high flow regime ($\Delta q = 0.3$), scouring ($\Delta\tau > 0$) can decrease the persistence probability, whereas appropriate jumping behavior ($\Delta\tau < 0$) can increase it. Parameters are $\bar{q} = 3.4$, $\sigma = 1.5$, and $\bar{\tau} = 2.5$.

simulation models, we derived and analyzed two spatially implicit stochastic models. Our approach has the advantage that analytical results can be obtained; the price to pay is that explicit space is approximated by an average emigration rate.

The transition from a spatially explicit advection-diffusion process to the average emigration rate occurs via the residence time, expressed as the inverse of the dominant eigenvalue of the advection-diffusion operator. In the same spirit, one can reduce a spatially explicit reaction-diffusion equation to a spatially implicit ordinary differential equation, from which one can obtain a fairly accurate description of the dynamic behavior of the spatially explicit equation (Strohm and Tyson, 2011; Vasilyeva and Lutscher, 2012; Vasilyeva, 2011).

Our approach assumes that the spatially averaged residence time is exponentially distributed. This assumption is convenient but unlikely to be true; however, the close match with the computational results by Kolpas and Nisbet (2010) gives reason to believe that the deviations from an exponential distribution have only small effects. We conjecture that the deviations from exponential are small as long as solutions of (10) converge quickly to the dominant eigenfunction, which is the case if the ratio of the subdominant to the dominant eigenvalue is large. Under temporal variation, the situation is less clear, and deviations could be larger. We are not aware of simulation results to compare our analytical results with. Such a detailed comparison is the subject of future work.

Our results for constant parameter values indicate that the thresholds in the deterministic models are simply to be replaced with a smooth transition from persistence to extinction around the same parameter values. This result also confirms the value of deterministic models in applied settings. For temporal variation, the importance of the initial phase for the long-term result stands out, in particular with long periods. Often, we find that variation in flow speed leads to a decrease in persistence probability, in particular with an initially high flow regime. This decrease is in line with the general ex-

pectation that temporal variation enhances extinction (Schreiber, 2010). The nonlinear relationship between flow rate and emigration probability adds to this effect. When the first phase is of low flow, then small variation can increase the persistence probability, an effect of the importance of the initial phase; but larger variation decreases persistence in the one-compartment model. We do, however, identify a number of scenarios in the drift-benthos model where this relationship does not hold. The most interesting effect where variation in flow speed actually increases persistence occurs in the drift-benthos model for intermediate values of transfer parameters. We speculate that for these values, an individual spends, on average, the phase of high flow on the benthos and the phase of low flow in the drift.

Out of the many possible correlations between parameter variation, we concentrated on the physical effect of scouring and the behavioral effect of adjusting the jumping rate to flow rate. The latter obviously implies that individuals can sense the flow speed. Our results demonstrate the extent to which these mechanism can augment or diminish the effect of variable flow. We suggest that our framework can also be applied to study the effect of ramping in hydroelectric dams. In particular when individual jumping and settling behavior is determined by daylight, then certain dam release schedules maybe more detrimental to river invertebrates than others. Our results can also be applied to some form of predation by fish, included as a death term in the drift compartment. We can interpret the 'emigration rate' as the sum of physical loss by advection and biological loss by predation. Then there could be correlations between flow speed and the presence of predators, which might amplify the combined 'emigration rate' or reduce the effect.

Acknowledgments

We thank Christina Cobbold and Olga Vasilyeva for insightful discussions. FL gratefully acknowledges funding in the form of an 'Early Researchers Award' from the Ontario Ministry of Research and Innovation.

References

Ballyk, M. and Smith, H. (1999). A model of microbial growth in a plug flow reactor with wall attachment. *Math. Biosci.*, **158**, 95–126.

Ballyk, M., Dung, L., Jones, D. A., and Smith, H. (1998). Effects of random motility on microbial growth and competition in a flow reactor. *SIAM J. Appl. Math.*, **59**(2), 573–596.

Boldin, B. (2007). Persistence and spread of gastro-intestinal infections: the case of enterotoxigenic *escherichia coli* in piglets. *Bull. Math. Biol.*, **70**(7), 2077–2101.

Byers, J. and Pringle, J. (2006). Going against the flow: Retention, range limits and invasions in advective environments. *Marine Ecol. Prog. Ser.*, **313**, 27–41.

Hershey, A., Pastor, J., Peterson, B., and Kling, G. (1993). Stable isotopes resolve the drift paradox for *baetis* mayflies in an arctic river. *Ecology*, **74**, 2315–2325.

Huisman, J., Arrayás, M., Ebert, U., and Sommeijer, B. (2002). How do sinking phytoplankton species manage to persist. *Am. Nat.*, **159**, 245–254.

Jin, Y. and Lewis, M. (2011). Seasonal influence on population spread and persistence in streams: Critical domain size. *SIAM Appl. Math*, **71**, 1241–1262.

John, F. (1971). *Partial Differential Equations*. Springer.

Kolpas, A. and Nisbet, R. (2010). Effects of demographic stochasticity on population persistence in advective media. *Bull. Math. Biol.*, **72**(5), 1254–1270.

Kot, M. (2001). *Elements of Mathematical Ecology*. Cambridge Univ. Press, Cambridge.

Lewis, M., Hillen, T., and Lutscher, F. (2009). Spatial dynamics in ecology. In M. Lewis, J. Keener, P. Maini, and M. Chaplain, editors, *Mathematical Biology*, volume 14 of *Park City Mathematics Series*. Institute of Advanced Studies.

Lutscher, F. and Seo, G. (2011). The effect of temporal variability on persistence conditions in rivers. *J. theor. Biol.*, **283**, 53–59.

Lutscher, F., Pachepsky, E., and Lewis, M. (2005). The effect of dispersal patterns on stream populations. *SIAM REV.*, **47**(4), 749–772.

Lutscher, F., Lewis, M., and McCauley, E. (2006). The effects of heterogeneity on population persistence and invasion in rivers. *Bull. Math. Biol.*, **68**(8), 2129–2160.

Lutscher, F., Nisbet, R., and Pachepsky, E. (2010). Population persistence in the face of advection. *Theor. Ecol.*, **3**, 271–284.

Maler, A. and Lutscher, F. (2010). Cell cycle times and the tumour control probability. *Math. Med. Biol.*, **27**(4), 313–342.

Pachepsky, E., Lutscher, F., Nisbet, R., and Lewis, M. A. (2005). Persistence, spread and the drift paradox. *Theor. Pop. Biol.*, **67**, 61–73.

Pasour, V. and Ellner, S. (2010). Computational and analytic perspectives on the drift paradox. *SIAM J. Appl. Dyn. Syst.*, **9**, 333–356.

Potapov, A. and Lewis, M. (2004). Climate and competition: The effect of moving range boundaries on habitat invasibility. *Bull. Math. Biol.*, **66**(5), 975–1008.

Pringle, J., Lutscher, F., and Glick, E. (2009). Going against the flow: the effect of non-gaussian dispersal kernels and reproduction over multiple generations. *Marine Ecol. Prog. Ser.*, **337**, 13–17.

Ryabov, A. and Blasius, B. (2008). Population growth and persistence in a heterogeneous environment: the role of diffusion and advection. *Math. Model. Nat. Phenom.*, **3**, 42–86.

Schreiber, S. (2010). Interactive effects of temporal correlations, spatial heterogeneity and dispersal on population persistence. *Proc. R. Soc. Lond. B*, **277**, 1907–1914.

Speirs, D. and Gurney, W. (2001). Population persistence in rivers and estuaries. *Ecology*, **82**(5), 1219–1237.

Strohm, S. and Tyson, R. (2011). The effect of habitat fragmentation on cyclic population dynamics: A reduction to ordinary differential equations. *Theor. Ecol.*

Vasilyeva, O. (2011). *Modeling and Analysis of Population dynamics in advective environments*. Ph.D. thesis, University of Ottawa.

Vasilyeva, O. and Lutscher, F. (2011). Population dynamics in rivers: analysis of steady states. *Can. Appl. Math. Quart.*, **18**(4), 439–469.

Vasilyeva, O. and Lutscher, F. (2012). Competition of three species in an advective environment. *Nonlinear Analysis: Real World Applications*, **13**(4), 1730–1748.

Zaider, M. and Minerbo, G. (2000). Tumour control probability: a formulation applicable to any temporal protocol of dose delivery. *Phys. Med. Biol.*, **45**, 279–293.

7 Appendix

7.1 Formulas for the drift model

We outline the calculations that lead to the formulae presented in Section 4.1. We consider the probability generating function,

$$F(t,x) = \sum_{n=0}^{\infty} p_n(t)x^n. \tag{29}$$

Using the set of equations (5), one can derive the first-order partial differential equation

$$\frac{\partial F}{\partial t} + (\beta x - \mu - \varepsilon)(1-x)\frac{\partial F}{\partial x} = 0, \tag{30}$$

together with the initial condition $F(0,x) = x^{n_0}$. Then we employ the method of characteristics (John, 1971) to find the solution $F(t,x)$. The solution $F(t,x)$ is constant along the characteristic curves $t(s) = s$ and

$$\frac{dx}{ds} = (\beta x - \mu - \varepsilon)(1-x). \tag{31}$$

This Riccati equation can be solved explicitly. For given $t > 0$, we then find $x(0)$ so that $x(t) = 0$. Then $p_0(t) = F(t,0) = F(0,x(0)) = x(0)^{n_0}$ is the extinction probability as in (18).

To obtain the formula for periodic coefficient functions, we note the following relations. Since

$$\int_0^{kT} \beta(z)dz = k \int_0^T \beta(z)dz, \tag{32}$$

and similarly for $\mu(z)$ and $\varepsilon(z)$, we see that $N(kT) = N(T)^k$. Then we can evaluate

$$\int_0^{kT} \frac{\beta(z)dz}{N(z)} = \sum_l^{k-1} \int_0^T \frac{\beta(z)dz}{N(z+lz)} = \int_0^T \frac{\beta(z)dz}{N(z)} \sum_l^{k-1} \frac{1}{N(T)^l}. \tag{33}$$

Together with the formula for the geometric series, this leads to the desired formula (21).

7.2 Formulas for the drift-benthos model

Following Maler and Lutscher (2010), we present a brief derivation of equation (7). We denote $p_{n,m}(t)$ as the probability that there are n drift individuals and m benthic individuals at time t. There are the following seven possibilities for having n drift and m benthic cells at time $t + \Delta t$.

1. There were $n+1$ drift and m benthic individuals at time t and one drift individual emigrated. The probability of this event is $p_{n+1,m}(t)(n+1)\varepsilon\Delta t + o(\Delta t)$.

2. There were n drift and $m+1$ benthic individuals at time t and one benthic individual died: probability $p_{n,m+1}(t)(m+1)\mu\Delta t + o(\Delta t)$.

3. There were n drift and $m-1$ benthic individuals at time t and one benthic individual gave birth: probability $p_{n,m-1}(t)(n+1)\beta\Delta t + o(\Delta t)$.

4. There were $n-1$ drift and $m+1$ benthic individuals at time t and one benthic individual moved to the drift: probability $p_{n-1,m+1}(t)(m+1)\tau\Delta t + o(\Delta t)$.

5. There were $n+1$ drift and $m-1$ benthic individuals at time t and one drift individual settled on the benthos: probability $p_{n+1,m-1}(t)(m-1)\sigma\Delta t + o(\Delta t)$.

6. There were n drift and m benthic individuals at time t and no events occurred: probability $p_{n,m}(t)\left(1 - n(\varepsilon+\sigma)\Delta t - m(\beta+\mu+\tau)\Delta t\right) + o(\Delta t)$.

7. There were some number of individuals at time t and more than one event occurred: probability $o(\Delta t)$.

Therefore $p_{n,m}(t+\Delta t)$ is equal to the sum of the seven probabilities given above. Subtracting $p_{n,m}(t)$ from this expression, dividing by Δt, and letting $\Delta t \to 0$, we get equation (7).

Now we define $P_n = \sum_m p_{n,m}$ and $Q_m = \sum_n p_{n,m}$, the probability that there be n drift individuals or m benthic individuals, respectively. Summing equation (7) with

respect to m, we obtain the following equation for P_n,

$$\begin{aligned}\dot{P}_n &= \varepsilon(n+1)P_{n+1} + \mu\sum_m (m+1)p_{n,m+1} + \sigma(n+1)P_{n+1} + \beta\sum_m (m-1)p_{n,m-1} \\ &\quad +\tau\sum_m (m+1)p_{n-1,m+1} - (\sigma+\varepsilon)nP_n - (\beta+\tau+\mu)\sum_m mp_{n,m}. \qquad (34)\end{aligned}$$

Now we form expectations $N_d = \sum_n P_n$ and $N_b = \sum_m Q_m$. From (34) we obtain an equation for N_d. (Note that $\sum_n \sum_m p_{n,m} = 1$.)

$$\begin{aligned}\dot{N}_d &= \varepsilon\sum_n n^2 P_n - \varepsilon N_d + \mu + \sigma\sum_n n^2 P_n - \sigma N_d + \beta \\ &\quad +\tau\sum_n\sum_m n(m+1)p_{n-1,m+1} - (\sigma+\varepsilon)\sum_n n^2 P_n - (\beta+\tau+\sigma).\end{aligned}$$

The only term that needs closer consideration is the following.

$$\begin{aligned}\sum_n\sum_m n(m+1)p_{n-1,m+1} &= \sum_n\sum_m (n-1)(m+1)p_{n-1,m+1} + \sum_n\sum_m (m+1)p_{n-1,m+1} \\ &= 1 + \sum_m (m+1)Q_{m+1} = 1 + N_b.\end{aligned}$$

Hence, we get the equation

$$\dot{N}_d = -\varepsilon N_d - \sigma N_d + \tau N_b. \qquad (35)$$

The derivation of the equation for N_b is similar, so that we arrive at system (9).

Chapter 3

Connectivity, passability and heterogeneity interact to determine fish population persistence in river networks

This paper is published in Journal of the Royal Society Interface [42];
Samia, Y., Lutscher, F., Hastings A. Connectivity, passability and heterogeneity interact to determine fish population persistence in river networks. *J. R. Soc. Interface.* 12: 20150435. 2015

The contribution by each author is as follows. The second and the third authors conceived the study and critically edited the manuscript; the first author carried out the analysis and numerical simulations and drafted the manuscript. All authors designed the study and gave their final approval for publication.

Connectivity, passability and heterogeneity interact to determine fish population persistence in river networks

Yasmine Samia
Department of Mathematics and Statistics
University of Ottawa, Ottawa, Canada

Frithjof Lutscher*
Department of Mathematics and Statistics, and Department of Biology
University of Ottawa, Ottawa, Canada

Alan Hastings
Department of Environmental Science and Policy
University of California Davis, CA, USA

*Corresponding author. Email: flutsche@uottawa.ca

Abstract

The movement of fish in watersheds is frequently inhibited by human-made migration barriers such as dams or culverts. The resulting lack of connectivity of spatial subpopulations is often cited as a cause for observed population decline. We formulate a matrix model for a spatially distributed fish population in a watershed, and we investigate how location and other characteristics of a single movement barrier impact the asymptotic growth rate of the population. We find that while population growth rate often decreases with the introduction of a movement obstacle, it may also increase due to a "retention effect". Furthermore, obstacle mortality greatly affects population growth rate. In practice, different connectivity indices are used to predict population effects of migration barriers, but the relation of these indices to population growth rates in demographic models is often unclear. When comparing our results with the Dendritic Connectivity Index, we see that the index cannot capture the retention effect nor the influences of obstacle mortality. We argue that structural indices cannot entirely replace more detailed demographic models to understand questions of persistence and extinction. We advocate the development of novel functional indices and characteristics.

Keywords

Fish population, watershed, migration barrier, connectivity index, population growth rate

1 Introduction

Freshwater ecosystems are in severe peril worldwide due to habitat degradation and fragmentation. Unlike terrestrial habitats, river systems are particularly susceptible to fragmentation due to their dendritic network geometry, i.e. the hierarchical arrangement of branching stream reaches [1, 2]. Populations inhabiting these dendritic networks have, by nature and topology, limited access to large parts of the watershed, even in the absence of any disconnecting structures [3–5].

Human development often adds disconnecting structures (e.g. dams or culverts) for transportation, energy generation, protection, or leisure. Nowadays, only a third of the world's largest rivers remain free-flowing from source to mouth [6]. While these developments have clear benefits to humans, they also have obvious effects on the geomorphological aspects of rivers as well as on their fauna and flora. For example, dams regulate flow speed and water level, modify sediment and nutrient supply in reaches upstream and downstream, and can pose an insurmountable obstacle for migrating fish, diadromous and potadromous [7]. The effects of damming on fish populations have been well documented, either through changes in patch occupancy [8], asymptotic growth rate [9, 10], extinction risk [1, 3, 11] or population demogenetics [3].

Great efforts are underway to understand the effects of human-imposed dispersal barriers on the fate of biological populations. Network-theoretic approaches are being used increas-

ingly to evaluate and explore the effects of obstacles on ecosystem function in terrestrial and aquatic ecosystems [12]. Resulting insights can be applied in development planning and conservation prioritization. A key focus is on *habitat connectivity* as an attempt to capture the existence and importance of dispersal pathways in spatially distributed habitat patches. Many indices exist, on the landscape level or patch level, to measure in some sense how connected one individual patch or the entire network of patches are [4, 12–17]. The intuitive common idea being promoted is that a higher connectivity index represents better conditions for the respective populations [4, 5, 15].

A recent review devoted specifically to connectivity metrics for watersheds explores the relationships between eight different connectivity metrics, some of which are global (a single metric for a watershed) some are local (a value for each patch in the watershed) [18]. They found that so-called "path-counting" metrics represent "an organism's ability to disperse throughout the watershed" and may therefore be used to assess the impact of barriers. All the metrics studied in [18] assume that each barrier is completely impassable, dividing a habitat in two disconnected sub-habitats. Many barriers, however, are somewhat passable [19]. A relatively recent path-counting metric that allows for partial passability is the *dendritic connectivity index* (DCI) [4]. Clearly, passability is species specific, and so the definition of this index was specialized [4] depending on the life history of the fish species under consideration: DCI_P for potadromous (migrating within freshwater) and DCI_D diadromous (migrating between fresh water and sea) species. In either case, DCI is a network-scale measure of connectivity, specific to freshwater systems, simple enough to examine the effects and interactions of multiple barriers and their permeability, i.e. the movement probability of individuals between sections connected by the obstacles [4, 16, 20].

What is missing for DCI is a detailed study of the relationship between the value of the index and meaningful population-level characteristics, such as persistence conditions or mean extinction times. In fact, such studies are largely missing for many indices applied to connectivity [12] and other areas, e.g. biodiversity [21]. A first step in uncovering the relation between structural connectivity (as measured by most indices) and functional connectivity (as expressed by population characteristics) was to compare the results of a movement-only, patch-occupancy simulation model with DCI [8]. In the present work, we include population growth and survival as well as a more detailed description of separate aspects of movement barriers into a spatially explicit patch model. We compare how movement barriers affect population persistence conditions, as measured by the long-term population growth rate, and DCI for different network geometries. Incorporating demographics to understand population persistence is obviously necessary, since persistence requires that an individual, on average, replaces itself over its lifetime [22]. Movement barriers in rivers not only inhibit migration, they often also are a significant source of direct mortality (e.g. power-generating dams) or indirect stress and increased energy expenditure of fish (e.g. fish ladders) that needs to be considered to understand demographic outcomes.

Our model is a strategic, generation-based model for a hypothetical potadromous fish species in randomly generated watersheds. We represent reaches of the river or stream as patches in our model and project changes in the density of the population on each patch

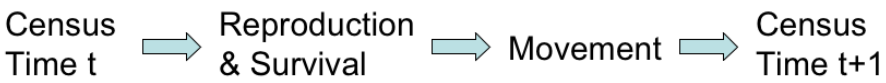

Figure 1: The life cycle of the model organism. We census the population after movement and before reproduction and survival.

through demographics and migration forward in time. The dominant eigenvalue of the resulting projection matrix then represents the asymptotic population growth rate; if it is greater than unity, then the population persists, if not, it becomes extinct [23]. Similar matrix models were previously applied to fish populations by various authors [9, 10, 24, 25] but with somewhat different goals. We give a detailed description of the model, the aspects of a barrier, and the generation of the network structure in the next section. We then explore in detail how the location of a single obstacle affects the population growth rate, and whether and to what extent this change can be predicted by a corresponding change in DCI. We find that only certain aspects of functional connectivity can be captured by DCI and argue that other known structural metrics are unlikely to capture those details. We advocate that more mechanistic models are necessary to predict the ecological impact of dispersal barriers in watersheds or to prioritize conservation efforts.

2 Model and Methods

We model the spatial population dynamics of a potadromous fish species in a dendritic river network. We represent each reach in the network as a patch of primary habitat where individuals reproduce and survive (see below). Direct connections between reaches are migration links between patches. The population density in each patch changes from year to year as individuals first reproduce locally and then migrate between patches. In a network of n patches, we denote the population density in patch i and year t as $N_{i,t}$. These densities change from year to year due to population dynamics and migration (see Figure 1) according to the equation

$$N_{i,t+1} = \sum_{j}^{n} c_{i,j} g_j(N_{j,t}) N_{j,t}. \tag{1}$$

Per capita survival and offspring production may depend on population density and patch attributes and are denoted by $g_j(N_{j,t})$. The probability that an individual, initially located in reach j resides in patch i at the end of the season is denoted by $c_{i,j}$.

Under the assumption that there is no Allee effect [26], we linearize model (1) at low density to evaluate conditions for population persistence. We denote $g_j'(0) = r_j + s_j$, where r_j is the per-capita number of offspring produced at site j and s_j is the survival probability in that reach. The linearized model then becomes

$$N_{i,t+1} = \sum_{j}^{n} c_{i,j}(r_j + s_j)N_{j,t}. \tag{2}$$

Using the (column) vector $\mathbf{N}(t) = (N_{1,t}, \ldots, N_{n,t})^T$ of population densities in each patch, we can write the linear model conveniently in matrix form as

$$\mathbf{N}(t+1) = B\mathbf{N}(t) \tag{3}$$

where the projection matrix B is given by the product of the migration matrix $C = (c_{i,j})$ and the diagonal matrices for production and survival, i.e.

$$B = C[R + S] \quad \text{with} \quad R = \text{diag}(r_j), \quad S = \text{diag}(s_j). \tag{4}$$

Before we can derive the exact form of the migration matrix, we explain in more detail the representation of reaches in the watershed.

2.1 Graphs of dendritic networks

A river network can be represented as a spatial graph [27]. We represent a river reach, or a suitable part thereof, by a node that is attributed with physical and ecological characteristics corresponding to the reach. A connection between reaches corresponds to an edge in the graph (Figure 2). While reaches 1, 2, 4, 5 in this Figure are delineated by confluences, reaches 3 and 6 could be separated by a physical disruption, such as a waterfall or culvert. Alternatively, the separation between 3 and 6 could be introduced to make all patches correspond to roughly similar length sections of the river network. The dendritic structure of the river network results in a tree graph [1, 2, 11]. We choose the river mouth to be the root of the tree.

The geometry of a (dendritic) network with n nodes is encapsulated in the adjacency matrix, A, a binary $n \times n$ matrix. This matrix is the fundamental structure of the migration matrix. Entries a_{ij} equal to one indicate a connection between reaches i and j, whereas zero entries indicate that reaches i and j are not adjacent, see Figure 2. By convention, diagonal elements are zero.

We consider the situation where each reach is adjacent to at most two upstream reaches. The simplest network then is a linear network, where each reach connects to exactly one upstream reach, the most complex is the complete binary network with exactly two. We generate intermediate geometries numerically according to a stochastic branching process [3]. Starting from the root, the tree graph is generated using a probability triplet, indicating the probabilities of a reach connecting to zero, one or two reaches upstream. The number of reaches and the height of the graph can vary. For example, networks in Figure 2(b) and Figure 3(a) can both be generated with the triplet $(0, 0.5, 0.5)$ and height 3, but have a different number of reaches. We constrain the stochastic generation process to triplets of the form $(0, \beta, 1 - \beta)$, where β is the probability of having one reach upstream. When $\beta = 0$, the complete binary tree is generated, and when $\beta = 1$, we get the linear network. We then

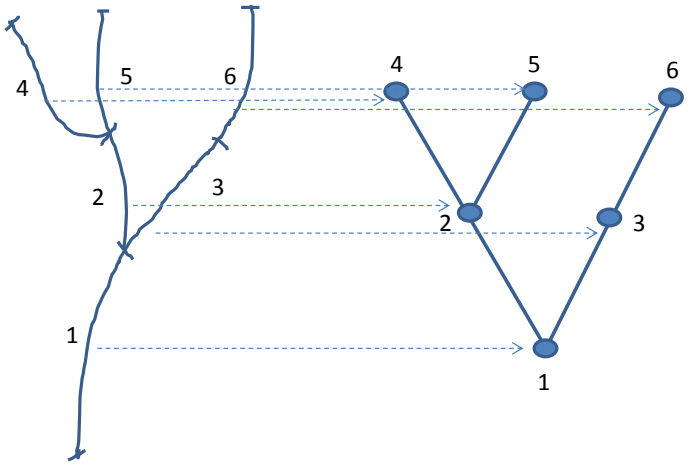

$$A = \begin{pmatrix} 0 & 1 & 1 & 0 & 0 & 0 \\ 1 & 0 & 0 & 1 & 1 & 0 \\ 1 & 0 & 0 & 0 & 0 & 1 \\ 0 & 1 & 0 & 0 & 0 & 0 \\ 0 & 1 & 0 & 0 & 0 & 0 \\ 0 & 0 & 1 & 0 & 0 & 0 \end{pmatrix}$$

(a) (b) (c)

Figure 2: (a) A river network with 6 reaches. (b) Spatial graph representation of the river network. (c) The corresponding adjacency matrix.

generate a graph until it contains a given height or number of nodes. We understand the simpler situations such as in Figures 2 and 3 as "modules" of a larger network, similar to the decomposition of foodwebs into building blocks [28].

2.2 The migration matrix C – no obstacles

As a first step to defining the migration matrix C, we model between-patch movement in the absence of obstacles. We distinguish between upstream and downstream movement. We obtain the "uninhibited movement matrix" M from the adjacency matrix A by multiplying each nonzero element in A with the appropriate downstream ($d_{i,j},\ i < j$) or upstream ($u_{i,j},\ i > j$) movement probability. The column sums in matrix M are bounded by unity. Matrix M for the simple 4-reaches network in Figure 3 is given by

$$M = \begin{pmatrix} 0 & d_{1,2} & 0 & 0 \\ u_{2,1} & 0 & d_{2,3} & d_{2,4} \\ 0 & u_{3,2} & 0 & 0 \\ 0 & u_{4,2} & 0 & 0 \end{pmatrix}. \tag{5}$$

To obtain migration matrix C from matrix M, we need to add the diagonal elements that represent the probability that an individual does not move. In the absence of mortality, C is a stochastic matrix, i.e., the column sums of C are one. We only make an exception to this rule in the first column where we consider two scenarios. In the "closed network"-scenario individuals do not leave the river network at the mouth, and the column sum in the first column is one. In the "open network"-scenario, individuals will leave the system through the river mouth, and the $(1,1)$-entry of C is zero. We regard these two cases as extreme

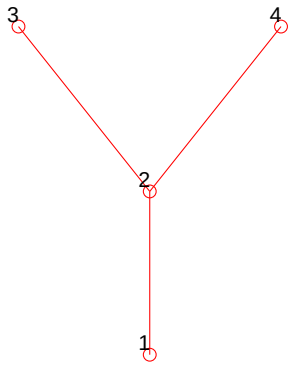

(a)

$$A = \begin{pmatrix} 0 & 1 & 0 & 0 \\ 1 & 0 & 1 & 1 \\ 0 & 1 & 0 & 0 \\ 0 & 1 & 0 & 0 \end{pmatrix}$$

(b)

Figure 3: (a) A dendritic graph representing a river network of 4 reaches, (b) The corresponding adjacency matrix to the graph on the left

cases; for a partially open network, one can choose any probability between the two cases. Hence the migration matrix C in the absence of migration obstacles is given by

$$C = \begin{pmatrix} * & d_{1,2} & 0 & 0 \\ u_{2,1} & 1 - d_{1,2} - u_{3,2} - u_{4,2} & d_{2,3} & d_{2,4} \\ 0 & u_{3,2} & 1 - d_{2,3} & 0 \\ 0 & u_{4,2} & 0 & 1 - d_{2,4} \end{pmatrix} \tag{6}$$

where

$$* = \begin{cases} 0 & \text{if the system is open} \\ 1 - u_{2,1} & \text{if the system is closed} \end{cases} \tag{7}$$

With this definition, individuals effectively move at most one patch up- or downstream per year. For more mobile species, one can use $\widetilde{C} = C^k$ for some $k > 1$ as the migration matrix. These two scenarios correspond to movement based on local versus global knowledge [8].

2.3 The migration matrix C – with obstacles

An obstacle or barrier, such as a dam, a culvert, or a hydropower station, can modify the probability of upstream and downstream movement between reaches, and it can also induce mortality in the movement process. To each obstacle we assign an upstream and downstream passability value (α_u and α_d, respectively, $0 \leq \alpha_u, \alpha_d \leq 1$), representing the proportion of individuals that can successfully cross the obstacle in the corresponding direction [4]. If the passability value is 1, then the obstacle is completely passable in the given direction. Contrarily, when the passability value is 0, the obstacle does not allow any transit through it. We represent the passability values of all obstacles in a passability matrix O. Matrix O is obtained from the adjacency matrix A by replacing the corresponding nonzero entries

with the passability values. For notational convenience, we set the diagonal elements to one, i.e. $o_{i,i} = 1$. Accordingly, the probability of failing to cross an obstacle is $1 - o_{i,j}$ for all nonzero entries $o_{i,j}$. We define the failure of passing matrix as $\tilde{O}$. If, for example, an obstacle is placed between reaches 2 and 3 in the simple network in Figure 3, then these matrices are given by

$$O = \begin{pmatrix} 1 & 1 & 0 & 0 \\ 1 & 1 & \alpha_d & 1 \\ 0 & \alpha_u & 1 & 0 \\ 0 & 1 & 0 & 1 \end{pmatrix} \quad \text{and} \quad \tilde{O} = \begin{pmatrix} 0 & 0 & 0 & 0 \\ 0 & 0 & 1-\alpha_d & 0 \\ 0 & 1-\alpha_u & 0 & 0 \\ 0 & 0 & 0 & 0 \end{pmatrix}. \tag{8}$$

Individuals who fail to cross an obstacle either stay in the reach from which they attempted to leave or die. Mortality can arise from the structure itself (e.g. fish being sucked into turbines at power-generating dams) or from increased energy expenditure in the attempt to cross the obstacle. We collect these mortality values in a matrix E where entry $e_{i,j}$ is the probability that an individual will die in the attempt to cross the obstacle from reach j to reach i. Mortality may depend on direction. Again, for a hypothetical obstacle between reaches 2 and 3 in the simple network in Figure 3, matrix E is given by

$$E = \begin{pmatrix} 0 & 0 & 0 & 0 \\ 0 & 0 & e_d & 0 \\ 0 & e_u & 0 & 0 \\ 0 & 0 & 0 & 0 \end{pmatrix}. \tag{9}$$

The resulting migration matrix C arises from careful bookkeeping of individual movement. For example, an individual can be in patch 2 if it moved upstream from patch 1 (with probability $u_{2,1}$), or downstream from patch 4 (with probability $d_{2,4}$), or successfully passed the obstacle downstream from patch 3 (with probability $\alpha_d d_{2,3}$), or it was already in patch 2 and stayed (with probability $1-d_{1,2}-\alpha_u u_{3,2}-(1-\alpha_u)e_u u_{3,2}-u_{4,2}$). The latter probability is obtained by considering individuals that did not move downstream to patch 1 nor upstream to patch 4, nor successfully got to patch 3 upstream, nor died while trying to get to patch 3 upstream. Based on these consideration, matrix C (for a closed network) is given by

$$C = \begin{pmatrix} 1-u_{2,1} & d_{1,2} & 0 & 0 \\ u_{2,1} & 1-d_{1,2}-\alpha_u u_{3,2}-(1-\alpha_u)e_u u_{3,2}-u_{4,2} & \alpha_d d_{2,3} & d_{2,4} \\ 0 & \alpha_u u_{3,2} & 1-\alpha_d d_{2,3}-(1-\alpha_d)e_d d_{2,3} & 0 \\ 0 & u_{4,2} & 0 & 1-d_{2,4} \end{pmatrix}. \tag{10}$$

In terms of matrices $\Delta_1 = \tilde{O} \circ E \circ M$ and $\Delta_2 = O \circ M$, the migration matrix C can be conveniently written as

$$C = \Delta_1 + I - \text{diag}\left(\sum_i (\Delta_1 + \Delta_2)_{i,j}\right). \tag{11}$$

Here, $\circ$ denotes the Hadamard product of entrywise multiplication of matrices.

The extension of this procedure to several obstacles is straight forward. In this work, we concentrate on the effect of adding (or removing) a single obstacle from a network.

2.4 Defining connectivity

There is a great variety of different indices to measure connectivity in general networks [12, 13]. Many indices are purely topological in that they consider only the existence of connections between patches. Those that include, in addition, patch attributes and at least to some extent also distances, are typically much more informative [17]. For a dendritic network, such indices tend to be too coarse. While terrestrial networks often contain many different paths between any two patches, there is only a single unique path connecting any two patches in a dendritic network. As a result, breaking any connection in a connected dendritic network will lead to two disconnected sub-networks, whereas a connected terrestrial ecological network often remains connected even if a connection is removed. Empirically more relevant is the observation that many barriers in watersheds are actually not complete impassable [19].

A relatively recent measure, developed specifically for watersheds and dendritic networks is the "dendritic connectivity index" DCI [4]. It is based on the probability that a fish can move between any two given points in the network. Hence, the index depends on movement behavior and includes the "strength" of a connection by looking at probabilities of movement. The idea behind this index for a potadromous species is the following. Suppose that there are K barriers, dividing a watershed into D sections. Denote the length of section j by L_j and the upstream and downstream passability of the m^{th} barrier by $\alpha_{u,m}$ and $\alpha_{d,m}$, respectively. For any two sections of the watershed, one multiplies the passabilities of all barriers that lie between these two sections as the total probability of passage between these two sections. The dendritic connectivity index for potadromous species is then given by

$$DCI_P = \sum_{i=1}^{D}\sum_{j=1}^{D}\left(\prod_{m=1}^{K}\alpha_{u,m}\alpha_{d,m}\right)\frac{L_i}{L}\frac{L_j}{L} \times 100, \tag{12}$$

where L denotes the total length of the system, see equations (2) and (3) in [4]. The value of $K = K(i, j)$ depends on the two sections chosen.

In the absence of obstacles to fish movement, DCI_P is equal to 100. Adding obstacles to the network decreases the connectivity index, unless obstacles are completely passable [4]. Other measures of habitat quality can replace length. In what follows, we scale the DCI_P so that the maximum corresponding value is 1.

2.5 Relating network connectivity to population persistence

To evaluate the effects of migration obstacles on the persistence of fish populations, we compare and contrast how the population growth rate of model (2) and the DCI_P vary with changes in obstacle location and other attributes (e.g. passability and mortality). The population growth rate is the dominant eigenvalue λ of the projection matrix B. When λ is

greater than unity, then the population will grow, otherwise, it will decline. An alternative measure for population persistence is the reproduction number R_0 that, for certain life-cycle models, can be obtained in a relatively simple and elegant way by graph-reduction arguments [29]. This method does not simplify calculations in our case, and the dominant eigenvalue gives additional information about time scales.

As the model contains many parameters, we consider certain strategically chosen simplified scenarios. In the baseline scenario, all reaches are of the same quality. However, river reaches generally differ in many aspects, such as river bed quality, primary producers, or temperature, which may enhance or reduce growth rates and/or survival probabilities for the fish population. For example, a typical classification distinguishes between warm-water loving species and cold-water loving species. Since water temperature generally increases downstream, the former do better downstream and the latter upstream. As two alternative scenarios, we therefore choose one where growth conditions are better upstream and one where they are better downstream.

For simplicity, we assume that all reaches located within the same level k (i.e. distance from the root of the tree or mouth of the river) are identical with respect to habitat quality.

In our dynamic model, we express habitat quality through parameters r_j, where higher values correspond to better conditions. For the calculation of the DCI_P, we express habitat quality as the length l_j of reach j. The length of a segment L_j is then the combined length of all reaches within a segment. For simplicity, we assume that all reaches located within the same level k are identical with respect to habitat quality. In particular, we write r_k and l_k for the habitat quality or length of any reach with distance $k-1$ from the root. To simplify matters even more, we introduce a single parameter that indicates how habitat quality changes between levels. We assume that the relative changes are constant between levels and write

$$\rho = \frac{r_{k+1}}{r_k} = \frac{l_{k+1}}{l_k}. \tag{13}$$

The base-line scenario of equal habitat quality everywhere is given by $\rho = 1$. When conditions are better upstream, we have $\rho > 1$ and when they are better downstream then $\rho < 1$. We then compare the qualitative behavior of λ and DCI_P in these three scenarios.

3 Results

We examine how the growth rate (λ) and the dendritic connectivity index (DCI_P) depend on the location of an obstacle in the system. We consider the three scenarios of a homogeneous network ($\rho = 1$), a network with better upstream conditions ($\rho > 1$) and a network where downstream conditions are better ($\rho < 1$). We investigate the influence of passability and mortality and river mouth conditions in each case.

We refer to the location of a barrier according to the level or height of the tree at which the obstacle is placed. In a linear network, there is only a single connection between any two levels, hence, there is a unique location for the barrier. In a complete binary tree, there are

2^k possible locations to place an obstacle at level k. By the symmetry of the complete binary tree, the growth rate and DCI_P will depend only on the level. In a randomly generated tree, there can be up to 2^k obstacle locations at level k. For each level k and probability triplet $(0, \beta, 1-\beta)$, we generated 50 networks of height 7 and recorded the average values of λ and DCI_P.

We begin with the effects of obstacle location on population growth rate. We choose the growth rate at the river mouth to equal $r_1 = 1.64$ and the survival probability to $s_j = 0.5$. We assumed that the probability of leaving a patch is 0.5 and that dispersal is unbiased, i.e. $d_{i,j} = u_{i,j} = 0.25$.

3.1 Homogeneous reaches ($\rho = 1$)

In a closed river system, when all reaches are of the same quality and there is no mortality associated with the barrier, the barrier or its location does not affect the population growth rate. Even though movement is affected, λ remains constant since conditions are the same everywhere.

If there is mortality at the obstacle ($e \neq 0$), the growth rate is lower than without the obstacle, and the actual value depends on location, see Figure 4, left panel. The lowest value of λ for the complete binary tree ($\beta = 0$) occurs when the obstacle is located at the first (i.e. lowest) level. For the linear network ($\beta = 1$), the lowest value of λ occurs when the barrier is in the middle of the network. (We confirmed this result numerically for linear networks of various sizes, only the network of height 7 is shown.) Thus, in both cases, the negative impact of the obstacle is largest when it separates the network into two evenly-sized parts. For randomly generated networks ($0 < \beta < 1$), the averaged population growth rate is in between the linear and the complete binary case. The obstacle location that has the most negative impact on growth rate depends on mortality and β. Increasing passability (α) will increase the growth rate since fewer individuals face mortality (plot not shown).

In an open network, an obstacle without mortality increases the growth rate for any location, and the highest growth rate occurs when the obstacle is located in the lowest level, independent of network topology, see Figure 4, middle panel. The obstacle prevents individuals from dispersing to the river mouth where they would leave the network. We refer to this mechanism as the "retention effect" of the obstacle. The effect is larger when the obstacle is placed close to the mouth. As the passability of the obstacle increases, λ decreases. As before, the averaged growth rate of randomly generated networks is bounded by the growth rate of the linear and the complete binary topology.

When an obstacle with mortality is placed into an open network, the resulting growth rate depends on the net effect between mortality (reducing λ) and retention (increasing λ), see Figure 4, right panel. When mortality is low enough, the retention effect is stronger when the obstacle is placed near the mouth. When the obstacle is placed higher up in the network, individuals face mortality in both directions: downstream from the mouth, upstream from the obstacle. This effect is particularly strong in the linear topology and is diluted in the complete binary case. The growth rate for random networks is, again, in between the two extremes. When obstacle mortality is high, the retention effect is too weak, and the growth

rate will always be below the default case without obstacles (plot not shown).

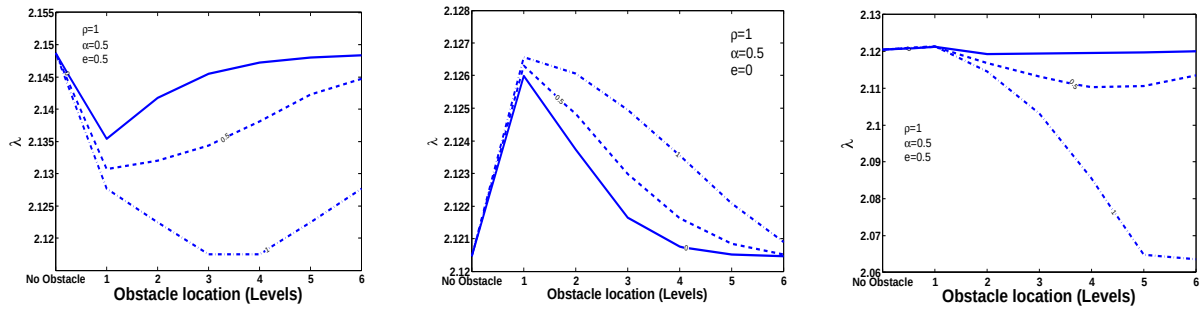

(a) (b) (c)

Figure 4: Relationship between the asymptotic growth rate (λ) and obstacle location in a network for the linear ($\beta = 1$, dash-dot), complete binary ($\beta = 0$, solid) and random ($\beta = 0.5$, dashed) topology. **Panel (a):** obstacle mortality in a closed system has the most negative effect when the network is partitioned into two similar-sized parts ($e = 0.5$). **Panel (b):** an obstacle without mortality induces the retention effect, which is strongest when the obstacle is near the mouth ($e = 0$). **Panel (c):** The net effect of retention and mortality in an open network ($e = 0.5$). In all cases, passability is $\alpha = 0.5$.

3.2 Reach quality increases downstream ($\rho < 1$)

When downstream reaches provide better habitat, an obstacle without mortality will increase the population growth rate in any network topology, even in a closed network. The effect is the strongest when the obstacle is at the lowest level, see Figure 5, top left. Similar to the retention effect, an obstacle at low levels traps individuals in the reaches of high quality and thereby increases λ. In fact, with the chosen parameters, the growth rate in patches of level 4 and up is less than unity. Only in the highest level do we have a net loss as $r_k + s_k < 1$. As the obstacle is moved upstream or passability is increased, the trapping effect is diminished and λ decreases.

When the obstacle engenders high enough fish mortality, we get completely opposite results (Figure 5, top right). The growth rate is lower than without obstacle, and the lowest value occurs when the obstacle is at the lowest level. As more individuals will be located in the downstream patches, they are more prone to obstacle induced mortality if they disperse. In this case, the more passable the obstacle, the higher the λ, because fewer individuals fail to successfully cross the obstacle and risk death. As we can expect, λ decreases with higher obstacle induced mortality.

When $\rho < 1$ and the system is open, the best growth conditions are downstream where the risk of loss is also the highest. An obstacle without mortality in the first level prevents individuals from reaching the best habitat and also from leaving the system. For intermediate passability values, the latter effect is stronger than the former, i.e. the growth rate is higher with the obstacle than without, see Figure 5, bottom left). The effect is much weaker when

the obstacle is placed higher upstream. The reason is that individuals above the obstacle are in low growth quality habitats, while those below the obstacle face loss downstream. Similar to the closed network case, a less passable obstacle results in a higher λ, preventing more individuals from dispersing to the river mouth.

Finally, if an obstacle in an open network induces fish mortality ($e \neq 0$), the retention effect of the obstacle in the first level is still present for low enough passability and mortality, and for any network topology, see Figure 5, bottom right. When the obstacle is located further from the mouth, the retention effect is weaker than the negative effects of mortality and open network. For the complete binary tree ($\beta = 0$), the lowest value of λ occurs at level 2, whereas it occurs at level 3 for the linear network ($\beta = 1$). Through simulations on larger networks, we found that these particular locations are independent of network height (plots not shown). Aside from the first level location, λ increases with increasing passability. In general, λ decreases when obstacle mortality is higher.

3.3 Reach quality increases upstream ($\rho > 1$)

For some fish species, the colder upstream reaches provide better habitat and maybe even a refuge against competition [30]. In this case, the difference between open and closed networks with respect to growth rate and obstacle location is marginal. With no obstacle-induced fish mortality ($e = 0$), λ increases as the obstacle is placed in higher levels, since individuals are trapped in patches of high quality. However, only for the linear topology ($\beta = 1$) does the highest growth rate occur with the obstacle in the highest level. For all non-linear topologies ($\beta < 1$), λ is the highest when the obstacle is in the second last level (see Figure 6, left panel). In the linear network, there is only one highest-quality patch, and with the obstacle just below it, individuals are trapped in the best growth conditions. In other topologies, an obstacle in the highest level traps individuals only in one of several best-quality patches. Individuals will still move away from all other high-quality patches, thereby reducing overall growth rate. An obstacle placed in the downstream levels has virtually no effect on λ since it is not harmful, but at the same time it locks individuals in low-growth conditions, obstructing them from moving to better habitats. Furthermore, as we have already seen in the other cases, λ is higher when the passability of the obstacle is lower, impeding more individuals from leaving the higher quality patches.

When the obstacle induces fish mortality ($e \neq 0$), then the positive trapping effect disappears. In non-linear topologies, the decrease in λ is very small and noticeable only for upstream locations. For the linear network however, λ drastically decreases as the obstacle location is moved upstream (see Figure 6, right panel). Essentially, the single best-quality patch carries a high mortality risk from the obstacle and loses its beneficial effect on population growth. As before with mortality, λ is higher for high passability values, allowing more individuals to safely traverse the obstacle. Clearly, increased mortality decreases λ in the linear network. For non-linear topologies, the sensitivity of λ with respect to mortality is marginal since there are so many high-quality patches that support population growth.

For an open network, the loss at the river mouth has no qualitative effect on these results, even when the obstacle location is in level 1. The retention effect disappears, and only the

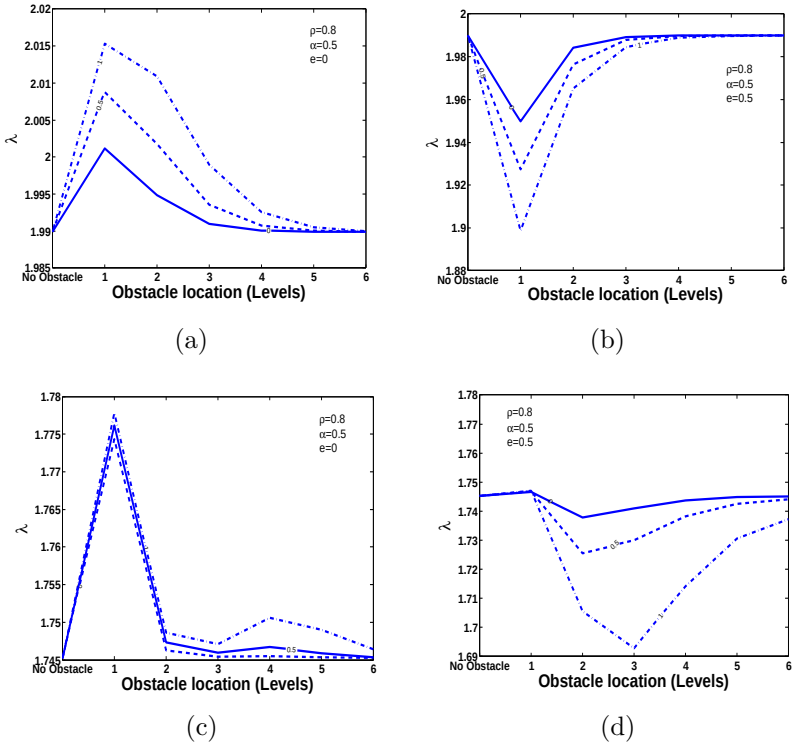

Figure 5: Relationship between the asymptotic growth rate (λ) and obstacle location in a network when downstream reaches are of higher quality. **Panel (a):** In a closed network, λ increases as a barrier traps individuals in the high-quality reach downstream ($e = 0$). **Panel (b):** With high enough obstacle mortality, the trapping effect disappears ($e = 0.5$). **Panel (c):** The trapping effect is also present in an open network ($e = 0$). **Panel (d):** Obstacle mortality in an open network can lead to mixed results: an obstacle in the first level is beneficial, in the second ($\beta = 0$) or third ($\beta = 1$) level it is the most devastating for population growth. Parameter values are $\rho = 0.8$ and $\alpha = 0.5$. Other parameters are as in the previous figure.

better growth conditions control the results.

3.4 Connectivity Index DCI_P

While the dendritic connectivity index (DCI_P) measures how barriers inhibit fish movement between sections in a watershed, it does not account for demographic dynamics, specifically not for mortality related to obstacles. It does, however, account for some aspect of habitat quality by considering length of a section, where longer sections correspond to higher quality. We calculated the DCI_P as a function of obstacle location in the three different settings of (a) homogeneous habitat quality ($\rho = 1$), (b) decreasing habitat quality upstream ($\rho < 1$), and (c) increasing habitat quality upstream ($\rho > 1$).

The greatest reduction in DCI_P arises when the obstacle separates the network into

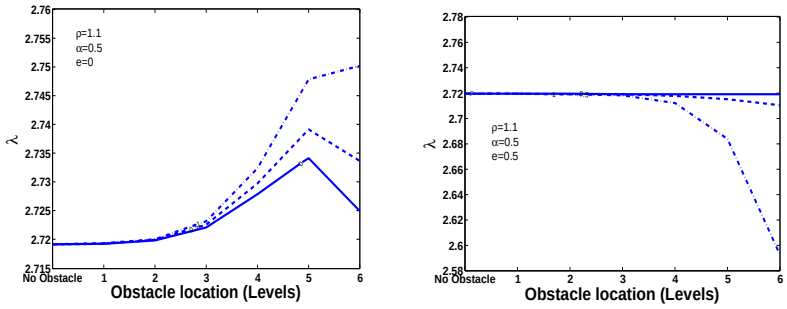

(a) (b)

Figure 6: Relationship between the asymptotic growth rate (λ) and the obstacle location in a network when upstream reaches are of higher quality. **Panel (a):** When there is no obstacle mortality, λ increases with level, except the highest level for non-linear topologies. **Panel (b):** When there is mortality, λ decreases with level, most strongly in the linear case and imperceptibly for the complete binary network. Parameters and line styles are as in previous figures.

two sections of (roughly) equal lengths (or quality), see Figure 7. For the complete binary network ($\beta = 0$), this location is at the lowest level, for the linear network ($\beta = 1$), it is at some intermediate level. When the habitat is homogeneous, the location is the middle level, when habitat quality is better downstream (upstream) the location is shifted downwards (upwards). The average DCI_P for 50 randomly generated networks shows an intermediate behavior between the two extreme cases.

Clearly, DCI_P decreases as the obstacle passability decreases. Obviously, the effects of open versus closed networks or of obstacle mortality cannot be evaluated with this index.

4 Discussion and conclusions

As more and more network-theoretic approaches are being employed to study the effects of movement barriers and habitat degradation on ecosystem function, the great challenge becomes "to determine how the connectivity structure of habitat networks constrains and enables ecological and evolutionary processes at various levels of biological organization" [12]. With this study, we contribute to this endeavor a comparison between two ecosystem-scale measures, namely (i) the long-term growth rate (λ) of a population dynamics model, and (ii) the dendritic connectivity index (DCI_P). More specifically, we evaluate the effect of the location of a single movement barrier in a watershed on these two quantities. The three most important insights from the population dynamics model are (i) that the effects in a randomly generated network are in some sense bounded by the effect in a linear and a complete binary network of the same height; (ii) that barriers can be beneficial to a population through a retention or trapping effect; and (iii) that mortality at an obstacle is the determining factor of the negative effects of the obstacle on population growth. The DCI_P can capture

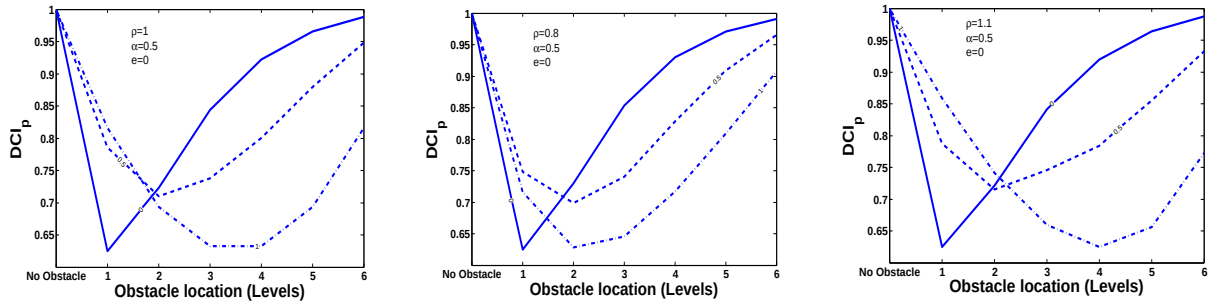

(a) (b) (c)

Figure 7: Relationship between the dendritic connectivity index DCI_P and the obstacle location in a network with different distribution of habitat quality. **Panel (a):** Homogeneous habitat ($\rho = 1$). **Panel (b):** Habitat quality increases downstream ($\rho = 0.8 < 1$). **Panel (c):** Habitat quality increases upstream ($\rho = 1.1 > 1$). In the absence of any obstacle, $DCI_P = 1$. Passability parameters are identical for the upstream and downstream direction ($\alpha = 0.5$).

these effects only to a certain (limited) degree. The relative size of the effects depends on parameter values, and a thorough sensitivity analysis will be required when empirical data are available for any species. At this point, we only note that for the chosen parameters, the typical maximal increase in population growth rate is an order of magnitude smaller that the maximal decrease.

To guarantee population persistence, an individual has to at least replace itself within a lifetime. In networks, not only the connectivity but viable reproduction "multiplied" by connectivity is the crucial quantity [22]. The importance of "loops" (e.g. ways to return to a patch) in the network topology has been stressed for terrestrial systems [31] and marine systems [22]. In river networks, loops can exist – and a population can persist – only when individuals move up- *and* downstream [32, 33]. Accordingly, the location of a barrier will determine how many loops it affects and therefore, how important it is for the persistence of a population. Because the path structure in a dendritic network is simple, a barrier affects more loops when it is located near the "middle" of the network. For a linear network, this location is halfway, for a complete binary network, it is the root. When habitat quality is changes along a gradient, this "middle" location changes accordingly.

Previous studies with population dynamics models considered only a complete binary network of 15 patches, and modeled dams and channelization as complete removal of patches [9, 24]. Fish moved on a fast time-scale through the entire (available) network. By contrast, we explored random topologies and slow-moving individuals. For a closed network, we arrive at the same result as in [9, 24] that a dam at the lowest level in the network has the most devastating effect on population growth. This commonality indicates a generic effect, independent of modeling approach. Our results are much more general (by allowing intermediate passability and considering random topologies) and more detailed (including obstacle mortality). From the comparison of all these different scenarios, we speculate that

the size of the remaining fragments and the interaction between movement and mortality rather than the level of disturbance seems to be the driving force.

We chose a population dynamics framework where population persistence emerges from the interplay of reproduction and mortality. We argue that this approach is valid in relatively stable hydrological conditions. An alternative approach considers colonization-extinction dynamics in highly variable environments, such as desert streams [1]. The importance of fragment size has been explored in the resulting stochastic patch-occupancy models either with [1,11] or without [8] population dynamics. The size of fragments or the largest connected component is also often the focus for prioritization in dam removal [34–37].

In patch-occupancy models, barriers and fragmentation typically results in population decline. Most uses of connectivity indices assume that barriers and fragmentation have negative effects on populations. Our study is the first to tease apart the effects of movement limitation from obstacle mortality. For that reason, we found the retention or trapping effects that can alleviate the negative effects of an obstacle with mortality. This positive effect of limiting migration is one of four recently advocated by Rahel [38], others being protection against invasive species, against disease, and eliminating hybridization. All these effects could be tested in an extension of our modeling framework. Incorporating (some of) these effects into patch-occupancy models is a challenge for the future.

Our strategic model focused on the effect of movement barriers while considering individuals with a very simple life cycle (growth to maturity in one year). Some previous models considered two [25] or three [9, 24] life stages. In addition, we only considered the scenario that upstream and downstream movement probabilities are equal, whereas many real populations show upstream-biased movement of adults [8] and potentially downstream-biased movement of early life stages [39]. A relatively simple first step to include differential upstream and downstream mobility in our model is to consider dispersal of the young-of-the-year separately. We modify equation (2) to

$$N_{i,t+1} = \sum_{j}^{n} (c_{i,j} s_j N_{j,t} + \tilde{c}_{i,j} r_j N_{j,t}) \tag{14}$$

where $c_{i,j}$ are the movement probabilities of adults as before and $\tilde{c}_{i,j}$ are the movement probabilities of juveniles. We still assume maturation within one year. While a complete study of this model is beyond the scope of this paper, we illustrate one effect under the extreme assumption that juveniles drift downstream only ($d_{juv} = 1$ and $u_{juv} = 0$), and that obstacles are completely passable for juveniles in the downstream direction.

In an open network with homogeneous reach quality, an obstacle in the first level still increases growth rate through a retention effect (for adults). At higher levels, however, the obstacle has a negative effect, stronger for the linear topology and weaker for the complete binary case, see Figure 8. This negative effect is not present in the comparable scenario without juvenile movement bias (Figure 4, middle panel). However, the qualitative behavior compares closely with the scenario that habitat quality decreases upstream (Figure 5, bottom right). Indeed, this similarity is not so surprising considering that if juveniles leave their native reach and travel downstream, then the contribution of upstream reaches to reproduction

is reduced.

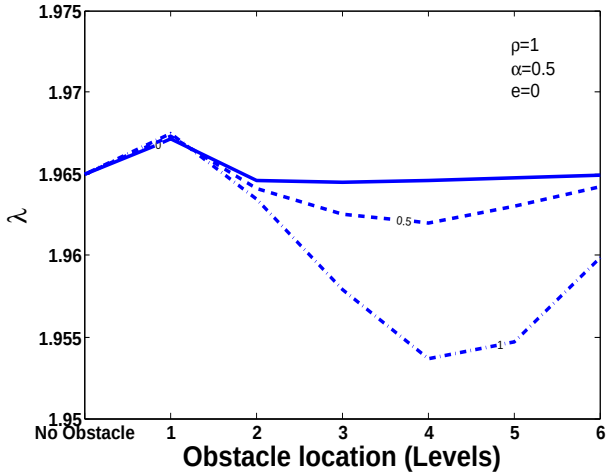

Figure 8: Relationship between the asymptotic growth rate (λ) and the obstacle location in an open network when juveniles exhibit a strong downstream bias ($d_{juv} = 1$ and $u_{juv} = 0$). Reaches are of equal quality ($\rho = 1$) and there is no obstacle mortality ($e = 0$). Passability for adults is $\alpha = 0.5$ and for juveniles $\alpha_{juv} = 1$.

The dendritic connectivity index (DCI_P) is a network-level index that measures not only the existence of a link between patches but also how hard it is to move between sections in a network with barriers [4]. Dendritic networks differ significantly from most terrestrial networks in that there is only one path between any two points in a dendritic network so that each new barrier will create a new section in the network. We saw that the DCI_P can capture certain effects of movement barriers on population dynamics but not all. When multiple life-stages involve multiple dispersal behaviors, a single network-level index is more unlikely to capture the resulting population dynamic effects. Patch-models for dispersal in the absence of growth and mortality, also found that DCI_P is only partly correlated with results [8]. While we used only DCI for comparison, it is clear that certain, potentially crucial, aspects of population growth cannot be captured by any structural indices. There is, therefore, a need to develop new indices for connectivity in dendritic networks and simultaneously systematically investigate their effect on population dynamic processes. This effect will strongly depend on migration characteristics and habitat requirements. Many indices have been developed for terrestrial networks [12], but even for those, the connection to population dynamics is not always clear. Some of these indices have been applied to river systems, for example the network-level "integral index of connectivity" (after which the DCI is modeled) and the measure of "betweenness-centrality" as an indicator of the importance of a given patch [15,16]. These measures could and should be compared to population dynamics indices such as reproductive value [23] or metapopulation capacity [40]. Probably more importantly, one needs to develop indices for the importance of a connection between patches in a similar fashion.

Real river systems often contain not only one but many migration barriers for fish. Our modeling approach readily extends to include several barriers, and exploring the combined effect is our ongoing research work. The principles of retention/trapping and mortality are combined and create an overall effect. Probably more crucially, some attributes of habitat quality are being transported downstream, an effect that is mostly absent from terrestrial ecosystems. Dams and culverts not only affect fish movement, they can also change the abiotic conditions in a stream or river by changing temperature, flow and other aspects. Including this downstream influence in modeling population dynamics in dendritic networks is another challenge for future theory.

Competing interests

We have no competing interests.

Authors' contributions

FL and AH conceived of the study; all three authors designed the study; YS carried out the analysis and drafted the manuscript; FL and AH critically edited the manuscript. All authors gave their final approval for publication.

Funding

YS is funded by an Alexander Graham Bell doctoral scholarship from the National Science and Engineering Research Council (NSERC); FL is funded by an NSERC Discovery Grant; AH is funded by NSF. All authors are grateful for funding by the Centre de Recherches Mathematiques (Montreal) of the workshop entitled "Sustainability of aquatic ecosystem networks" (2013, Fredericton, New Brunswick, Canada).

Appendix

The MATLAB files used for calculations and to create the plots in this work are available from the journal website. The executable main file is named `SingleObstacle_MainFile.m`; all other files are function files that feed into this main file.

References

[1] Fagan WF. Connectivity, fragmentation, and extinction risk in dendritic metapopulations. *Ecology*, 83(12):3243–3249, 2002.

[2] Grant EHC, Lowe WH, and Fagan WF. Living in the branches: population dynamics and ecological processes in dendritic networks. *Ecol. Lett.*, 10(2):165–175, 2007.

[3] Labonne J, Ravigné V, Parisi B, and Gaucherel C. Linking dendritic network structures to population demogenetics: the downside of connectivity. *Oikos*, 117(10):1479–1490, 2008.

[4] Cote D, Kehler DG, Bourne C, and Wiersma YF. A new measure of longitudinal connectivity for stream networks. *Landsc. Ecol.*, 24(1):101–113, 2009.

[5] Padgham M and Webb JA. Multiple structural modifications to dendritic ecological networks produce simple responses. *Ecol. Model.*, 221(21):2537–2545, 2010.

[6] World Wildlife Fund. Free-flowing rivers: Economic luxury or ecological necessity?, 2006.

[7] Cumming GS. The impact of low-head dams on fish species richness in Wisconsin, USA. *Ecol. Appl.*, 14(5):1495–1506, 2004.

[8] Perkin JS, Gido KB, Al-Taáni O, and Scoglio C. Simulating fish dispersal in stream networks fragmented by multiple road crossings. *Ecol. Model.*, 257:44–56, 2013.

[9] Charles S, Bravo de La Parra R, Mallet J-P, Persat H, and Auger P. Population dynamics modelling in an hierarchical arborescent river network: an attempt with salmo trutta. *Acta biotheor.*, 46(3):223–234, 1998.

[10] Charles S, Bravo de La Parra R, Mallet J-P, Persat H, and Auger P. Annual spawning migrations in modelling brown trout population dynamics inside an arborescent river network. *Ecol. Model.*, 133(1):15–31, 2000.

[11] Fagan WF, Grant EHC, Lynch H, and Unmack PJ. Riverine landscapes: ecology for an alternative geometry. *Spatial ecology*, pages 85–100. Chapman and Hall/CRC, 2009.

[12] Rayfield B, Fortin M-J, and Fall A. Connectivity for conservation: a framework to classify network measures. *Ecology*, 92(4):847–858, 2011.

[13] Calabrese JM and Fagan WF. A comparison-shopper's guide to connectivity metrics. *Front. Ecol. Environ.*, 2(10):529–536, 2004.

[14] Fischer J and Lindenmayer DB. Landscape modification and habitat fragmentation: a synthesis. *Glob. Ecol. Biogeogr.*, 16(3):265–280, 2007.

[15] Erős T, Schmera D, and Schick RS. Network thinking in riverscape conservation–a graph-based approach. *Biol. Conserv.*, 144(1):184–192, 2011.

[16] Erős T, Olden JD, Schick RS, Schmera D, and Fortin M-J. Characterizing connectivity relationships in freshwaters using patch-based graphs. *Landsc. Ecol.*, 27(2):303–317, 2012.

[17] Moilanen A and Nieminen M. Simple connectivity measures in spatial ecology. *Ecology*, 83(4):1131–1145, 2002.

[18] Malvadkar U, Scatena FN, and Leon M. A comparison of connectivity metrics on watersheds and implications for water management. *River Res. Appl.*, 31(2):256–267, 2015.

[19] Pépino M, Rodríguez MA, and Magnan P. Fish dispersal in fragmented landscapes: a modeling framework for quantifying the permeability of structural barriers. *Ecol. Appl.*, 22(5):1435–1445, 2012.

[20] Fullerton AH, Burnett KM, Steel EA, Flitcroft RL, Pess GR, Feist BE, Torgersen CE, Miller DJ, and Sanderson BL. Hydrological connectivity for riverine fish: measurement challenges and research opportunities. *Freshwater Biol.*, 55(11):2215–2237, 2010.

[21] McCarthy MA, Moore AL, Krauss J, Morgan JW, and Clements CF. Linking indices for biodiversity monitoring to extinction risk theory. *Conserv. Biol.*, 28(6):1575–1583, 2014.

[22] Hastings A and Botsford LW. Persistence of spatial populations depende on returning home. *Proc. Natl. Acad. Sci. USA*, 103(15):6067–6072, 2006.

[23] Caswell H. *Matrix population models: construction, analysis, and interpretation* . Second edition. Sinauer Associates, Sunderland, Massachusetts, USA, 2001.

[24] Charles S, Bravo de La Parra R, Mallet J-P, Persat H, and Auger P. A density dependent model describing *salmo trutta* population dynamics in an arborescent river network. effects of dams and channelling. *C. R. Acad. Sci. III Sci.*, 321(12):979–990, 1998.

[25] Goldberg EE, Lynch HJ, Neubert MG, and Fagan WF. Effects of branching spatial structure and life history on the asymptotic growth rate of a population. *Theor. Ecol.*, 3(3):137–152, 2010.

[26] Courchamp F, Berec L, and Gascoinge J. *Allee effects*. Oxford University Press, 2008.

[27] Dale MRT and Fortin M-J. From graphs to spatial graphs. *Annu. Rev. Ecol. Evol. Syst.*, 41(1):21, 2010.

[28] McCann K. *Food Webs*, volume 50 of *Monographs in Population Biology*. Princeton University Press, 2011.

[29] de Camino-Beck T and Lewis MA. A new method for calculating net reproductive rate from graph reduction with applications to the control of invasive species. *Bull. Math. Biol.*, 69:1341–1354, 2007.

[30] McMahon TE, Zale AV, Barrows FT, Selong JH, and Danehy RJ. Temperature and competition between bull trout and brook trout: A test of the elevation refuge hypothesis. *Trans. Am. Fish. Soc.*, 136:1313–1326, 2007.

[31] Artzy-Randrup Y and Stone L. Connectivity, cycles, and persistence thresholds in metapopulation networks. *PLoS Comp. Biol.*, 6(8):e1000876, 2010.

[32] Sarhad J, Carlson R, and Anderson KE. Population persistence in river networks. *J. Math. Biol.*, 69:401–448, 2014.

[33] Lutscher F, Pachepsky E, and Lewis MA. The effect of dispersal patterns on stream populations. *SIAM Appl. Math*, 65(4):1305–1327, 2005.

[34] Kuby MJ, Fagan WF, ReVelle CS, and Graf WL. A multiobjective optimization model for dam removal: An example trading off salmon passage with hydropower and water storage in the Willamette basin. *Adv. Water Res.*, 28(8):845–855, 2005.

[35] O'Hanley JR. Open rivers: Barrier removal planning and the restauration of free-flowing rivers. *J. Environ. Manage.*, 92:3112–3120, 2011.

[36] Januchowski-Hartley SR, McIntyre PB, Diebel M, Doran PJ, Infante DM, Joseph C, and Allan JD. Restoring aquatic ecosystem connectivity requires expanding inventories of both dams and road crossings. *Front. Ecol. Environ.*, 11(4):211–217, 2013.

[37] Branco P, Segurado P, Santos JM, and Ferreira MT. Prioritizing barrier removal to improve functional connectivity in rivers. *J. Appl. Ecol.*, 2014.

[38] Rahel FJ. Intentional fragmentation as a management strategy in aquatic systems. *BioScience*, 63(5):362–372, 2013.

[39] Morrissey MB and Ferguson MM. Individual variation in movement throughout the life cycle of a stream-dwelling salmonid fish. *Mol. Ecol.*, 20(2):235–248, 2011.

[40] Ovaskainen O and Hanski I. Spatially structured metapopulation models: Global and local assessment of metapopulation capacity. *Theor. Pop. Biol.*, 60:281–302, 2001.

Chapter 4

Downstream flow and upstream movement determine the value of a stream reach for potadromous fish populations

This paper is accepted for publication in Theoretical Ecology pending minor revisions [41]; Samia, Y., Lutscher, F. 2016. Downstream flow and upstream movement determine the value of a stream reach for potadromous fish populations. *Theoretical Ecology* (accepted pending minor revisions).

The contribution by each author is as follows. Both authors conceived and designed the study. The first author carried out the analysis and drafted the manuscript. The second author critically edited the manuscript. Both authors gave their final approval for publication.

Downstream flow and upstream movement determine the value of a stream reach for potadromous fish populations

Yasmine Samia
Department of Mathematics and Statistics
University of Ottawa
Ottawa, ON, K1N6N5, Canada

Frithjof Lutscher
Department of Mathematics and Statistics, and Department of Biology
University of Ottawa
Ottawa, ON, K1N6N5, Canada

Corresponding author:
Frithjof Lutscher. email: flutsche@uottawa.ca. fax: 1-613-562-5776

Abstract

Given that human activities often have negative impacts on biological populations, a common question is to find the location of greatest positive or least negative impact. Local habitat suitability is frequently used to evaluate viability of fish populations in river networks. Upper stream reaches are often undervalued, in particular when they are not navigable or do not contain commercially interesting fish. Since water flow transports certain local conditions downstream and individuals navigate river networks upstream and downstream, impacts of local perturbations can manifest elsewhere in the system, and overall effects of disturbances should be assessed on a network level. We study a model for a potadromous fish population in a system of connected stream reaches. We consider different geometries to evaluate how downstream transport and individual movement interact to determine the location of greatest and least impact of a single or two concurrent disturbances. Our results show how upper stream reaches can be highly significant for population persistence if downstream transport of abiotic conditions or upstream movement of individuals is strong.

1 Introduction

To understand how local alterations to river reaches affect the overall state of a river system in general, and its fish populations in particular, is of paramount importance for conservation efforts and land management (Stanfield *et al.*, 2014). While conservation principles and mathematical models for terrestrial systems of inter-connected habitat patches have been studied for a long time, river networks possess some characteristically distinct features that require novel approaches to understanding the processes and mechanisms that drive population dynamics (Lowe, 2006). The dendritic geometry of branching river reaches and the downstream transport of physical conditions by water are two of these features that need to be considered when evaluating the effects of local alterations on global ecosystem properties (Fagan, 2002; Goldberg *et al.*, 2010; Padgham and Webb, 2010). Our work aims to illuminate some of the complex interactions between abiotic conditions and population dynamic responses to local perturbations in river networks.

Different reaches in river networks have different functions that contribute to the overall well-being of the river system. While the main river channel and downstream reaches typically sustain a larger variety of species (Nilsson *et al.*, 1994), headwaters regulate floods and sedimentation and support downstream food chains (Meyer *et al.*, 2007; Bishop *et al.*, 2008; Thorp *et al.*, 2006). However, these upper reaches of a watershed are often overlooked when management efforts mainly focus on exploitable and navigable parts of the river (Stanfield *et al.*, 2014). We regularly become aware of the strong connection between upstream disturbances and downstream effects when disastrous spills occur upstream and wipe out life downstream; for example recently from an old gold mine along the Animas river in Colorado (Moreno and Billeaud, 2015). But not all effects are so drastic or immediate. A recent workshop discussed the question of which and how many headwater drainage features could be sacrificed to development and agricultural use before fish assemblages downstream would be seriously affected (Stanfield *et al.*, 2014).

Given the enormous consequences of disturbances, empirical work is hazardous, limited or impossible, so mathematical models are necessary to understand principles and mechanisms. While there are many hydrological models describing water flow, they often do not include ecological dynamics, but see Jin *et al.* (2014). Ecological dynamics in river networks are frequently modeled with deterministic or stochastic patch- or metapopulation models (Charles *et al.*, 1998b,a, 2000; Fagan, 2002; Goldberg *et al.*, 2010; Labonne *et al.*, 2008; Padgham and Webb, 2010; Samia *et al.*, 2015). These models usually consider movement of individuals between river reaches but not transport of local disturbances to downstream locations through river flow.

Downstream transport of chemical pollution was addressed explicitly in a series of detailed tactical ecotoxicological models by Chaumot *et al.* (2002, 2003a,b) in the context of cadmium effects on brown trout in a complete binary network of 15 reaches. Toxicant effects differed with the spatial pattern of exposure; in particular, the effect of pollution at the river mouth was much higher than in upstream reaches. This effect of space could be understood as a function of the proportion of adults exposed to pollution (Chaumot *et al.*, 2003b) and interacts with migratory patterns during spawning (Chaumot *et al.*, 2003a).

In this work, we develop and analyze a more general, strategic model to examine how the locations of a single or two separate local disturbances in a river network affect the fate of a hypothetical potadromous fish population. In our framework, a transportable disturbance can be chemical pollution but also other abiotic aspects, such as temperature or turbidity, that can affect reproductive rates and can be transported downstream by river flow. The model is based on our earlier work on the effect of movement barriers (e.g. dams or culverts) on the population growth rate in different dendritic geometries (Samia *et al.*, 2015). One of our results there was that studying two, in some sense 'extreme', geometries sufficed to understand the behavior of the system in more natural, randomly generated networks. These two are the linear and the complete binary arrangement of river reaches. In the linear case, all reaches form a single linear chain, reminiscent to the River Nile when viewed from space. In the complete binary case, each reach is fed by exactly two immediate upstream reaches, comparable more to the vast network of the Amazon river. Our results here are based on these two extreme geometries. We introduce a disturbance in any reach in the network and evaluate how it changes the asymptotic population growth rate. This growth rate is a crucial quantity in demography in that it indicates whether the population will persist or go extinct (Caswell, 2001). We study how this effect depends on the ease with which the disturbance is transported downstream and on the movement pattern of the fish. From our analysis, we formulate general principles for how these two mechanisms affect the location of the 'most vulnerable reach'; i.e., the location where the population growth rate responds most strongly to the disturbance. By considering the joint effect of two disturbances, we also contribute to the study of cumulative effects of external drivers on population dynamics. Our results demonstrate the potential importance of a single reach on the fate of a population and can be applied to conservation efforts and land-use planing.

2 The Model

Our model tracks the density of a potadromous fish species in a dendritic river network from one year to the next. Each reach in the network is considered a (homogeneous) patch of primary habitat and is represented as a node in the spatial graph. An edge connecting nodes indicates a confluence of two reaches; see Figure 1. We denote by $N_{i,t}$ the density of the species in reach i in year t. Between subsequent years, individuals survive with probability s_i and produce, on average, r_i offspring. For simplicity, there is no stage structure; i.e., offspring become mature adults within one year. An individual moves from reach j to reach i with probability $c_{i,j}$. Then the densities in a network of n reaches evolve from year to year according to the equation (Samia *et al.*, 2015)

$$N_{i,t+1} = \sum_{j}^{n} c_{i,j}(r_j + s_j)N_{j,t}. \tag{1}$$

This linear model is adequate to determine persistence conditions for the population as long as there are no Allee effects (Courchamp *et al.*, 2008). We discuss a more realistic, nonlinear extension in the appendix, and we show that the behavior of the linear model completely predicts the behavior of the nonlinear model.

Model equation (1) can be formulated as a linear matrix model for state vector $\mathbf{N}(t) = (N_{1,t}, \ldots, N_{n,t})^T$ as

$$\mathbf{N}(t+1) = B\mathbf{N}(t), \tag{2}$$

where the projection matrix B is the product of the migration matrix $C = (c_{i,j})$ and the diagonal matrices for production and survival; i.e.,

$$B = C[R + S] \quad \text{with} \quad R = \text{diag}(r_j) \quad \text{and} \quad S = \text{diag}(s_j). \tag{3}$$

Matrix C is a (sub-) stochastic matrix that describes individual movement. We assume that individuals move by at most one reach per year, and we denote by $d_{i,j}$ ($u_{i,j}$) the probability to move downstream (upstream) from patch j to patch i. We assume that there is no loss or mortality related to movement, except possibly at the mouth of the river network. In particular, the column sums of matrix C equal unity, except possibly for the first column. For the mouth of the river, we consider two extreme scenarios. If the first column sum equals unity, we speak of a *closed system*. No individuals leave through the river mouth. If $c_{1,1} = 0$, we speak of an *open system*. An individual that does not move upstream from the mouth leaves the system; for more details, see Samia *et al.* (2015). For example, the connectivity

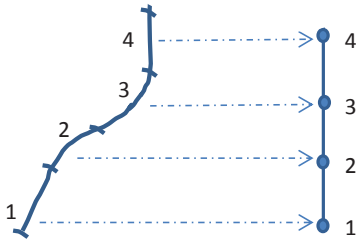

(a)

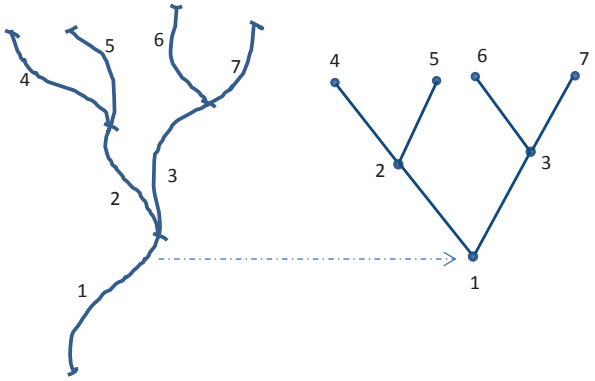

(b)

Figure 1: Representation of (a) a linear river network of 4 reaches (and 4 levels) and (b) a complete binary network of 7 reaches (on three levels) as spatial graphs. River reaches are represented by nodes and connections by edges.

matrices corresponding to the networks in Figure 1 are given by

$$C = \begin{pmatrix} * & d_{1,2} & 0 & 0 \\ u_{2,1} & 1 - d_{1,2} - u_{3,2} & d_{2,3} & 0 \\ 0 & u_{3,2} & 1 - d_{2,3} - u_{4,3} & d_{3,4} \\ 0 & 0 & u_{4,3} & 1 - d_{3,4} \end{pmatrix} \tag{4}$$

for the linear network, and by

$$C = \begin{pmatrix} * & d_{1,2} & d_{1,3} & 0 & 0 & 0 & 0 \\ u_{2,1} & 1 - d_{1,2} - u_{4,2} - u_{5,2} & 0 & d_{2,4} & d_{2,5} & 0 & 0 \\ u_{3,1} & 0 & 1 - d_{1,3} - u_{6,3} - u_{7,3} & 0 & 0 & d_{3,6} & d_{3,7} \\ 0 & u_{4,2} & 0 & 1 - d_{2,4} & 0 & 0 & 0 \\ 0 & u_{5,2} & 0 & 0 & 1 - d_{2,5} & 0 & 0 \\ 0 & 0 & u_{6,3} & 0 & 0 & 1 - d_{3,6} & 0 \\ 0 & 0 & u_{7,3} & 0 & 0 & 0 & 1 - d_{3,7} \end{pmatrix} \tag{5}$$

for the complete binary network, where

$$* = \begin{cases} 0 & \text{if the system is open} \\ 1 - u_{2,1} & \text{if the system described by (4) is closed} \\ 1 - u_{2,1} - u_{3,1} & \text{if the system described by (5) is closed} \end{cases} \tag{6}$$

We now describe how local and upstream conditions affect downstream population vital rates. For simplicity, we consider the case that only offspring production (r_i) and not adult survival (s_i) are affected. We distinguish the contribution of three groups of influences on production within a reach: (i) instream conditions (γ_i), such as benthic substrate or level of shading; (ii) landscape conditions (q_i), such as natural, industrial or agricultural run-off; and (iii) upstream conditions (h_i), such as nutrient loading or temperature, which indirectly account for influences of upstream landscape conditions. Accordingly, we write the local growth rate as

$$r_i = \exp(\gamma_i + q_i + h_i) > 0. \tag{7}$$

We consider instream conditions to be fixed at their respective reach, whereas landscape and upstream conditions can be transported to downstream reaches by water flow. Hence, considering only local, instream conditions — i.e., setting $q_i = h_i = 0$ — our model reduces to the one we had previously used to study the effect of movement barriers on population persistence (Samia *et al.*, 2015). We choose $q_i = 0$ to be the neutral value, so that $q_i > 0$ indicates a positive effect of landscape conditions on fish growth and $q_i < 0$ a negative effect such as contaminants entering the river. Our analysis below focuses on the latter scenario.

To calculate the effect of upstream conditions on local growth rates, we take a weighted average of transportable upstream conditions according to relative discharge and discounted for distance. Specifically, if reaches j and k are directly upstream of reach i (see Figure 1), we set

$$h_i = f_{ij}(q_j + h_j)\text{disc}_{ij} + f_{ik}(q_k + h_k)\text{disc}_{ik}, \tag{8}$$

where $f_{ij} \geq 0$ is the fraction of discharge from reach j into reach i, given by

$$f_{ij} = \frac{\text{discharge from } j}{\text{total discharge in } i},$$

and $\text{disc}_{ij} \geq 0$ is the discounting factor between reaches i and j. We measure discharge at the end of each reach, so that the total discharge in a reach equals the sum of the discharges of the reaches immediately upstream plus the lateral input. Furthermore, we assume that the discounting factor decreases with distance, and set

$$\text{disc}_{ij} = e^{-\nu_i l_i},$$

where l_i is the length of reach i. If the buffering factor ν_i is high, then there is little or no downstream transport. The upstream influence on downstream reproduction is low. This situation occurs if run-off contaminants are quickly moved into hyporheic storage zones and broken down there. On the other hand, if ν_i is low, then there is strong downstream transport. Upstream conditions have a large influence on downstream fish production.

3 Methods and assumptions

We measure how a local (negative) disturbance affects the fish population, depending on the strength of downstream transport, fish movement preference and habitat heterogeneity. We report our results in terms of the location of the disturbance. In particular, we determine which reach is the most vulnerable (or valuable) for the population. More specifically, we use the dominant eigenvalue (λ) of projection matrix B as our quantity of interest since it represents the asymptotic population growth rate. The population can grow only if $\lambda > 1$. We report how λ changes with respect to location and strength of the disturbance. For large disturbances, we report absolute changes (e.g. we plot λ as a function of the location of the disturbance), while, for small perturbations, we use standard sensitivity analysis to report rates of change; i.e., we calculate the derivative $d\lambda/dq_i$, see Caswell (2001).

We formulated our model in sufficient generality so that it is applicable to many different real-world river systems, from the linearly shaped Nile to the highly branched Amazon. However, for our detailed investigations reported here, we choose several carefully selected model simplifications that allow us to theoretically explore common principles rather than specific systems. We choose two extreme types of networks, a *linear network* where each non-boundary reach has exactly one upstream and one downstream neighbor, and a *complete binary network* where each non-boundary reach has exactly two upstream and one downstream neighbors. Our previous work shows that the dominant eigenvalue of intermediate, randomly generated networks is bounded by these two extremes (Samia *et al.*, 2015). We illustrate our results using a linear network with seven reaches. In this case, each reach represents a different level (i.e., distance from the mouth of the river). For a complete binary network, we use one with 127 reaches (corresponding to seven levels) and one with 7 reaches (corresponding to three levels). Our qualitative results do not change when more levels are involved.

We make the simplifying assumptions that all reaches are of the same length, that the amount of lateral influx is negligible compared to downstream discharge, that the buffering factor and survival rates are constant throughout the network and that all reaches within one level are identical with respect to local conditions. Therefore the value of γ_i depends only on the level of the reach. In the simplest case, we consider a homogeneous network, where all local conditions are equal. To represent heterogeneity, we consider a fixed ratio ρ of local growth rates between levels,

$$\rho = \frac{\gamma_{\text{ level } (k+1)}}{\gamma_{\text{ level } k}}.$$

In particular, the case $\rho > 1$ models a species that does better upstream (e.g., cold-water preference), whereas setting $\rho < 1$ models a species that reproduces better downstream.

Movement probabilities consist of an overall probability (p) to move away from the current reach and a movement bias. In the absence of movement bias, the probability to move downstream is $d_{i,j} = p/2$ and the probability to move upstream is either also $u_{i,j} = p/2$ (in the linear network) or $u_{i,j} = p/4$ to each of the two upstream connecting reaches (in the complete binary network). With bias upstream, the downstream movement probability is $d_{i,j} = p/4$, and the upstream probabilities are adjusted accordingly. With bias downstream, the numbers are reversed. The probability to move upstream from the highest level is zero. The probability of moving downstream from the mouth of the river depends on whether the network is closed or open (see previous section). We initialize discharge in the highest level

of the network as a constant, identical for all top-level reaches, and then calculate discharge throughout the network.

Unless otherwise noted in the text or figure caption, we choose parameter values as listed in Table 1.

parameter	meaning	value
s_i	survival probability	0.5
ν_i	buffer factor	0.01 (low)
		1 (high)
q_i	landscape conditions	0 (neutral)
		-5 (disturbance)
l_i	reach length	10
γ_i	instream conditions	0.5
p	overall moving probability	0.5

Table 1: Default parameter values used for numerical results.

4 Results

Even with the simplifying assumptions made in the previous section, there is still a large number of scenarios to explore. Between two network types (linear, binary), two mouth conditions (open, closed) and three local quality options ($\rho = 1$, $\rho > 1$ and $\rho < 1$), there are twelve scenarios, and for each there are three mechanisms to check (downstream transport, movement bias and movement probability). We begin by introducing a single disturbance (strong or weak) at exactly one reach and evaluating the response in λ. Then we consider the interaction of two disturbances and ask what their cumulative effect is. The results of our numerical explorations are summarized in the following sections.

4.1 Single disturbance in a homogeneous network ($\rho = 1$)

We choose the linear, homogeneous, closed network as our baseline scenario. We illustrate the three main findings in this case and report how they depend on the shape and other properties of the network.

I. The importance of reaches shifts in the direction of movement bias. Figure 2(a) depicts the value of λ in the linear network depending on the level (reach) at which the disturbance is located. The value of λ in the undisturbed network is given where

the curves intersect the y-axis. If a strong, negative disturbance is placed anywhere in the network, the population growth rate decreases; see Appendix 6.1 for the proof. In the absence of movement bias and downstream transport (i.e., when buffering is strong), the largest decrease occurs when the disturbance is placed in the center of the network, i.e. the middle reach (solid line). We shall refer to the location with the strongest effect as the *critical disturbance location* or the *most vulnerable reach*. With upstream (downstream) bias, the critical location moves upstream (downstream); see the dashed and dash-dot lines, respectively, in Figure 2(a).

When the network is open, downstream reaches are inherently more risky for individuals because they might leave the network at the river mouth (Samia *et al.*, 2015). Accordingly, the most vulnerable reaches shift upstream, but their relative order on the three curves in Figure 2(a) remains the same (plot not shown).

II. Downstream transport increases the importance of upstream reaches. The bars in Figure 2(b) indicate the sensitivity of λ with respect to a small disturbance at the corresponding location (i.e., $d\lambda/dq_i$). In the absence of downstream transport (i.e. buffering is strong) and movement bias, λ is (almost) equally sensitive to disturbances in all reaches (dark bars in Figure 2(b)). In contrast, λ is much more sensitive to disturbances in upstream reaches when buffering is weak and the disturbance is transported downstream (light bars in Figure 2(b)). The critical disturbance location is then shifted upstream. In fact, the difference between strong and weak buffering can make the difference between population persistence ($\lambda > 1$) and population extinction ($\lambda < 1$). For example, when a strong enough negative disturbance is placed in an upstream reach and buffering is weak, then the population may face extinction, even though it would be able to persist if a disturbance of the same strength had been placed further downstream or buffering was strong; see Figure 2(c). This qualitative result is exactly the same for an open network (plot not shown).

Comparing the (solid) line for unbiased movement in Figure 2(a) and the constant sensitivity in the absence of transport in Figure 2(b), we note that sensitivity analysis for small disturbances may not reveal the system's response to large disturbances, even though the system is linear. The dark bars indicting sensitivity in the absence of downstream transport seem constant on this scale, so that one could conclude that all reaches are equally vulnerable to disturbance. However, the bars actually differ by very small amounts. In particular, the highest sensitivity of λ to a negative disturbance is observed at reach 4, while its lowest corresponding sensitivity to negative disturbances is at reaches 1 and 7. When a large disturbance is applied, these differences are amplified, and the higher vulnerability in the center reach becomes visible in Figure 2(a).

III. Movement rate enhances but does not change the pattern. When the overall

rate of movement (p) is small, then λ is virtually constant, but when the movement rate is large, then λ decreases significantly when a strong negative disturbance is introduced. The critical disturbance location, however, is independent of p, see Figure 2(d). With a high movement rate, individuals will pass through the disturbed reach more frequently, and therefore the effect is more pronounced. For an open network, again, the pattern is exactly the same (plot not shown).

IV. A broadly branched network decreases the importance of a single upstream reach and increases the importance of the centre. In a complete binary network, the centre is located at the mouth of the river. At the same time, there are 2^k identical reaches on level k so that the importance of an individual reach is naturally diminished. These insights are crucial to understand the location of the most vulnerable reach in a complete binary network.

In a closed network, this most vulnerable reach is still the center of the network, which is now the river mouth. Hence the critical location is the lowest level. Upstream (downstream) bias does not shift this location but rather diminishes (enhances) the overall negative effect of the disturbance on λ; see Figure 3(a).

Even with downstream transport, the most vulnerable patch remains the river mouth, but many reaches in higher levels are almost equally vulnerable; see Figure 3(b). In contrast, when there is no downstream transport, the effect of a disturbance is significantly smaller for any level upstream of the mouth; see Figure 3(a).

The heightened importance of upstream reaches through downstream transport of disturbances is also visible in the sensitivity analysis in Figure 3(c). In the absence of transport, λ is by far the most sensitive to disturbances in the first level (river mouth), but, with transport, disturbances in the second level are almost as important. If a binary network is open, then the most central location is also the most dangerous since individuals leave the network through the river mouth. Accordingly, an additional disturbance to the river mouth has no significant effect on the population growth rate. Therefore λ is much less sensitive to the disturbance location than to movement bias, where upstream bias keeps individuals away from the river mouth and therefore increases λ (plot not shown). A comparison of the sensitivity analysis also confirms that, in this case, downstream transport of conditions increases the importance of upstream reaches for population persistence, with the critical location being around the mid-height of the network; see Figure 3(d). This particular location now plays the role of the center, and changing its quality affects incoming individuals from both upstream and downstream reaches.

To complete the description of our results, we mention that, in all cases, the overall movement rate (p) has the effect of enhancing the existing pattern without changing it qualitatively.

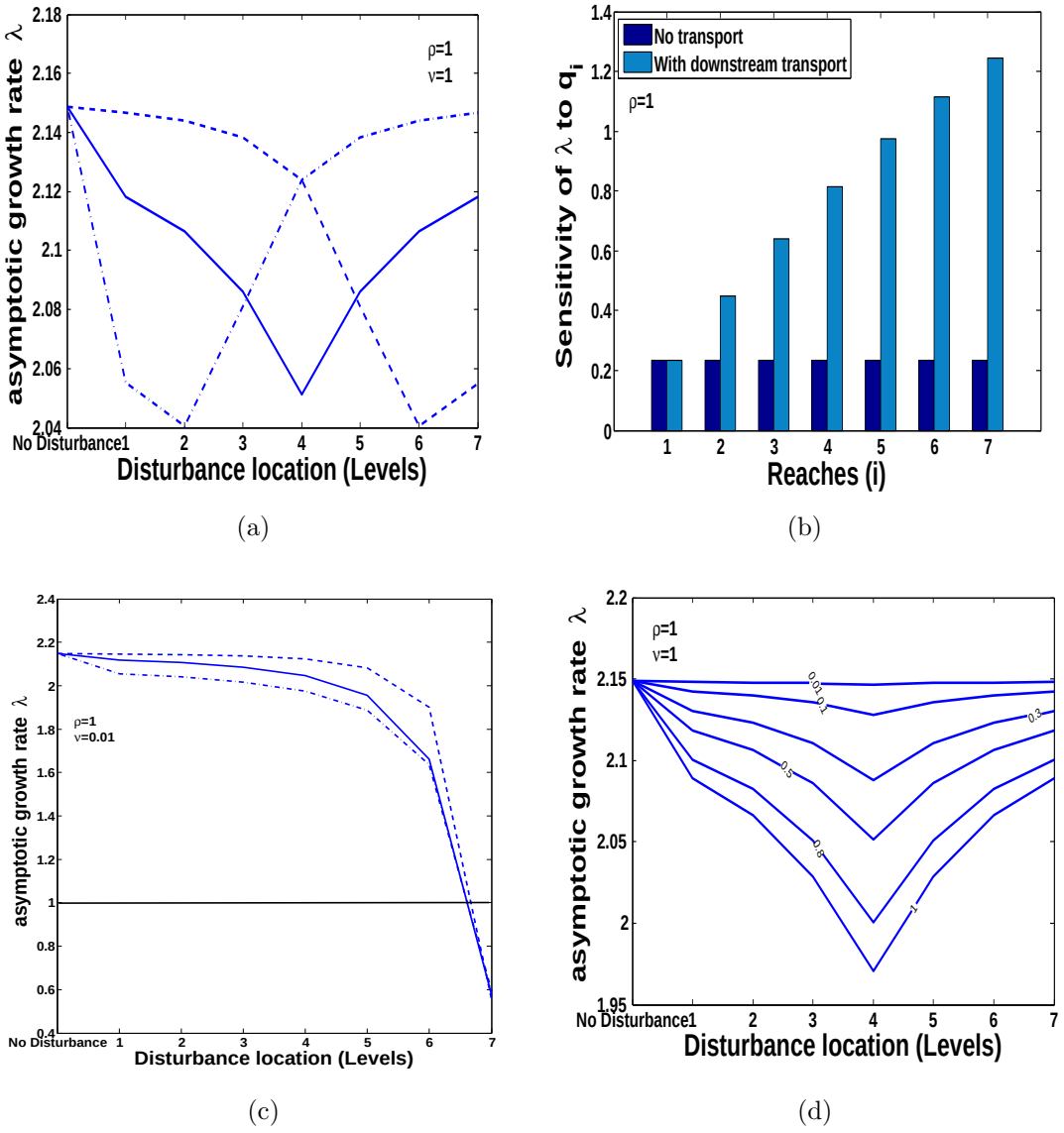

Figure 2: The effect of movement bias, downstream transport and movement probability on the population growth rate λ in a linear, homogeneous closed network. (a) Population growth rate as a function of disturbance location for unbiased (solid), upstream biased (dashed) and downstream biased (dash-dot) movement. (b) Sensitivity of λ with respect to disturbance location without (dark) and with (light) downstream transport. (c) Growth rate as a function of disturbance location with downstream transport and movement bias as in (a). (d) Growth rate as a function of disturbance location for different values of overall movement probability. Parameters are as in Table 1 and in the annotations of the plots.

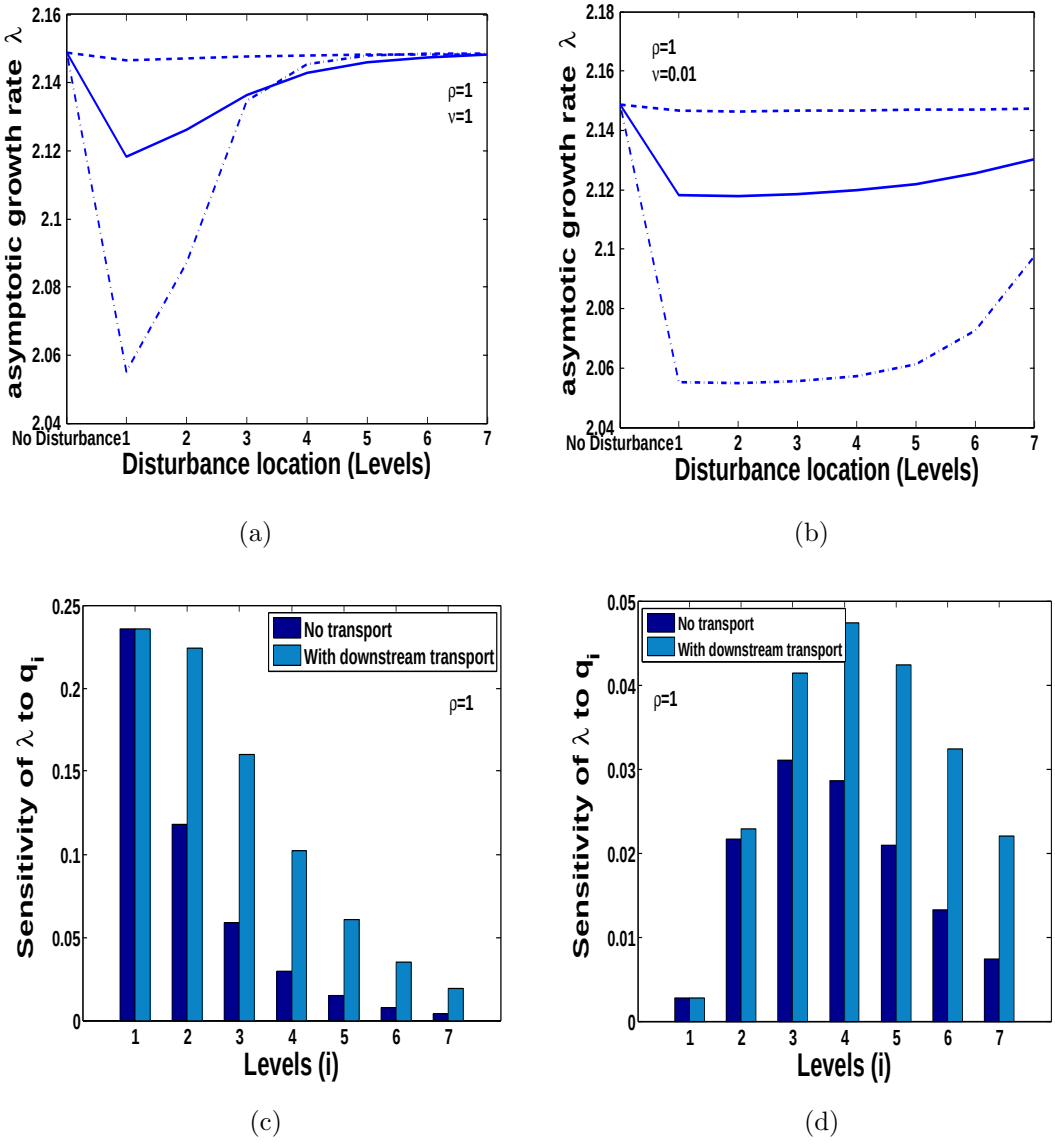

Figure 3: The effect of movement bias and downstream transport on the population growth rate λ in a homogeneous complete binary network. (a) Population growth rate as a function of disturbance location for unbiased (solid), upstream biased (dashed) and downstream biased (dash-dot) movement, in the absence of downstream transport. (b) Same as (a) but with downstream transport. (c) Sensitivity of λ with respect to disturbance location without (dark) and with (light) downstream transport in a closed network. (d) Same as (c) but in an open network. Parameters are as in Table 1 and in the annotations of the plots.

4.2 Single disturbance in a heterogeneous network

The scenario that population growth rate is homogeneous in the network is not very realistic in practice. Habitat heterogeneity in river networks often occurs via gradients, say, as water temperature and nutrient load usually increase downstream whereas shading decreases. Accordingly, we explore how the insights from the previous sections carry over to such gradient environments.

V. The importance of a reach increases when the population growth rate in that reach increases. This insight is not at all surprising, but it is modulated and sometimes overwritten by the four previous findings above. We look at some of these aspects in more detail and begin with the scenario where the growth rate increases downstream.

Growth rate increases downstream ($\rho < 1$)

When population growth rates are higher downstream, the importance of downstream locations is enhanced (if possible) and that of upstream locations is diminished. For closed networks, the effects are qualitatively similar to the case of a homogeneous network, just shifted downstream (plots not shown): the river mouth is typically the most vulnerable reach in the absence of downstream transport of the disturbance. With transport (i.e., weak buffering) upstream reaches become more important again. Upstream (downstream) movement bias gives smaller (larger) population growth rates. Sensitivity of λ with respect to disturbances in upstream reaches increases considerably with downstream transport.

The situation is more interesting when the network is open because of two conflicting effects. The reach at the mouth of the river has the highest productivity but at the same time carries the greatest risk of washout from the system. This risk of washout in fact decreases the importance of downstream reaches. Mid-level reaches become more important in the linear and binary networks. Figure 4(a) demonstrates how downstream transport enhances the importance of upstream reaches in the linear network; Figure 4(b) is the corresponding plot for the complete binary network.

As before, increasing the overall movement rate (p) enhances the pattern. When there is no transport, increasing p can also shift the critical location upstream; with strong transport, the critical location is and remains upstream.

Growth rate increases upstream ($\rho > 1$)

When the population growth rate is higher upstream, the upstream reaches are inherently more important. Upstream bias in movement enhances this trend, as does

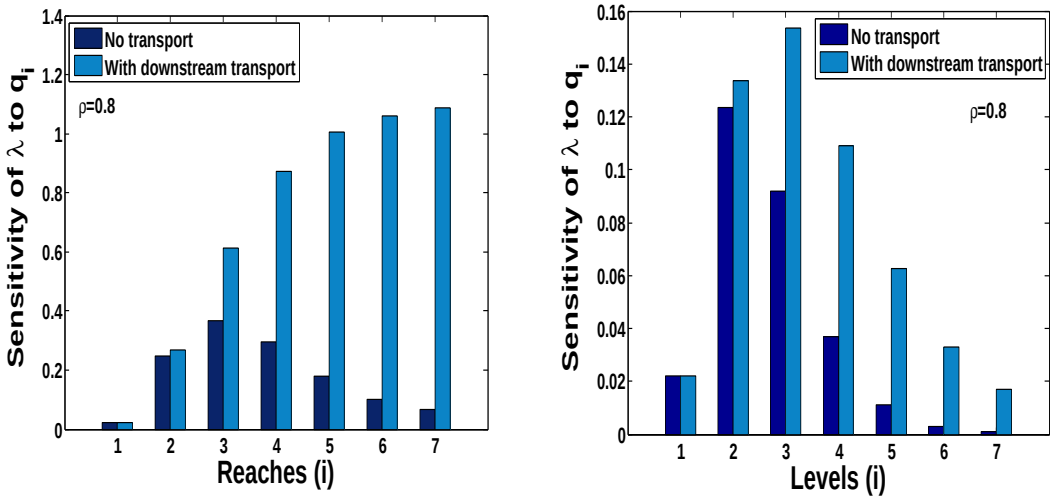

(a) (b)

Figure 4: The effect of downstream transport when downstream locations provide better growth conditions. Sensitivity of λ with respect to disturbance location without (dark) and with (light) downstream transport in (a) an open linear network and (b) in an open complete binary network. Growth rate increases downstream; i.e., $\rho < 1$. Parameters are as in Table 1 and in the annotations of the plots.

downstream transport of disturbances. In a linear network, the critical disturbance location is moved upstream, as compared to the homogeneous case. This effect is clearly visible in the absolute values of λ and in the sensitivities, and it is independent of whether the river mouth is open or closed. Without transport, the critical location in the linear network is the second highest level, and the population can persist in all cases; see Figure 5(a). With transport, the critical location is the highest level, and the population is not viable when the disturbance is located there ($\lambda < 1$); see Figure 5(b). The sensitivity of λ with respect to a disturbance in the highest level with transport is nearly twice that without transport; see Figure 5(c).

In the complete binary network, both open and closed, the importance of the river mouth as the central reach is diminished since growth rates are higher upstream. The population growth rate is most sensitive to disturbances in the second highest level when there is no transport, and in the highest level when there is transport; see Figure 5(d). We note, however, that the sensitivity values are very small. While the importance of the river mouth is diminished by the upstream increase in growth rate, the importance of any single upstream reach is diminished by the fact that there are 2^k such reaches on level k. Accordingly, the population growth rate appears almost constant with respect to disturbance location (plot not shown).

4.3 Two disturbances and cumulative effects

So far, we have considered how the population growth rate in a pristine river network is affected by the location of a single disturbance, large or small. But what happens when there is already a disturbance present in the network? Where would an additional disturbance have the largest effect, and what is the cumulative effect of the two disturbances? We answer this question by sensitivity analysis; i.e., by calculating the change in λ with respect to the location of a second disturbance, given the location of the existing disturbance.

Whereas there are only n possible locations for a single disturbance in a network of n patches, we now have to deal with n^2 possible pairs of locations for the two disturbances. For that reason, we illustrate our results only for linear and complete binary networks of seven reaches each. (Accordingly, the binary network will have only three levels). We checked our findings for larger networks, and found the same qualitative patterns; a detailed comparison of numerical results for complete binary networks of different heights is provided in Appendix D of the thesis.

VI. A secondary disturbance has the strongest effect when it is far from the existing disturbance with respect to the network topology. Figure 6(a) shows the sensitivity of λ in a linear network with respect to a small disturbance in reaches 1–7 for a given

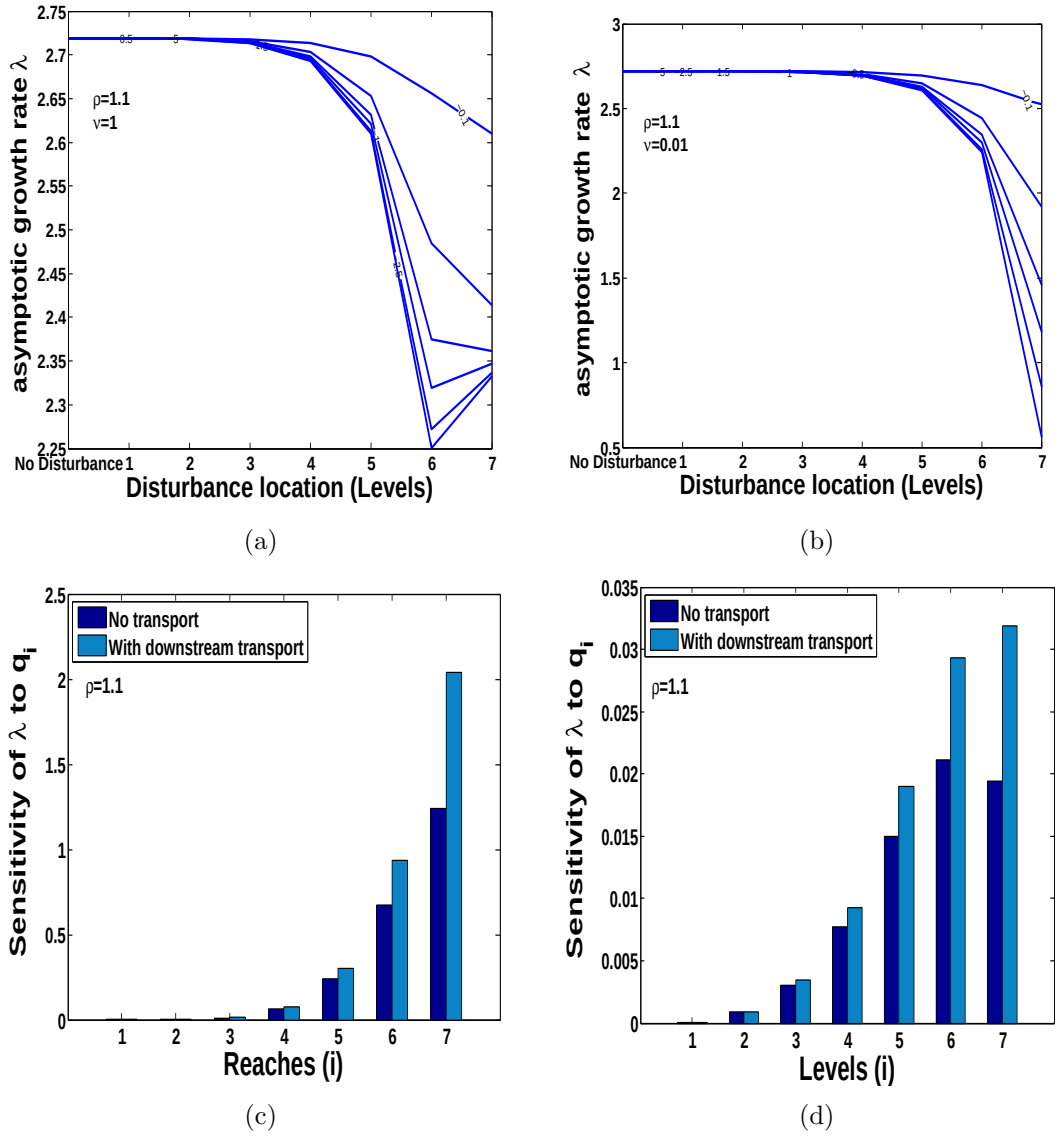

Figure 5: The effect of downstream transport when upstream locations provide better growth conditions. Population growth rate λ in a linear network for unbiased (solid), upstream-biased (dashed) and downstream-biased (dash-dot) movement without transport (a) and with transport (b). Sensitivity of λ with respect to disturbance location without (dark) and with (light) downstream transport in (c) an open linear network and (d) in an open complete binary network. Growth rate increases upstream, i.e. $\rho > 1$. Parameters are as in Table 1 and in the annotations of the plots.

existing disturbance in reaches 1–7 as a 3D bar plot. In the absence of downstream transport and movement bias, the population growth rate is insensitive to a further small disturbance at the same site. The bars along the diagonal are essentially zero. The largest sensitivity arises when the additional disturbance is far away from the already-disturbed site. When the existing disturbance is downstream (in reaches 1–3), the highest bars are at the source (reach 7), whereas when the existing disturbance is upstream (reaches 5–7), then the highest bars are at the river mouth (reach 1). Downstream transport shifts this pattern such that upstream locations are much more influential; only when the original disturbance is in the highest reaches do additional disturbances in the downstream locations have a significant effect on λ; see Figure 6(b). With upstream movement bias, the same effect arises. Downstream movement bias shifts the importance of locations downstream, but when conditions are transported downstream as well, the most influential locations are again upstream (plot not shown).

In a complete binary network (see Figure 1 for labeling of the reaches), the pattern is similar when keeping in mind the importance of the central location of the river mouth. In the absence of downstream transport and movement bias, the sensitivity is smallest for disturbances occurring at the already-disturbed site and largest at the river mouth (reach 1) if the original disturbance is anywhere else; see Figure 6(c). With downstream transport, the most influential locations are the ones farthest away from the existing disturbance; i.e., in the highest upstream reaches on the half of the network that is opposite (with respect to the river mouth) of the original disturbance; see Figure 6(d). For example, if the original disturbance is in reach 2, then the furthest reaches are 6 and 7. Just as with the linear network, this pattern also arises with upstream bias and persists with upstream or downstream bias, as long as there is downstream transport. When there is downstream bias but no downstream transport, the river mouth regains its status of the most influential location (plot not shown).

Qualitatively, these findings remain true when the network is not homogeneous but rather contains the gradient structure for either $\rho > 1$ or $\rho < 1$. As before, upstream (downstream) levels become more important when upstream (downstream) conditions are better. However, downstream transport and upstream movement bias continue to make the upstream reaches the most vulnerable ones.

5 Discussion

Questions about how water safety and biodiversity are affected by river network alterations — e.g., through climate change, urban sprawl or agriculture — are of

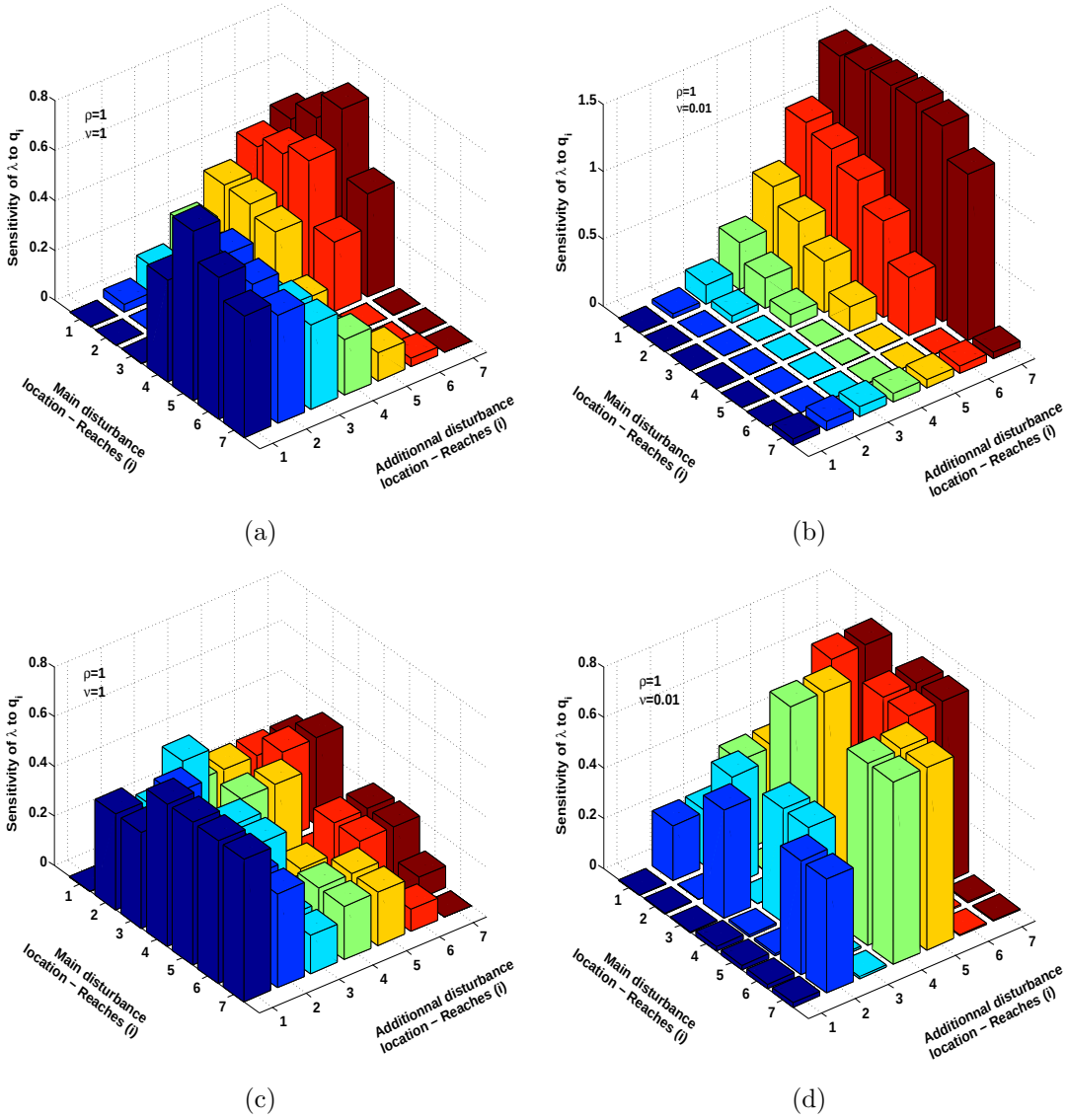

Figure 6: Cumulative effects for two disturbances in different geometries. Sensitivity of λ to a secondary disturbance in a closed linear network (a) without transport and (b) with transport, as well as in a closed complete binary network (c) without and (d) with transport. Parameters are as in Table 1 and in the annotations of the plots.

paramount importance. The complexity of river ecosystems, governed by the interactions of geomorphology, hydrology, connectivity and ecology, poses great challenges in the understanding of mechanisms and effects. Management of these systems frequently relies on hydrological models and local habitat suitability measures to evaluate the impact of alterations on a given species but tends to neglect ecological feedbacks (Anderson *et al.*, 2006). Since water flow transports many physical and geochemical aspects from upper to lower reaches, questions about the importance of upper reaches and about cumulative downstream effects are particularly pressing (Stanfield *et al.*, 2014). Our strategic analytical model contributes some mechanistic insights into these questions.

We studied how the asymptotic growth rate of a hypothetical potadromous fish species changes with respect to disturbances in one or two reaches in the network, especially how the change depends on transport of the disturbance. In this way, we identified the most vulnerable reach for a negative disturbance. Clearly, local habitat suitability is important (see *V*), but movement bias (see *I*) and downstream transport (see *II*) can move the critical location upstream of the best local habitat and increase the importance of upper reaches. Species with high movement rates show a more pronounced but qualitatively similar pattern as species with low movement rates (see *III*). A single upstream reach is less influential in a highly branched structure (see *IV*), but the cumulative effect of two disturbances is greater when the second disturbance is far away from the first in the network distance (see *VI*).

Our results highlight the importance of upstream reaches in a dendritic network when disturbance attributes are easily transported downstream. As the asymptotic growth rate is a global indicator for the entire network, our study complements mechanistic models on smaller scales that looked at response length for population distribution on a reach level (Anderson *et al.*, 2005). Vice versa, this finding suggests that mitigation or restoration immediately downstream of a disturbance would have the greatest benefits. Such measures can include buffer zones (Correll, 1996) and other measures to shorten uptake length (Lutscher and McCauley, 2013).

Our results also point out that details of the movement behavior of fish in river networks can be crucial for population persistence and need to be accounted for when assessing potential effects of disturbances. This aspect of the study complements our previous work where we considered movement behavior around barriers, such as dams or culverts (Samia *et al.*, 2015). Populations with upstream movement bias are more vulnerable to disturbances in upper reaches. For example, we would expect upstream bias in cold-water species so that upstream disturbances could be more detrimental for bull trout (*Salvelinus confluentus*), which require <13°C temperatures, than for brook trout (*Salvelinus fontinalis*), which can tolerate up to 22°C temperatures.

While it is clear that our model does not apply to fish species with completely different movement patterns (e.g. anadromous), an important next step is to include a more detailed fish life history into the model and evaluate how the general principles from our strategic model apply. For example, White Sucker (*Catostomus commersonii*) migrate on a local scale to spawning habitat, and fry and adults have different movement patterns (Geen *et al.*, 1966).

Rarely do disturbances arise in completely pristine river networks these days; most times preexisting disturbances are present. Our work also sheds light on how disturbances interact. We thereby contribute to the research on cumulative effects that is now frequently mandated by government regulations. Upstream movement and downstream transport also alter the patterns of cumulative effects and shift importance to upstream reaches (see *VI*). The findings relate to the well-known SLOSS (single large or several small) debate for conservation planing (Wilcox and Murphy, 1985). Clearly, in river networks, one needs to account for distance according to the network structure rather than geographic distance. Our results for two disturbances indicate that movement patterns and transport of conditions change the optimal conservation design. However, our work assumes that there are no Allee effects, and it is known that population response to fragmentation can change with the shape of density dependence (Dewhirst and Lutscher, 2009).

From a management point of view, our results can be used to determine the least harmful location for, say, development or risk of toxic contamination in a network. This location is typically near mouth of the river but it is moved upstream if transport and upstream movement bias are strong. The effects of transportable contaminants on fish populations were studied with a much more detailed tactical model of brown trout (Chaumot *et al.*, 2002, 2003a,b). Their and our models captured only one species and only potadromous movement. One can easily think of scenarios where the downstream location in a highly branched network would be the most vulnerable reach; for example, in an anadromous species (e.g. salmon) where all individuals that return to spawn in a certain watershed have to pass through its mouth. Accordingly, our model should be extended to include multiple species with varying habitat requirements and migration patterns.

Our modeling framework is a matrix model for a multi-patch population, and as such has a distinct history of successful application in (spatial) demographics (Caswell, 2001; Charles *et al.*, 2009). In particular, sensitivity analysis and simulation tools are well developed, and have recently been extended to age-stage structured populations (Caswell, 2012), which can be interpreted as age-patch models. We were able to assess the importance of each reach in a river network through the effect of its quality on the population growth rate. The latter indicator is a robust

population endpoint to assess stress in ecology (Forbes and Calow, 2002; Stark and Banks, 2003) and is a projective variable that describes the demographic state of the population (Caswell, 1996); hence it is well suited to answer decision-making questions. Other descriptive population endpoints exist, such as the asymptotic population distribution and the reproductive value. These features were considered by Chaumot *et al.* (2002, 2003a,b).

One novel aspect in our model is the transport of conditions from one patch to others. Most patch models, either deterministic compartmental models or stochastic metapopulation models, assume that local patch quality is independent of neighboring patch quality. This assumption is clearly not tenable for river networks. Our work strongly suggests that spatial correlations in patch quality have great importance for theoretical population dynamics as well as applied decision-making. We therefore advocate that mathematical tools and quantities — for example indicators of the importance of individual patches to overall population growth rate, viability, and steady-state distribution (Ovaskainen and Hanski, 2003) — be generalized to include spatial correlations induced by river-flow transport or other mechanisms such as ground water.

Acknowledgements

YS is grateful for an Alexander Graham Bell doctoral scholarship from the Natural Science and Engineering Research Council of Canada (NSERC). FL acknowledges an NSERC discovery grant. Both authors thank Alan Hastings for initial discussions. We also thank Les Stanfield and all the participants for discussions during the 'Trim the Tribs' workshop, held in Ottawa (2012) with financial support from the Toronto and Region Conservation Authority.

6 Appendix

6.1 The effect of a strong negative disturbance on the asymptotic growth rate

In this section of the appendix, we analytically prove that, if a strong disturbance is placed anywhere in the network, the population growth rate decreases. We state this result in the following theorem:

Theorem 1 *Consider the linear model given by equation (1)*

$$N_{i,t+1} = \sum_{j=1}^{n} c_{i,j}(r_j + s_j)N_{j,t}$$

and let $r_i = e^{(\gamma_i + q_i + h_i)} > 0$ *be the local growth rate in reach* i*. The dominant eigenvalue* λ *of the corresponding linear matrix model (equation (2))*

$$\boldsymbol{N}(t+1) = B\boldsymbol{N}(t)$$

is an increasing function of the local growth r_i*.*

Proof Let $\mathbf{w}$ and $\mathbf{v}$ be the respective right and left eigenvectors corresponding to the dominant eigenvalue λ of the projection matrix $B = (b_{i,j})$. We consider the rate of change of λ with respect to the local growth rate r_i at any reach i. Since the asymptotic growth rate λ depends on the entries of matrix B and these entries depend themselves on the growth rate r_i, we use the chain rule to write:

$$\frac{d\lambda}{dr_i} = \frac{d\lambda}{db_{i,j}} \cdot \frac{db_{i,j}}{dr_i}.$$

As detailed in Caswell (2001),

$$\frac{d\lambda}{db_{i,j}} = \frac{v_i w_j}{\langle \mathbf{w}, \mathbf{v} \rangle},$$

where $\langle \mathbf{w}, \mathbf{v} \rangle$ is the scalar product of $\mathbf{v}$ and $\mathbf{w}$. Matrix B is non-negative, irreducible and primitive (see Appendix 6.2 for a detailed explanation). Hence, by the Perron–Frobenius theorem, the right and left eigenvectors corresponding to the dominant eigenvalue λ are real and strictly positive; in particular, the scalar product $\langle \mathbf{w}, \mathbf{v} \rangle$ is positive. On the other hand, $\dfrac{db_{i,j}}{dr_i}$ is positive by the construction of matrix B. Therefore

$$\frac{d\lambda}{dr_i} > 0$$

and any decrease in the local growth rate r_i caused by a negative disturbance decreases λ, independently of the location of the disturbance.

6.2 A nonlinear extension to the linear model (1)

In this work, we study only the stability of a linear model for the population. This model is valid for small population densities (as long as there is no Allee effect), but not at large densities, when intra-specific competition cannot be neglected. In this appendix, we formulate a corresponding nonlinear model, and we show that the linear model that we studied completely determines the behavior of the corresponding nonlinear model. More specifically, we show that the zero state of the nonlinear model is globally asymptotically stable if and only if the dominant eigenvalue of the linear model is less than unity. Vice versa, the nonlinear model has a unique, positive, globally asymptotically stable steady state if and only if the dominant eigenvalue of the linear model is greater than unity. In other words, it is sufficient to study the linear model, as we did in this work.

We begin by introducing a recruitment function of Beverton–Holt type into our model. The model then becomes:

$$N_{i,t+1} = \sum_{j=1}^{n} c_{i,j} f_j(N_{j,t}) = \sum_{j=1}^{n} c_{i,j} g_j(N_{j,t}) N_{j,t}, \tag{9}$$

where $f_j(N) = g_j(N)N$, and the local per-capita reproduction and survival term is

$$g_j(N_{j,t}) = \frac{r_j}{1 + e_j N_{j,t}} + s_j. \tag{10}$$

Here e_j measures the strength of intra-specific competition on reproduction. The other parameters are as defined in equation (1). The linearization of model (9) at the zero steady-state is precisely the linear model (1) since $f_i'(0) = g_i(0) = r_i + s_i$.

We begin by justifying, for the linear model (1), the existence of a real dominant eigenvalue that determines the stability of the zero solution. By construction, matrix B is non-negative since all entries are obtained from adding and multiplying rates of movement and demography, which are non-negative. This matrix is also irreducible because it is associated to a strongly connected graph; i.e., there is a path from any node to any other node. Moreover, matrix B is primitive since it is irreducible and has a positive trace. Then, by the Perron–Frobenius theorem (Caswell, 2001), we have that (i) there exists a real, positive eigenvalue λ that is the simple root of the characteristic equation $\det(B - \lambda I) = 0$; (ii) λ is strictly greater in magnitude than any other eigenvalue; and (iii) the right and left eigenvectors corresponding to λ are real and strictly positive. In particular, if $\lambda < 1$, then all solutions of the linear system converge to zero, but if $\lambda > 1$, then there is a biologically relevant (i.e., positive) solution that diverges to infinity.

We now prove the following theorem for the nonlinear system.

Theorem 2 *If $\lambda < 1$, then the zero steady state of (9) is globally asymptotically stable. On the other hand, if $\lambda > 1$, the zero steady state is unstable and there exists a unique positive steady-state, $\mathbf{N}^* = (N_1^*, \ldots, N_n^*)$, that is globally asymptotically stable for all non-negative solutions $\mathbf{N} \neq \mathbf{0}$.*

Proof The proof rests on two essential properties of the functions f_i: namely, these functions are monotone increasing and concave. The proof follows the same ideas as those used in Van Kirk and Lewis (1997), Lutscher and Lewis (2004), Krasnosel'skii and Zabreiko (1984) and Krasnosel'skii (1964) for models with continuous spatial variable.

First, let us assume $\lambda < 1$. As noted before, all non-negative solutions of the linear model converge to zero. The per-capita growth in (9) is bounded by the growth at zero, independent of the population size; that is:

$$0 < g_j(N) = \frac{r_j}{1 + e_j N} + s_j < r_j + s_j = g_j(0) \text{ for all } j.$$

Equivalently, we have $f_j(N) \leq f_j'(0)N$ for all j. Since matrix C is (sub-) stochastic, we find

$$N_{i,t+1} = \sum_{j=1}^{n} c_{i,j} f_j(N_{j,t}) \leq \sum_{j=1}^{n} c_{i,j} g_j(0) N_{j,t}.$$

In particular, solutions of the nonlinear model are bounded in each component by solutions of the linear model with the same initial condition. Since the latter solutions converge to zero by assumption, solutions of the nonlinear model do the same.

Next, let us assume $\lambda > 1$. We begin by checking the asymptotic derivative at infinity. Specifically, we need to find functions, denoted by $g_j(\infty)$, such that

$$|g_j(N) - g_j(\infty)| \leq \frac{\text{const.}}{|N|} \text{ for large } N. \tag{11}$$

Due to the form of $g_j(N)$, we can choose $g_j(\infty) = s_j$ for all j, since

$$|g_j(N) - g_j(\infty)| = |\frac{r_j}{1 + e_j N}| \leq \frac{r_j}{e_j |N|} \tag{12}$$

By definition, the asymptotic derivative at infinity (Krasnosel'skii, 1964) of the nonlinear model (9) is given by CS where C is the movement matrix and S the diagonal matrix of survival probabilities. Since the dominant eigenvalue of C is bounded by unity and since $g_j(\infty) = s_j < 1$ for all j, the dominant eigenvalue of CS is bounded by $\max_j s_j < 1$.

Since the dominant eigenvalue at zero is greater than unity, solutions increase component-wise when small. Since the eigenvalue of the asymptotic derivative at infinity is less than unity, solutions decrease component-wise when large. Since the nonlinearities f_j are monotone, solutions of the recursion (9) are monotone. Therefore there has to exist at least one positive steady state, $\mathbf{N}^*$; see Proposition 3 in Lutscher and Lewis (2004) and Theorem 4.11 in Krasnosel'skii (1964).

Furthermore, f_j is increasing with respect to the population size and g_j is decreasing with respect to the population size. This means that f_j is monotone increasing and concave. Hence, by Proposition 4 in Lutscher and Lewis (2004) and Theorem 6.3 in Krasnosel'skii (1964), the positive steady state is unique. Moreover, by Theorem 6.6 in Krasnosel'skii (1964), every solution $\mathbf{N} \neq \mathbf{0}$ converges to $\mathbf{N}^* > 0$. Therefore the positive steady state is globally asymptotically stable when $\lambda > 1$.

References

Anderson, K.E., Paul, A., McCauley, E., Jackson, J., and Post, J. (2006). Instream flow needs in streams and rivers: the importance of understanding ecological dynamics. *Front. Ecol. Environ.*, **4**(6), 309–318.

Anderson, K.E., Nisbet, R.M., Diehl, S., and Cooper, S. (2005). Scaling population responses to spatial environmental variability in advection dominated systems. *Ecol. Lett.*, **8**, 933–943.

Bishop, K., Buffam, I., Erlandsson, M., Folster, J., Laudon, H., Seibert, J., and Temnerud, J. (2008). Aqua incognita: the unknown headwaters. *Hydrol. Process*, **22**(8), 1239.

Caswell, H. (1996). Demography meets ecotoxicology: untangling the population level effects of toxic substances. In M. Newman and C. Jagoe, editors, *Ecotoxicology: A hierarchical treatment*. Boca Raton, FL (USA): CRC Press, Lewis Publishers. Pages 255–292. CRC Press.

Caswell, H. (2001). *Matrix population models*. Wiley.

Caswell, H. (2012). Matrix models and sensitivity analysis of populations classified by age and stage: a vec-permutation matrix approach. *Theor. Ecol.*, **5**, 403–417.

Charles, S., Bravo de La Parra, R., Mallet, J.-P., Persat, H., and Auger, P. (1998a). A density dependent model describing *salmo trutta* population dynamics in an

arborescent river network. effects of dams and channelling. *CR Acad Sci III-Vie*, **321**(12), 979–990.

Charles, S., Bravo de La Parra, R., Mallet, J.-P., Persat, H., and Auger, P. (1998b). Population dynamics modelling in an hierarchical arborescent river network: an attempt with salmo trutta. *Acta biotheor.*, **46**(3), 223–234.

Charles, S., Bravo de La Parra, R., Mallet, J.-P., Persat, H., and Auger, P. (2000). Annual spawning migrations in modelling brown trout population dynamics inside an arborescent river network. *Ecol. Model.*, **133**(1), 15–31.

Charles, S., Billoir, E., Lopes, C., and Chaumot, A. (2009). Matrix population models as relevant modeling tools in ecotoxicology. In J. Devillers, editor, *Ecotoxicology Modeling, Emerging topics in Ecotoxicology: Principles, Approaches and Perspectives*, volume 2, pages 261–298. Springer.

Chaumot, A., Charles, S., Flammarion, P., Garric, J., and Auger, P. (2002). Using aggregation methods to assess toxicant effects on population dynamics in spatial systems. *Ecol. Appl.*, **12**(6), 1771–1784.

Chaumot, A., Charles, S., Flammarion, P., and Auger, P. (2003a). Do migratory or demographic disruptions rule the population impact of pollution in spatial networks? *Theor. pop. biol.*, **64**(4), 473–480.

Chaumot, A., Charles, S., Flammarion, P., and Auger, P. (2003b). Ecotoxicology and spatial modeling in population dynamics: An illustration with brown trout. *Environ. toxicol. chem.*, **22**(5), 958–969.

Correll, D. (1997). Buffer zones and water quality protection: general principles. In Haycock, N., Burt, T., Goulding, K., Pinay, G. (eds) *Buffer zones: their processes and potential in water protection. The proceedings of the international conference on buffer zones*, Quest Environmental, pages 7–20.

Courchamp, F., Berec, L., and Gascoinge, J. (2008). *Allee effects*. Oxford University Press.

Dewhirst, S. and Lutscher, F. (2009). Dispersal in heterogeneous habitats: thresholds, spatial scales and approximate rates of spread. *Ecology*, **90**(5), 1338–1345.

Fagan, W.F. (2002). Connectivity, fragmentation, and extinction risk in dendritic metapopulations. *Ecology*, **83**(12), 3243–3249.

Forbes, V.E. and Calow, P. (2002). Population growth rate as a basis for ecological risk assessment of toxic chemicals. *Phil. Trans. B*, **357**(1425), 1299–1306.

Geen, G., Northcote, T., Hartman, G., and Lindsey, C.C. (1966). Life histories of two species of catostomid fishes in Sixteenmile Lake, British Columbia, with particular reference to inlet stream spawning. *J. Fish. Res. Board Can.*, **23**(11), 1762–1787.

Goldberg, E.E., Lynch, H.J., Neubert, M.G., and Fagan, W.F. (2010). Effects of branching spatial structure and life history on the asymptotic growth rate of a population. *Theor. Ecol.*, **3**(3), 137–152.

Jin, Y., Hilker, F., Steffler, P., and Lewis, M. (2014). Seasonal invasion dynamics in a spatially heterogeneous river with fluctuating flows. *Bull. Math. Biol.*, **76**(7), 1522—1565.

Krasnosel'skii, M.A. (1964). *Positive Solutions of Operator Equations*. Noordhoff LTD, Groningen.

Krasnosel'skii, M.A. and Zabreiko, P.P. (1984). *Geometrical Methods of Nonlinear Analysis*. Springer Verlag, Berlin.

Labonne, J., Ravigné, V., Parisi, B., and Gaucherel, C. (2008). Linking dendritic network structures to population demogenetics: the downside of connectivity. *Oikos*, **117**(10), 1479–1490.

Lowe, W. (2006). The trouble with rivers. *BioSci.*, **56**(3), 260–263.

Lutscher, F. and Lewis, M.A. (2004). Spatially-explicit matrix models. *J. Math. Biol.*, **48**(3), 293–324.

Lutscher, F. and McCauley, E. (2013). A probabilistic framework for nutrient uptake length. *Theor. Ecol.*, **6**(1), 71–86.

Meyer, J.L., Strayer, D.L., Wallace, J.B., Eggert, S.L., Helfman, G.S., and Leonard, N.E. (2007). The contribution of headwater streams to biodiversity in river networks. *J. Am. Water Res. Assoc.*, **43**(1), 86–103.

Moreno, I. and Billeaud, J. (2015). Wastewater from Colorado Mine Reaches New Mexicos. *The Big Story, Associated Press*. Published online on 09-August-2015.

Nilsson, C., Ekblad, A., Dynesius, M., Backe, S., Gardfjell, M., Carlberg, B., Hellqviist, S., and Jansson, R. (1994). A comparison of species richness and traits of riparian plants between a main river channel and its tributaries. *J. Ecol.*, **82**(2), 281–295.

Ovaskainen, O. and Hanski, I. (2003). How much does an individual habitat fragment contribute to metapopulation dynamics and persistence? *Theor. pop. biol.*, **64**, 481–495.

Padgham, M. and Webb, J.A. (2010). Multiple structural modifications to dendritic ecological networks produce simple responses. *Ecol. Model.*, **221**(21), 2537–2545.

Samia, Y., Lutscher, F., and Hastings, A. (2015). Connectivity, passability and heterogeneity interact to determine fish population persistence in river networks. *J. Roy. Soc. Interface*, **12**(110), 20150435.

Stanfield, L., Del Guidice, L., Lutscher, F., Trudeau, M., Alexander, L., Fagan, W., Fertik, R., Mackereth, R., Richardson, J., Shrestha, N., Tetreault, G., and Wipfli, M. (2014). A discussion paper on: Cumulative effects from alteration of headwater drainage features and the loss of ecosystem integrity or river networks. Technical report, Ontario Ministry of Natural Resources.

Stark, J.D. and Banks, J.E. (2003). Population-level effects of pesticides and other toxicants on arthropods. *Ann. Rev. Entomology*, **48**(1), 505–519.

Thorp, J.H., Thoms, M.C., and Delong, M.D. (2006). The riverine ecosystem synthesis: biocomplexity in river networks across space and time. *River Res. Appl.*, **22**(2), 123–147.

Van Kirk, R.W. and Lewis, M.A. (1997). Integrodifference models for persistence in fragmented habitats. *Bull. Math. Biol.*, **59**(1), 107–137.

Wilcox, B. and Murphy, D. (1985). Conservation strategy: The effect of fragmentation on extinction. *Am. Nat.*, **125**(6), 879–887.

Chapter 5

Discussion, Conclusion and Future work

5.1 Discussion

Persistence of populations in river networks is a fundamental issue in population ecology. These lotic environments impose, through water flow, a risk of inhabiting organisms being washed out of their suitable habitat. The ability of populations to persist despite this natural environmental stress is an exceptional phenomenon that has attracted a lot of interest and is referred to as the 'drift paradox'. Furthermore, how persistence and extinction dynamics depend on alterations to rivers and changes in ecological conditions is of paramount importance for effective management of river ecosystems. With all the peril that threatens river ecosystems, from small-scale variations in ecological conditions to habitat fragmentation and pollution, the response of species to such disturbances is a serious contemporary concern for conservation ecology. Overall, the aim is to minimize extinction risk of species.

Mathematical models serve as a two-way translation means from concrete real-world problems into abstract representations and theoretical analysis and vice versa. Even though they necessarily involve simplifications and idealising assumptions, they have proven their value in providing conceptual frameworks that allow for detailed investigation of ecological

questions. Population models are frequently used to theoretically explore processes and test hypotheses relating to biological systems under several environmental conditions. More importantly, these models draw their strength from their potential to generate explanations and uncover mechanisms that underly ecological phenomena.

We have presented three approaches to the problem of persistence in river networks using mathematical modelling. Our first contribution addresses the 'drift paradox' question in a single river reach, through a stochastic framework. We construct and analyse two spatially implicit stochastic models, analogous to earlier deterministic modelling approaches. Demographic stochasticity is formulated as birth, death or emigration events, whereas environmental stochasticity is explored through temporal variation of water flow. The stochastic models that we present are related to their deterministic analogues through the emigration rate, which is derived from the dominant eigenvalue of the deterministic movement operator. We investigate the effects of stochasticity on the persistence probability of two categories of stream invertebrates: organisms that are always dispersing in the water column, and those that spend sometime resting or crawling on the benthos. For each of these categories, we present our results under constant environmental conditions first and then include temporal variation.

Overall, our results illustrate how local population persistence depends on stochasticity via emigration rates and temporal variation. In particular, we find that, for the single-compartment model, a small variation in flow speed can increase persistence probability, whereas large temporal variations lead to a decrease in the persistence probability. More interestingly, when the benthos compartment is considered, the persistence probability often increases, depending on the transition rates between drift and benthos. These particular results suggest that some physical and behavioral mechanisms can counterbalance or enhance the effect of flow variation.

Persistence of a population in flowing environments and the 'drift paradox' are interesting questions of equal theoretical and practical importance. Corresponding applications are mainly advantageous in the design and management of environmental reserves as well as in

restoration projects.

Results of the stochastic models that we developed compare relatively well to those of deterministic analogues. This fact underscores the robustness of the deterministic theory with respect to stochastic demographic effects, for which the transition from definite persistence to definite extinction is smoothed out. At the same time, this finding indicates that the stochastic model complements the deterministic approach by generating more detailed results.

A key decision in mathematical modelling is whether to model processes as deterministic or stochastic. The persistence of stream populations and the 'drift paradox' are fairly well-documented concepts, especially through deterministic models, which are considerably simpler to analyse. Our stochastic work then comes to explore other aspects of already-acknowledged models and hence complements the deterministic theory. On the other hand, for our next two contributions on persistence at a network scale, we choose the deterministic framework, because the corresponding theory is still under development without many previous results that we can compare ours to. Accordingly, including stochasticity is a subject of future work that is beyond the scope of this thesis.

In our second contribution, we address the problem of population persistence in fragmented dendritic river networks. Population dynamics are modeled through a discrete-time matrix model, where the updating matrix accounts for demographic processes as well as the explicit spatial structure of the river. The effects of a single obstacle on fish migration appear as a decrease in the movement probabilities between the two reaches where the obstacle is located. We evaluate the effects of a single obstacle from two perspectives, by considering it as a disconnecting structure of both the population and the river network. At the population level, an obstacle inhibits fish migration, thus dividing the population and clustering individuals into two partially connected groups; its corresponding effect on population persistence is quantified through the asymptotic growth rate of the population. At the network level, fragmentation by a single obstacle disconnects river reaches, splitting the network into two disjoint components. The corresponding effect is described through a structural connectiv-

ity index especially developed for potadromous fish in dendritic networks. The comparison between the two metrics in different scenarios (homogeneous or heterogeneous growth conditions) and on different dendritic topologies (linear, complete binary and random networks) reveals that structural indices do not capture all effects of movement barriers on population dynamics. In particular, we show that an obstacle can enhance persistence when it does not induce mortality or when it prevents individuals form leaving the network. Therefore, decreased connectivity does not necessarily correspond to a decrease in the likelihood of persistence.

We represent rivers as spatial dendritic graphs and adapt a systematic method to randomly generate these graphs numerically. From a graph-theoretic point of view, interesting novel insights from our work suggest that the linear and complete binary topologies are extreme cases that bound eigenvalues of dendritic networks of random shape. In practice, this result is extremely helpful for applied ecologists, because it simplifies the application of our model to real-world rivers that are not necessarily of an exact linear or binary shape. Once we know the outcome on these two extreme topologies, we can interpolate and predict results for any dendritic spatial structure.

We formulate our results by considering the critical location where a disconnection would have the most detrimental effect on the asymptotic growth rate. Site selection is fundamental in conservation ecology and management purposes, for best directing protection efforts towards locations where potential fragmentation will have the greatest impact. Our approach enables a deeper understanding of population response to fragmentation of rivers and contributes to designing better interventions to optimise species persistence.

Our model is strategic in the sense that it is flexible enough to apply to any dendritic geometry, any fish species that reproduces and disperses within river reaches (potadromous) and any obstacle to migration that partially inhibits individuals movement. For instance, it is well suited to describe the impacts of river damming on resident fish populations. The work presented in Chapter 3 complements our first contribution through the mathematical modelling of potential effects of dams on river populations, namely regulating water flow

and inhibiting fish migration. Further, the model we present serves as a baseline matrix population model that we adapt in our third contribution to assess the impacts of other types of disturbances in rivers.

The third of our contributions tackles the problem of fish persistence in river networks under negative transportable environmental disturbances. From a modelling standpoint, it is an adaptation of the matrix population model developed in our second paper, from which we remove fragmentation effects and include disturbances that affect local population growth rates. From an ecological perspective, it is a scale-up of the unidirectional water-flow concept described in the first paper to a whole river network and also an application to a specific aspect of this flow by which negative influences rather than organisms travel downstream. In practice, the model we present is appropriate to illustrate, for instance, many cases of river pollution.

We explore the extent to which downstream conditions are controlled by the inputs from upstream reaches. In addition to habitat heterogeneity, we consider two ecologically relevant scenarios: the case of a flowing river that eases the downstream transport of conditions, as opposed to the presence of lentic patches, where water is stationary or relatively still, such as buffer zones that absorb disturbances and prevent their downstream transport. After considering a single disturbance, we investigate the sensitivity of the persistence conditions, described by the asymptotic population growth, to an additional negative disturbance. Similar to our previous contribution, we pinpoint critical locations where disturbances generate serious consequences for population persistence.

Primarily, our results highlight the importance of upstream reaches in a given network through the downstream transport of conditions. More importantly, we assess the relevant contribution of each habitat patch to population persistence on the network scale. Our main insights shed light on the importance of the spatial structure of the network, as well as the movement preferences of individuals and local habitat quality in determining population persistence or extinction.

Our third study complements the work presented in our second contribution. While

the former evaluates the importance of a connection in a river network, the latter explores the importance of a habitat patch. Both studies provide a guideline for sustainable river ecosystems management and effective species conservation. Most of all, they contribute to the cumulative effects assessment of multiple environmental stresses on population persistence in rivers.

5.2 Conclusion

River systems are often the location of diverse environmental and anthropogenic disturbances, simultaneously affecting the overall state of the ecosystem and resident organisms. We have contributed in this thesis to a basis for cumulative impact assessment on persistence of populations in river systems. Each of the three studies that we conducted illustrates, through mathematical modelling, the response of organisms occupying river reaches to a given natural or human-caused disturbance. Namely, we tackle the 'drift paradox' question in our first contribution, which by nature represents a persistence challenge for stream populations. We add to this effect external temporal variation in water flow, which can be caused by either environmental variability such as seasonality or artificial control of flow as the case of flow-regulating dams. Using a stochastic framework, we show that the acute persistence threshold from analogous deterministic models is replaced by an interval of threshold values that smoothes the transition from persistence to extinction. Moreover, we identify, through numerical analysis, population mechanisms that counterbalance or adapt to the variation in water flow. In the following contribution, we address the problem of fragmentation of rivers, which is another aspect of river damming and a serious threat to persistence of populations. Disconnecting rivers affects both the geomorphological aspect of the river network and the dispersal routes of fish populations. We quantify corresponding effects using a dendritic connectivity index for potadromous fish (DCI_p) and the asymptotic population growth rate, then compare both quantities for various scenarios of habitat heterogeneity. Coupling matrix population models with numerical computations reveals the discrepancy between what eco-

logical indices measure and what population persistence conditions truly are. It also sheds light on the role played by the spatial structure of the system. The strategic framework that we develop represents a baseline for the spatially explicit modelling of populations in dendritic river networks. The interplay between water-transportable conditions and population persistence is explored in our third contribution and applies, for instance, to river pollution, where negative effects from upstream reaches are transported to downstream sites. It is a generalization of the concept of unidirectionality of the water-flow, from our first paper, to the network level, and a specification of another particular role that the water flow plays. The matrix model that we use is an adaptation from our second paper, with the inclusion of transport in local growth quality. We identify the global importance and contribution of each local habitat reach to population persistence. With all these contributions, we design a mathematical framework to answer persistence questions in rivers and to assess cumulative effects of various relatively controllable or uncontrollable disturbances. This work provides valuable contributions to conservation ecology and sustainable management efforts.

5.3 Future work

The work we presented throughout this thesis sets the basis for a cumulative impact assessment regarding the persistence of river populations. The strategic models that we developed are characterized by their simplicity in translating complex ecological situations into mathematical equations, their completeness by including necessary and sufficient ecological aspects of the question of concern and their flexibility to extend to different scales, topologies and contexts. In the following, we give a brief perspective of the possible extensions of our work. Any future contribution will necessarily rely on the basic elements incorporated in our models.

Future research questions related to our stochastic approach to the 'drift paradox' apply to either the single or the two-compartment models. One of the extensions is the inclusion of temporal variability in the net growth rate or even the dispersal rate. This variability illustrates for instance effects of climate change, such as severe drought periods, on persis-

tence of organisms that are not adapted to survive in such conditions. Similarly, exchange rates between the benthos and the drift compartments could depend on variations in time or in flow speed. Another application of the drift-benthos model considers mortality risk threatening organisms dispersing in the drift that can be caused, for example, by predation by fish. Thus it requires including an additional death term in the drift compartment. Of course, the combined effects of predation and variation in flow speeds would be another question to explore.

A wider range of applications is open for our deterministic matrix population model, two of which are already studied in our second and third contributions. A more realistic approach to the effect of fragmentation on river populations is to consider multiple barriers, not just a single one. Both the construction of our updating matrix and the dendritic connectivity index can readily account for multiple obstacles and thus move the cumulative impact assessment one step forward. Another extension of the same model would include age-structured populations, where the interplay between spatial structure, heterogeneity and dispersal preferences can have a different outcome than what we have previously found. Other obvious aspects that can be tackled based on our model are species competing for similar resources, the case of more mobile individuals, who can travel larger distances and get to non-adjacent patches in one time step, and also different life histories like diadromous fish species that do not spend all their life cycle in rivers but migrate to oceans. Similar potential research ideas apply to the same model in the context of downstream transport of upstream effects. In particular, transportable conditions can also affect survival probabilities; hence corresponding adaptations should be included in the model. Formulating a stochastic analogue to this model is also a future exploration area, for which results could compare or contrast those of the deterministic models.

We recommend first tackling each of these aspects separately, to uncover underlying mechanisms. Once we understand each case separately, we can think of combining different scenarios. Perhaps the most complicated setup that one could pose is having multiple disturbances and multiple barriers in one river system, which is more realistic, but its un-

derstanding requires a detailed explanation of each aspect separately.

Cumulative effects assessment on river populations is a multi-scale concept and is built through the analysis of one effect at a time. We have contributed to this endeavour by the present thesis, which provides a clear and precise strategic mathematical framework and represents, from both ecological and mathematical perspectives, a milestone in the assessment of cumulative impacts on populations in rivers.

Appendix A

Supplementary material to Chapter 2: Derivation of the stochastic model

Birth-Death-Emigration process

A linear birth-death-emigration process is a continuous-time Markov process. The derivation of this process for the single compartment model is explained in what follows. Let $X(t)$ be the number of individuals at time t. $X(t)$ is now a random variable. Let $p_n(t) = P[X(t) = n],\ n = 0, 1, 2, \ldots$ represent the probability that there are n individuals at time t. Assume that each individual can give birth to a new individual, can die or can leave the domain in some small time Δt. Assume also that the probability of more than one event in Δt is a higher order function of Δt. Individuals are also assumed to be independent. For a single individual, we have the following probabilities:

$$
\begin{aligned}
P[\text{1 birth in } (t, t+\Delta t] | X(t) = 1] &= \beta \Delta t + o(\Delta t) \\
P[\text{1 death in } (t, t+\Delta t] | X(t) = 1] &= \mu \Delta t + o(\Delta t) \\
P[\text{1 emigration in } (t, t+\Delta t] | X(t) = 1] &= \varepsilon \Delta t + o(\Delta t) \\
P[\text{no change in } (t, t+\Delta t] | X(t) = 1] &= 1 - (\beta + \mu + \varepsilon)\Delta t + o(\Delta t) \\
P[\text{several events in } (t, t+\Delta t] | X(t) = 1] &= o(\Delta t).
\end{aligned}
$$

The order symbol $o(\Delta t)$ denotes quantities for which

$$\lim_{\Delta t \to 0} \frac{o(\Delta t)}{t} = 0.$$

We now consider a population that consists of n individuals. To have exactly one birth event among n individuals, we must have only one individual giving birth and $n-1$ individuals who do not give birth nor die nor emigrate. There are n ways for this to happen. Hence:

$$\begin{aligned} P[\text{1 birth in } (t, t+\Delta t] | X(t) = n] &= n[\beta \Delta t + o(\Delta t)][1 - (\beta + \mu + \varepsilon)\Delta t + o(\Delta t)]^{n-1} \\ &= n\beta \Delta t + o(\Delta t). \end{aligned}$$

Similarly, we write:

$$\begin{aligned} P[\text{1 death in } (t, t+\Delta t] | X(t) = n] &= n\mu \Delta t + o(\Delta t) \\ P[\text{1 emigration in } (t, t+\Delta t] | X(t) = n] &= n\varepsilon \Delta t + o(\Delta t) \\ P[\text{no change in } (t, t+\Delta t] | X(t) = n] &= 1 - [(\beta + \mu + \varepsilon)n]\Delta t + o(\Delta t). \end{aligned}$$

With these probabilities, we write a master equation for the probability of having n individuals at a given time t, $p_n(t)$, which is again the sum of all possible probabilities: birth, death or emigration at time t. In fact, emigration acts just like an additional death term.

There are n individuals at time $t + \Delta t$ if:

- there were $n-1$ individuals at time t and one birth event occurred in Δt. The corresponding probability is $(n-1)\beta p_{n-1}(t)\Delta t + o(\Delta t)$
- there were $n+1$ individuals at time t and one death or emigration event occurred in Δt. The corresponding probability is $(n+1)(\varepsilon + \mu)p_{n+1}(t)\Delta t + o(\Delta t)$
- there were already n individuals at time t and no events occurred in Δt. The corresponding probability is $1 - [n(\beta + \mu + \varepsilon)]p_n(t)\Delta t + o(\Delta t)$.

Thus we have:

$$p_n(t+\Delta t) = (n-1)\beta\Delta t p_{n-1}(t) + [(n+1)(\mu+\varepsilon)]\Delta t p_{n+1}(t) + [1-n(\beta+\mu+\varepsilon)\Delta t]p_n(t) + o(\Delta t)$$
$$\Rightarrow \frac{p_n(t+\Delta t)-p_n(t)}{\Delta t} = (n-1)\beta p_{n-1}(t) + [(n+1)(\mu+\varepsilon)]p_{n+1}(t) - n(\beta+\mu+\varepsilon)p_n(t) + o(\Delta t). \tag{A.0.1}$$

As $\Delta t \to 0$, we get a differential equation for p_n:

$$\frac{dp_n}{dt} = (n-1)\beta p_{n-1} + [(n+1)(\mu+\varepsilon)]p_{n+1} - n(\beta+\mu+\varepsilon)p_n, \tag{A.0.2}$$

with the initial condition:

$$p_n(0) = \begin{cases} 1, & n = n_0 \\ 0, & n \neq n_0. \end{cases}$$

This is exactly equation (5) in our paper. The master equation for the two-compartment model is derived in a similar logic; see Appendix 7.2, page 33.

The expected value of this process is, by definition, $N(t) = \sum np_n(t)$. It is straightforward, but tedious, to show that the expected value satisfies equation (6) of the paper. The corresponding theory and derivation process are well known. In what follows, we include the derivation of equation (6) for the convenience of the reader.

$$\begin{aligned}
\frac{dN}{dt} &= \sum_{n=0}^{\infty} n\frac{dp_n}{dt} \\
&= \sum_{n=0}^{\infty} n\beta(n-1)p_{n-1} + \sum_{n=0}^{\infty} n(\mu+\varepsilon)(n+1)p_{n+1} - \sum_{n=0}^{\infty} n^2(\beta+\mu+\varepsilon)p_n \\
&= \sum_{n=0}^{\infty} n^2\beta p_{n-1} - \sum_{n=0}^{\infty} n\beta p_{n-1} + \sum_{n=0}^{\infty} n^2\mu p_{n+1} + \sum_{n=0}^{\infty} n^2\varepsilon p_{n+1} + \sum_{n=0}^{\infty} n(\mu+\varepsilon)p_{n+1} - \sum_{n=0}^{\infty} n^2\beta p_n \\
&\quad - \sum_{n=0}^{\infty} n^2\mu p_n - \sum_{n=0}^{\infty} n^2\varepsilon p_n.
\end{aligned} \tag{A.0.3}$$

Now we expand the sums containing p_{n-1} and p_{n+1} separately:

$$\sum_{n=0}^{\infty} n^2\beta p_{n-1} = \sum_{k=-1}^{\infty}(k+1)^2\beta p_k = 0 + \sum_{k=0}^{\infty}(k+1)^2\beta p_k = \sum_{k=0}^{\infty} k^2\beta p_k + \sum_{k=0}^{\infty} 2k\beta p_k + \sum_{k=0}^{\infty}\beta p_k$$
$$= \sum_{k=0}^{\infty} k^2\beta p_k + 2\beta N + \beta$$

$$\sum_{n=0}^{\infty} n\beta p_{n-1} = \sum_{k=-1}^{\infty}(k+1)\beta p_k = \sum_{k=0}^{\infty}(k+1)\beta p_k = \sum_{k=0}^{\infty} k\beta p_k + \sum_{k=0}^{\infty}\beta p_k = \beta N + \beta$$

$$\sum_{n=0}^{\infty} n^2\mu p_{n+1} = \sum_{k=1}^{\infty}(k-1)^2\mu p_k = \sum_{k=1}^{\infty} k^2\mu p_k - 2\sum_{k=1}^{\infty} k\mu p_k + \sum_{k=1}^{\infty}\mu p_k$$
$$= \sum_{k=0}^{\infty} k^2\mu p_k - 2\sum_{k=0}^{\infty} k\mu p_k + \sum_{k=0}^{\infty}\mu p_k - \mu p_0$$
$$= \sum_{k=0}^{\infty} k^2\mu p_k - 2\mu N + \mu - \mu p_0$$

$$\sum_{n=0}^{\infty} n^2\varepsilon p_{n+1} = \sum_{k=1}^{\infty}(k-1)^2\varepsilon p_k = \sum_{k=1}^{\infty} k^2\varepsilon p_k - 2\sum_{k=1}^{\infty} k\varepsilon p_k + \sum_{k=1}^{\infty}\varepsilon p_k$$
$$= \sum_{k=0}^{\infty} k^2\varepsilon p_k - 2\sum_{k=0}^{\infty} k\varepsilon p_k + \sum_{k=0}^{\infty}\varepsilon p_k - \varepsilon p_0$$
$$= \sum_{k=0}^{\infty} k^2\varepsilon p_k - 2\mu N + \varepsilon - \varepsilon p_0$$

$$\sum_{n=0}^{\infty} n(\mu+\varepsilon)p_{n+1} = \sum_{k=1}^{\infty}(k-1)(\mu+\varepsilon)p_k = \sum_{k=1}^{\infty} k(\mu+\varepsilon)p_k - \sum_{k=1}^{\infty}(\mu+\varepsilon)p_k$$
$$= \sum_{k=0}^{\infty} k(\mu+\varepsilon)p_k - \sum_{k=0}^{\infty}(\mu+\varepsilon)p_k + (\mu+\varepsilon)p_0$$
$$= \sum_{k=0}^{\infty} k(\mu+\varepsilon)p_k - (\mu+\varepsilon) + (\mu+\varepsilon)p_0.$$

We now replace each of these sums in the original equation (A.0.3) to get equation (6):

$$\begin{aligned}\frac{dN}{dt} =& \sum_{n=0}^{\infty} n^2\beta p_n + 2\beta N + \beta - \beta N - \beta + \sum_{n=0}^{\infty} n^2\mu p_n - 2\mu N + \mu - \mu p_0 \\ & \sum_{n=0}^{\infty} n^2\varepsilon p_n - 2\mu N + \varepsilon - \varepsilon p_0 - \sum_{n=0}^{\infty} n(\mu+\varepsilon)p_n - (\mu+\varepsilon) + (\mu+\varepsilon)p_0 \\ & - \sum_{n=0}^{\infty} n^2\beta p_n - \sum_{n=0}^{\infty} n^2\mu p_n - \sum_{n=0}^{\infty} n^2\varepsilon p_n \\ =& \beta N - \mu N - \varepsilon N \\ =& (\beta - \mu - \varepsilon)N.\end{aligned}$$

For this birth-death-emigration process, $p_n(t)$ depends on $p_n(t)$, $p_{n-1}(t)$ and on $p_{n+1}(t)$, which makes it complicated to solve. This is why we introduce the probability-generating function

$$F(t,x) = \sum_{n=0}^{\infty} p_n(t)x^n$$

that allows us to solve the problem for all the $p_n(t)$ at once. The corresponding calculations are outlined in Appendix 7.1.

Appendix B

Lexicon of ecological terms

Connectivity Landscape connectivity is defined as "the degree to which the landscape facilitates or impedes movement among resource patches" [45]. Two connectivity classes are distinguished: structural connectivity and functional connectivity. Structural connectivity refers to connectivity that is entirely based on the landscape structure and topology, with no dependence on the biological or behavioral attributes of individuals. On the other hand, functional connectivity considers organisms' behaviour and responses to elements of the landscape.

Benthic Refers to the ecological region at the lowest level of a lake, a river or an ocean. Organisms living in the benthic zone are called **benthos**.

Diadromous A life history describing fish species whose life cycle occurs partly in fresh water and partly in marine waters. Distances between reproduction and feeding zones can be up to many thousands of kilometres.

Energy expenditure The amount of energy that an individual needs to carry a physical function.

Lotic environment Refers to running-water habitats such as rivers or streams, as opposed to a **lentic environment**, which refers to standing waters such as lakes and ponds.

Potadromous A life history describing fish species whose entire life cycle takes place within freshwaters of river systems. Reproduction and feeding locations may be separated by short (a few meters) or long (hundreds of kilometers) distances.

Primary producers Organisms in an ecosystem that produce biomass from inorganic compounds (algae, grass, plants, plankton) and start the food chain. They are also known as *autotrophs*.

Reach A section of a river of defined length.

Scouring A process by which swiftly moving water scrubs river sides and the river bed, washing out primary producers from the benthic region and transporting them in the water column. In the first paper of this thesis (Chapter 2), scouring is modelled by increasing the jumping rate of benthic individuals when the flow rate increases.

Appendix C

Supplementary material to Chapter 3: Matlab codes and pseudocodes

In this appendix, the MATLAB® codes that were used to generate random dendritic networks and to assess the effect of a single obstacle on population persistence are provided. Short function files are written in pseudocodes. However, the code for the main file is given verbatim since pseudocode extending over several pages is visually not appealing. In section 1, the main code is provided. In section 2, pseudocodes for the function files used within the main code are given. In section 3, we list the codes for two modified functions that we used to generate random networks. We do not write corresponding pseudocodes, first to respect the authors' copyrights, and also because we used them as posted on the MathWorks website. We note that the actual Matlab codes for all the functions that we used are available as supplementary material to [42] on the journal's website.

C.1 The main Code

The main file to generate figures of Chapter 2 is SingleObstcaleMainFile. Running this file generates two-dimensional plots of λ and DCI_p versus the obstacle location (within the levels).

I first generate a network according to the triplet $(0, \beta, 1-\beta)$ where β is the probability of having one adjacent upstream reach to each given reach. A linear network is generated with $\beta = 1$, while a complete binary tree is generated with $\beta = 0$. For random networks, I use $\beta = 0.5$ and generate 50 random networks; values of λ and DCI_p are then averaged over these networks.

The main sections of this code are the following:

- first I generate a network and extract its adjacency matrix to build from it other population dynamics matrices. One can also plot the tree to visualize it.
- second, I define some growth quality values for each reach.
- then I introduce obstacles by changing passability and mortality values as needed. Here, one can choose to have a closed or an open network. The connectivity matrix is generated for each case, and both the dominant eigenvalue λ and the connectivity index DCI_p are calculated, then averaged over levels and networks (if applicable).
- the results are plotted in two figures: one for λ vs. obstacle location, and one for DCI_p vs. obstacle location.

The functions called within the main file are described in pseudocodes in section 2.

```
clear all; clc;

%%%%%%%%%%%%%%%%%%%%%%%%%%%%%%%%%%%%%%%%%%%%%%%%%%%%%%%%%%%%%%%%%%%%%%%%%%%%
%%% Generate random network (using GenerateRandomTree.m code)%%%%%%
%%%%%%%%%%%%%%%%%%%%%%%%%%%%%%%%%%%%%%%%%%%%%%%%%%%%%%%%%%%%%%%%%%%%%%%%%%%%
ngen=2;     %number of generations added to the first node, the tree height
    will then be ngen+1
counter_beta=0;

for beta=0   % generate different network topologies (complete binary tree,
    random and linear)
    counter_beta=counter_beta+1;

    prob_vec = [0 beta 1-beta];     % the dendrtic network is generated
        according to this probability triplet
    max_nodes=127;  % we can limit the number of nodes to a maximum. Here I am
         using the number of nodes in a complete biary tree of 7 levels.

    if beta==0 || beta==1
       NbNetworks=1;
    else NbNetworks=50;     % choose how many random networks to generate with
         beta=0.5. You will then need to average the values over all of them.
    end

    for k=1:NbNetworks

        [parents,nkids,nparents]=GenerateParentVector(prob_vec,ngen,max_nodes)
            ;     % Generate the parents vector of the tree
        % parents: is a vector (a_i) where entries are the parents of node i
        % nkids: is the number of leaves or nodes in the last level
        % nparents: is the a vector where entries are the number of nodes in
            each level

        parent=parents;
        n = length(parent);     % number of nodes in the network
        [M1,post]=AdjMatrixSO(parents,n);  % Get the Ajacency Matrix M1
            without reordering

        %%% Plot the tree
        %%%-------------
        % The following 7 lines can be commented out if one does not wish to
            plot the tree
        figure(1); trimtreeplot(parents);      % Plot the tree
        [x,y,h] = trimtreelayout(parents);    % Get the x and y coordinates of
             the nodes; h is the height of the tree
        x = x';
        y = y';
        name1 = cellstr(num2str((1:n)'));   % create labels for the nodes
        text(x(:,1), y(:,1), name1,'VerticalAlignment','bottom','
            HorizontalAlignment','right')      % Label the nodes
        title({'Dendritic Network'},'FontSize',12,'FontName','Times New Roman'
```

```
    );

%%%%%%%%%%%%%%%%%%%%%%%%%%%%%%%%%%%%%%%%%%%%%%%%
%%% Define the network characteristics%%%%%
%%%%%%%%%%%%%%%%%%%%%%%%%%%%%%%%%%%%%%%%%%%%%%%%
NbConnections=n-1;  % maximum number of connections (edges) in the
    network. In our context, this will correspond to the maximum
    number of obstacles that one can introduce in the system. In our
    paper, we only look at one obstacle.
M11=triu(M1)-eye(size(M1)); % Get the upper triangular part of
    adjacency matrix
[x11,y11]=find(M11==1);  % Find the coordinates vectors of non zeros
    elements of adjacency matrix which correspond to the coordinates (
    i,j) of the nodes connected by an edge

counter_rho=0;       % this counter is useful when one wants to test
    different values of rho automatically
for rho=1    % rho is the gradient of habitat quality. In our paper,
    we use values 1 (for homogeneous reaches), 0.8 (when reach quality
     increases downstream) and 1.1 (when reach quality increases
    upstream)
     counter_rho=counter_rho+1;

     [LengthVector,L]=LengthVec(nparents,post,rho); % Associate a
         length/weight to each node according to the gradient rho. We
         let all reaches in the same level have the same length. L is
         the sum of the lengths of reaches in the network

     rho_LocAtt=rho;      % gradient for local attributes
     rho_survival=1;      % gradient for survival. the value 1 is for
         homogeneous survival throughout the network.
     loc0=0.5;            % initial value of local attributes
     [LocAttrib,s]=WidthVelocityLocAttVecSO(nparents,post,rho_LocAtt,
         rho_survival,loc0);    % generate a vector for local attributes
          or conditions, and a vector of survival probabilities at
         different reaches

     r=exp(LocAttrib');    % local growth vector
     rs=diag(r+s',0);    % diagonal matrix combining growth and survival

     %%%%%%%%%%%%%%%%%%%%%%%%%%%%%%%%
     %%% Introduce obstacles %%%%%
     %%%%%%%%%%%%%%%%%%%%%%%%%%%%%%%%
     prob=0.5; % probability of moving at all
     delta=0;    % obstacle induced mortality. In our paper, we use
         values 0 (for no mortality) and 0.5 (for 50% mortality of
         individuals)
     counter=0;

     for NbObstacles=0:1; % 0 is for no obstcales, 1 is for one
         obstacle. The code can be edited to account for more than one
```

```
obstacle.
if NbObstacles==0
    B=[];   % preallocate the projection matrix
    lambda=[]; % preallocate the lambda vector
    counter=counter+1;

    alpha=1;    % alpha is the passability of each obstacle.
        When there are no obstacles in the system, alpha is
        always 1 (completely passable).
    DCIP(counter,1)=1; % When there are no obstacles, the
        connectivity index is always 1.

    %%% Define the population dynamics related matrices and
        choose to open or close the system at the bottom
    %%%-----------------------------------------------------
    % U: is a lower triangular matrix with upstream movement
        probabilities between nodes
    % D: is an upper triangular matrix with downstream
        movement probabilities between nodes
    % M_tild: is the uninhibited movement matrix; corresponds
        to M in the paper
    % O: is the obstacles matrix
    % O_tild: is the failing of passing matrix
    % Delta: is the obstacle induced mortality matrix
    % Delta1, Delta2: are as defined ion the paper. Delta3=
        Delta1+Delta2
    % C: is the conectivity matrix

    %%% Depending on the situation, adjust the following
        function for closed or open networks
    %%%-----------------------------------------------------
    [U,D,M_tild,O,O_tild,Delta,Delta1,Delta2,Delta3,C]=
        MatricesNoObstaclesSO(M1,n,prob,nkids,delta);

    B=C*rs;     %updating matrix from a generation (with
        migration) to the other
    lambda(counter,1)=max(eig(B)); % the dominant eigenvalue
        for each case

elseif NbObstacles>0 && NbObstacles<= NbConnections
    alpha=0.5;      % 50% partial passability
    alpha_u=alpha;
    alpha_d=alpha;

    counter=counter+1;
    NbSections=NbObstacles+1;
    m=[];

  %%% Choose the possible obstacle locations. Can also be set
      manually for a single obstacle, but is automated to be
      easily edited for multiple obstacles
```

```
        %%%-------------------------------------------------------------
          m=nchoosek(1:n-1,NbObstacles);   %get all possible
              obstacles locations according to the given number of
              obstcales wanted (combination process)
          B=[];
          qmax=size(m,1);       % maximum number of obstacle locations

          for q=1:qmax
               %%% Build the obstacles associated matrices with
                   obstacles
               %%%-------------------------------------------------------
               [U,D,M_tild,O,O_tild,Delta,Delta1,Delta2,Delta3,C]=
                   MatricesWithObstaclesSO(M1,n,prob,x11,y11,alpha_u
                   ,alpha_d,q,m,delta);

                 B=C*rs;         % updating matrix
                 lambda(counter,q)=max(eig(B));    % find the
                     dominant eigenvalue of matrix B

              %%% Construct a matrix containing the different groups
                   of nodes (sections) formed by the obstacles
              %%%-------------------------------------------------------
               if alpha==1
                   DCIP(counter,q)=1;
               else
                   [S,SectionLengthVec,C2]=
                       SectionsAndPassabilitiesMatricesSO(NbSections,
                       NbConnections,x11,y11,LengthVector,O,parent,
                       parents,ngen,n,alpha); % Construct passability
                        matrix to calculate DCIp
                   % S: is a matrix regrouping nodes to form sections
                        separated by the obstacles. It is only used
                       to construct C2.
                   % SectionLengthVec: is a vector whose entries are
                       the lengths of the two sections formed by
                       introducing the obstacle
                   % C2: is the passability between sections matrix
                       used to calculate DCIp

                   [DCIP(counter,q)]=DCIpMultipleObstacles(NbSections
                       ,SectionLengthVec,C2);     % Calculate DCIp for
                        each obstacle location
               end
          end

      elseif NbObstacles> NbConnections
               fprintf('The Nb of obstacles should be smaller than
                   the Nb of Connections')
      end
  end
```

```
            DCIpAvrg=[];
            LamAvrg=[];

            %%% Average DCIp and lambda over levels
            %%%-----------------------------------------
            [DCIpAvrg1,LamAvrg1]=AverageOverLevelsDCIpLambdaSO(nparents,post,
                DCIP(2,:),lambda(2,:));
            DCIpAvrg(:,k)=[DCIP(1,1); DCIpAvrg1']; % put values in one vector
            LamAvrg(:,k)=[lambda(1,1); LamAvrg1'];

        end
        %%% Average over the different random networks
        %%%-----------------------------------------------
        DCIpAvrgNet=sum(DCIpAvrg,2)./sum(DCIpAvrg~=0,2);
        LamAvrgNet=sum(LamAvrg,2)./sum(LamAvrg~=0,2);

    end
    DCIPAvrg(counter_beta,:)=DCIpAvrgNet'; % transpose to row vectors
    LAMAvrg(counter_beta,:)=LamAvrgNet';

    %%%%%%%%%%%%%%%%%%%%%%%%%%
    %%% Plot the results %%%%%
    %%%%%%%%%%%%%%%%%%%%%%%%%%
    figure(2);
    h1=plot(0:ngen,DCIPAvrg(counter_beta,:));
    clabel([beta 0:ngen ;length(DCIPAvrg(counter_beta,:)) DCIPAvrg(
        counter_beta,:)],h1,'LabelSpacing',1000);
    ylabel('DCI_p')
    xlabel('Obstacle location (Levels)')
     set(gca,'Xtick',0:6,'XTickLabel',{'No Obstacle','1','2','3','4','5','6'})
         ;
    title({['\rho =',num2str(rho),', passability \alpha =',num2str(alpha),',
        mortality e=',num2str(delta)]})
    hold on;

    figure(3);
    h2=plot(0:ngen,LAMAvrg(counter_beta,:));
    clabel([beta 0:ngen ;length(LAMAvrg(counter_beta,:)) LAMAvrg(counter_beta
        ,:)],h2,'LabelSpacing',1000);
    ylabel('\lambda')
    xlabel('Obstacle location (Levels)')
     set(gca,'Xtick',0:6,'XTickLabel',{'No Obstacle','1','2','3','4','5','6'})
         ;
    title({['\rho =',num2str(rho),', passability \alpha =',num2str(alpha),',
        mortality e=',num2str(delta)]})
    hold on;
end
```

C.2 Pseudocodes for function files

Algorithm C.2.1: GENERATEPARENTVECTOR($probvec, ngen, maxnodes$)

```
% Generate the parents vector for each tree graph
maxkids = length(probvec) − 1            % maximal number of children
cumprob = [cumsum(probvec)1]             % distribution function
parents = 0
extinct = 0
nkids = 1            % number of children in the last generation
for i ← 1 to ngen
do { % indices of individuals in the previous generation
     gprevi = length(parents) − nkids + 1 : length(parents)
     npar ← nkids
     nparents(i) = npar            % Count the number of reaches/nodes in every level
     % generate a set of numbers of children for all individuals according to the distribution
     runi = rand(1, npar)            % a uniform sample
     % add the kids to the tree
     nkids = 0
     for j ← 1 to maxkids
     do { % find indexes of the parents who give birth to j children
          jpi = gprevi(find((runi > cumprob(j)) and (runi ≤ cumprob(j + 1))))
          if not isempty(jpi)
          then { parents ← [parentsrepmat(jpi, 1, j)]
                 parents ← sort(parents)
                 parentsi ← parents            % redefine the same vector to cut if needed
                 % cut the tree if the number of nodes exceeds the maximum number of nodes
                  you want to have
                 if length(parents) > maxnodes
                 then { parents ← [parentsi(1 to maxnodes)]
                        parents ← sort(parents)
                        nkids ← nkids + length(jpi) ∗ j − length(parentsi(maxnodes + 1 to end))
                 else { parents ← sort(parents)
                        nkids ← nkids + length(jpi) ∗ j
          }
     % exit if no individuals left
     if nkids ← 0
     then { extinct = 1
            break
     }
if nkids ≠ 0
  then nparents ← [nparentsnkids]            % Add the number of nodes/reaches of the last generation
  else nparents ← nparents
if extinct
  then return (Extinct in generation i)
  else return (Stopped in generation ngen)return (parents, nkids, nparents)
```

Algorithm C.2.2: AdjMatrixSO($parents, n$)

```
% Get the adjacency matrix of the graph
parent ← parents
j = find(parent)
A_1 = sparse(parent(j), j, 1, n, n)
A_1 ← A_1 + A1' + speye(n, n)
M_1 = full(A_1)
[ignore, post] = etree(A_1)
return (M_1, post)
```

Algorithm C.2.3: LengthVec($nparents, post, rho$)

```
% This routine sets all reaches in the same level to the same length
l = 1
t = 1
i = 1
l_0 = 10
while l ≤ length(nparents) and nparents(l) ≠ 0
  do { for j ← post(t) to post(t) + nparents(l) − 1
         do LengthVector(j) = ρ^(i−1) * l_0
       i ← i + 1
       t ← t + nparents(l)
       l ← l + 1
L ← sum(LengthVector)
return (L, LengthVector)
```

Algorithm C.2.4: WidthVelocityLocAttVecSO($nparents, post, rho_{LocAtt}, rho_{survival}, loc_0$)

```
% Use the gradient ρ to generate a vector of local qualities and survival probabilities
 for each reach
l = 1
t = 1
i = 1
s_0 = 0.5
% Make all reaches at the same level have the same survival and local attributes
while l ≤ length(nparents) and nparents(l) ≠ 0
  do { for j ← post(t) to post(t) + nparents(l) − 1
         do { s(j) = (ρ_survival)^(i−1) * s_0
              LocAttrib(j) = (ρ_LocAtt)^(i−1) * loc_0
       i ← i + 1
       t ← t + nparents(l)
       l ← l + 1
return (LocAttrib, s)
```

Algorithm C.2.5: MATRICESNOOBSTACLESSO$(M_1, n, prob, nkids, \delta)$

% Generate the population dynamics related matrices for a closed network without obstacles
$O \leftarrow M_1$
$\tilde{O} \leftarrow zeros(n, n)$
$M_1(1 : size(M_1) + 1 : end) \leftarrow 0$
$d = prob/2$
$u = prob/2$
$Upper \leftarrow triu(M_1)$
$D = d * Upper$
$Lower \leftarrow tril(M_1)$
$Sum = sum(Lower)$
$U \leftarrow zeros(size(Lower))$
for $i \leftarrow 1$ **to** $size(Lower, 1)$
do { **if** $Sum(:, i) \neq 0$
then $U(:, i) = u * (Lower(:, i)/(Sum(:, i)))$
else $U(:, i) = zeros(1, n)'$
$\tilde{M} = U + D$ % movement restricted matrix
$\Delta \leftarrow zeros(n, n)$
$\Delta_1 = \tilde{O} * \Delta * \tilde{M}$
$\Delta_2 = O * \tilde{M}$
$\Delta_3 = \Delta_1 + \Delta_2$
$\Delta_3 = eye(n) - diag(sum(\Delta_3))$
$C = \Delta_2 + \Delta_3$
% For an Open system at the bottom (root) set the first entry to be 0
$C(1, 1) = 0$
return $(U, D, \tilde{M}, O, \tilde{O}, \Delta, \Delta_1, \Delta_2, \Delta_3, C)$

Algorithm C.2.6: MATRICESWITHOBSTACLESSO$(M_1, n, prob, x11, y11, \alpha_u, \alpha_d, q, m, \delta)$

```
% Generate the population dynamics related matrices for a closed network with obstacles
O ← M1
Õ ← zeros(n, n)
for i ← 1 to size(m, 2)
  do { O(x11(m(q, i)), y11(m(q, i))) = α_d
       O(y11(m(q, i)), x11(m(q, i))) = α_u
       Õ(x11(m(q, i)), y11(m(q, i))) = 1 − α_d
       Õ(y11(m(q, i)), x11(m(q, i))) = 1 − α_u
       % Mortality associated to obstacles Matrix
       Δ ← zeros(n, n)
       Δ(x11(m(q, i)), y11(m(q, i))) = δ
       Δ(y11(m(q, i)), x11(m(q, i))) = δ
M1(1 : size(M1) + 1 : end) = 0
d = prob/2
u = prob/2
Upper ← triu(M1)
D = d ∗ Upper
Lower ← tril(M1)
Sum = sum(Lower)
U ← zeros(size(Lower))
for i ← 1 to size(Lower, 1)
  do { if Sum(:, i) ≠ 0
       then U(:, i) = u ∗ (Lower(:, i)/(Sum(:, i)))
       else U(:, i) = zeros(1, n)′
M̃ = U + D
Δ1 = Õ ∗ Δ ∗ M̃
Δ2 = O ∗ M̃
Δ3 = Δ1 + Δ2
Δ3 = eye(n) − diag(sum(Δ3))
C = Δ2 + Δ3
% For an Open system at the bottom (root) set the first entry to be 0
C(1, 1) = 0
return (U, D, M̃, O, Õ, Δ, Δ1, Δ2, Δ3, C)
```

Algorithm C.2.7: SectionsAndPassabilitiesMatricesSO($NbSections, NbConnections, x11, y11, LengthVector, O, parent, parents, ngen, n, \alpha$)

```
% Build the sections matrix S, and the passabilities between sections matrix C_2
 to calculate DCI_p
S ← zeros(NbSections, (2 * n))
count = 0
S_1 ← [ ]
S_2 ← [ ]
for j ← 1 to NbConnections
do { if O(x11(j), y11(j)) = 1
       then { if isempty(find(S = x11(j)))
                then { count ← count + 1
                       S_1 ← [ ]
                       S(count, :) = [S_1  x11(j)  y11(j)  zeros(1, (2 * n) − length(S_1) − 2)]
                       S_1 = S(count, :)
                       S_1 ← S_1(S_1 ≠ 0)
              else if not isempty(find(S = x11(j)))
                then { [t, f] ← find(S = x11(j))
                       t ← t(1)
                       S_1 ← S(t, :)
                       S_1 ← S_1(S_1 ≠ 0)
                       S(t, :) = [S_1  x11(j)  y11(j)  zeros(1, (2 * n) − length(S_1) − 2)]
     else if O(x11(j), y11(j)) = α
       then { if isempty(find(S = x11(j)))
                then { count ← count + 1
                       S_1 ← [ ]
                       S(count, :) = [S_1  x11(j)  zeros(1, (2 * n) − length(S_1) − 1)]
                       S_1 = S(count, :)
                       S_1 ← S_1(S_1 ≠ 0)
              if isempty(find(S = y11(j)))
                then { count ← count + 1
                       S_2 ← [ ]
                       S(count, :) = [S_2  y11(j)  zeros(1, (2 * n) − length(S_2) − 1)]
                       S_2 = S(count, :)
                       S_2 ← S_2(S_2 ≠ 0)

              else if not isempty(find(S = y11(j)))
                then { [t, f] = find(S = x11(j))
                       t ← t(1)
                       S_2 = S(t, :)
                       S_2 ← S_2(S_2 ≠ 0)
                       S(t, :) = [S_2  y11(j)  zeros(1, (2 * n) − length(S_2) − 1)]
                       S(t, :) ← S_2
% Construct a vector containing the length of each section formed by the obstacles
SectionLengthVec ← [ ]
for j ← 1 to size(S, 1)
do { SS = S(j, :)
     SS ← SS(SS ≠ 0)
     SS = unique(SS)
     for i ← 1 to length(SS)
       do {L(i) = LengthVector(SS(i))  SectionLengthVec(j) = sum(L)
     L ← [ ]
```

```
% Construct the passabilities matrix
C2 ← ones(NbSections, NbSections)
for i ← 1 to NbSections
  do { SS1 = S(i,1)
       for j ← 1 to NbSections
         do { if j = i
              then C2(i,j) = 1
              else if j > i
                then { SS2 ← S(j,1)
                       if O(SS1,SS2) ≠ 0
                         then C2(i,j) = O(SS1,SS2) * O(SS2,SS1)      % entries of C2 are powers of
                                                                       alpha_d * alpha_u
                       else if O(SS1,SS2) = 0
                         then { path ← [ ]
                                [p1] = NodesDown(parent, SS1, parents, ngen)
                                [p2] = NodesDown(parent, SS2, parents, ngen)
                                [a, ai, bi] = intersect(p1, p2)
                                if not isempty(find(a ≠ 1))
                                  then { a ← max(a(find(a ≠ 1)))
                                         c ← find(p1 = a)
                                         p1 ← p1(1 to c)
                                         b ← find(p2 = a)
                                         p2 ← p2(1 to b) }
                                path = [p1  fliplr(p2)]
                                for k ← 1 to length(path) − 1
                                  do pp(k) = O(path(k), path(k+1)) * O(path(k+1), path(k))
                                C2(i,j) = prod(pp)
                                pp ← [ ] } } }
C2 = triu(C2) − eye(length(C2)) + triu(C2)′
return (S, SectionLengthVec, C2)
```

Algorithm C.2.9: NODESDOWN($parent, y_1, parents, ngen$)

```
% Find the nodes location downstream of a given node
p ← [ ]                % preallocate p
p(1) ← parent(y_1)
if p(1) ≠ 0
  then { p_1 ← p(1)
         j = 2
         while j ≤ (length(p) + 1)
           do { for i ← j
                do { if parents(p(i − 1)) ≠ 0
                     then { p(i) ← parents(p(i − 1))
                            p_1 = [p_1  p(i)]
                     else p_1 ← p_1
                j ← j + 1
         p_1 ← [y_1  p_1]          % downstream ancestors of node t1
  else p_1 ← y_1
% We can also find the path from node t1 all the way down to node 1,
 then all the way up to the same node t1
p_2 = sort(p_1)
p_2 ← [p_1  p_2(2 to end)]
return (p_1, p_2)
```

Algorithm C.2.10: DCIPMULTIPLEOBSTACLES($NbSections, SectionLengthVec, C2$)

```
% Calculate the connectivity index DCIp
a ← zeros(NbSections, NbSections)
l ← SectionLengthVec
L ← sum(l)
for i ← 1 to NbSections
  do { for j ← 1 to NbSections
       do a(i, j) = l(i) ∗ l(j) ∗ C2(i, j)
DCIP = sum(sum(a))/(L^2)
return (DCIP)
```

Algorithm C.2.11: AVERAGEOVERLEVELSDCIPLAMBDASO($nparents, post, DCIPk, Lambdak$)

```
% Average values of DCIp and lambda over levels to get one value for each level
t = 1
l = 2        % when averaging over the second row of lambda and DCIp; use 1 when there is one row
i = 1
while l ≤ length(nparents) and nparents(l) ≠ 0
  do { j ← post(t) to post(t) + nparents(l) − 1
       DCIpAvrg(i) = sum(DCIPk(j))/nparents(l)
       LamAvrg(i) = sum(Lambdak(j))/nparents(l)
       i ← i + 1
       t ← t + nparents(l)
       l ← l + 1
return (DCIpAvrg, LamAvrg)
```

C.3 Matlab codes needed for plotting a tree graph

C.3.1 Code for 'trimtreelayout' function

```
function [x,y,h,s] = trimtreelayout(parent,post)
%   TRIMTREELAYOUT A modified standard function TREELAYOUT.
%     Produces different heights for the leaves. They appear in
%     their respective layer instead of the deepest layer. The
%     format is the same as for TREELAYOUT, see below.
%
%   [x,y,h,s] = trimtreelayout(parent,post)
%
%
%   TREELAYOUT Lay out tree or forest.
%   [x,y,h,s] = treelayout(parent,post)
%       parent is the vector of parent pointers, with 0 for a root.
%       post is a postorder permutation on the tree nodes.
%       (If post is omitted we compute it here.)
%       x and y are vectors of coordinates in the unit square at which
%       to lay out the nodes of the tree to make a nice picture.
%       Optionally, h is the height of the tree and s is the
%       number of vertices in the top-level separator.
%
%   See also ETREE, TREEPLOT, ETREEPLOT, SYMBFACT.

%   Copyright 1984-2000 The MathWorks, Inc.
%   $Revision: 5.11 $  $Date: 2000/06/08 20:18:46 $
%
%   Modified by RG 01-Nov-1 to plot the leaves in the right layer
%

% This is based on the C code in sptrees.c by John Gilbert.
% Leaves are spaced evenly on the x axis, and internal
% nodes are centered over their descendant leaves with
% y coordinate proportional to height in the tree.

n = length(parent);

 pv = [];
 if (size(parent,1)>1), parent = parent(:)'; end
 if (nargin<2) & ~all(parent==0 | parent>(1:n))
     % This does not appear to be in the form generated by ETREE.
      if (any(parent>n) | any(parent<0) | any(parent~=floor(parent)) ...
          | any(parent==[1:n]))
         error('Bad vector of parent pointers.');
      end
      [parent,pv] = fixparent(parent);
 end

if nargin < 2,
```

```
    % Create the adjacency matrix A of the given tree,
    % and get the postorder with another call to etree.

    j = find(parent);
   A = sparse (parent(j), j, 1, n, n);
    A = A + A' + speye(n,n);
    M=full(A);
    [ignore, post] = etree(A);
%    post
end;

% Add a dummy root node #n+1, and identify the leaves.

parent = rem(parent+n, n+1) + 1;  % change all 0s to n+1s
isaleaf = ones(1,n+1);
isaleaf(parent) = zeros(n,1);

% In postorder, compute heights and descendant leaf intervals.
% Space leaves evenly in x (in postorder).

xmin = n(1,ones(1,n+1)); % n+1 copies of n
xmax = zeros(1,n+1);
height = zeros(1,n+1);
nkids = zeros(1,n+1);
nleaves = 0;

for i = 1:n,
    node = post(i);
    if isaleaf(node),
        nleaves = nleaves+1;
        xmin(node) = nleaves;
        xmax(node) = nleaves;
    end;
    dad = parent(node);
    %RG
%    height(dad) = max (height(dad), height(node)+1);
    xmin(dad)   = min (xmin(dad),   xmin(node));
    xmax(dad)   = max (xmax(dad),   xmax(node));
    nkids(dad)  = nkids(dad)+1;
end;

% RG compute heights
% traverse the tree from the root downwards in a layer-manner
lay_ind = n+1;
par_ind = n+1;
while(1)
  lay_ind = find(ismember(parent, lay_ind));
  if isempty(lay_ind)
    break;
  end
  par_ind = [par_ind lay_ind];
```

```
  height(par_ind) = height(par_ind)+1;
end
height(1:n) = height(1:n)-1;

% Compute coordinates, leaving a little space on all sides.

% treeht = height(n+1) - 1; % plots the tree upwards from root to leaves with
    root on the x axis
treeht = height(n+1) ;  % plots the tree upwards from root to leaves inside
    the xy plane
deltax = 1/(nleaves+1);
deltay = 1/(treeht+2);
x = deltax * (xmin+xmax)/2;
% y = deltay * (height+1);  % plot the tree downwards from root to leaves
y = deltay * (treeht-height);  % plot the tree upwards from root to leaves

% Omit the dummy node.

x = x(1:n);
y = y(1:n);

% Return the height and top separator size.


h = treeht;
s = n+1 - max(find(nkids~=1));

if ~isempty(pv)
   x(pv) = x;
   y(pv) = y;
end

% ---------------------------
function [a,pv] = fixparent(parent)
%FIXPARENT  Fix order of parent vector
%   [A,PV] = FIXPARENT(B) takes a vector of parent nodes for an
%   elimination tree, and re-orders it to produce an equivalent vector
%   A in which parent nodes are always higher-numbered than child
%   nodes.  If B is an elimination tree produced by the TREE
%   functions, this step will not be necessary.  PV is a
%   permutation vector, so that A = B(PV);

n = length(parent);
a = parent;
a(a==0) = n+1;
pv = 1:n;

niter = 0;
while(1)
   k = find(a<(1:n));
   if isempty(k), break; end
```

```
    k = k(1);
    j = a(k);

    % Put node k before its parent node j
    a  = [ a(1:j-1)  a(k)  a(j:k-1)  a(k+1:end)] ;
    pv = [pv(1:j-1) pv(k) pv(j:k-1) pv(k+1:end)] ;
    t = (a >= j & a < k);
    a(a==k) = j;
    a(t) = a(t) + 1;

    niter = niter+1;
    if (niter>n*(n-1)/2), error('Bad vector of parent pointers.'); end
end

a(a>n) = 0;
a;
```

C.3.2 Code for 'trimtreeplot' function

```
function trimtreeplot(p,c,d)
% TRIMTREEPLOT A modified standard function TREEPLOT. Plots the
%   leaves differently from TREEPLOT. They appear in their
%   respective layer instead of the deepest layer so that the tree
%   appears as "trimmed". The format is the same as for TREEPLOT,
%   see below.
%
% trimtreeplot(p [,c,d])
%
% TREEPLOT Plot picture of tree.
%   TREEPLOT(p) plots a picture of a tree given a vector of
%   parent pointers, with p(i) == 0 for a root.
%
%   TREEPLOT(P,nodeSpec,edgeSpec) allows optional parameters nodeSpec
%   and edgeSpec to set the node or edge color, marker, and linestyle.
%   Use '' to omit one or both.
%
%   See also ETREE, TREELAYOUT, ETREEPLOT.

%   Copyright (c) 1984-98 by The MathWorks, Inc.
%   $Revision: 5.8 $  $Date: 1997/11/21 23:44:59 $
%
%   Modified by RG 01-Nov-1 to use trimtreelayout instead of
%   TREELAYOUT

% RG use another treelayout
%[x,y,h]=treelayout(p);
[x,y,h]=trimtreelayout(p);

f = find(p~=0);
pp = p(f);
X = [x(f); x(pp); repmat(NaN,size(f))];
```

```
Y = [y(f); y(pp); repmat(NaN,size(f))];
X = X(:);
Y = Y(:);

if nargin == 1,
    n = length(p);
    if n < 500,
        plot (x, y, 'ro', X, Y, 'r-');
    else,
        plot (X, Y, 'r-');
    end;
else,
    [ignore, clen] = size(c);
    if nargin < 3,
        if clen > 1,
            d = [c(1:clen-1) '-'];
        else,
            d = 'r-';
        end;
    end;
    [ignore, dlen] = size(d);
    if clen>0 & dlen>0
        plot (x, y, c, X, Y, d);
    elseif clen>0,
        plot (x, y, c);
    elseif dlen>0,
        plot (X, Y, d);
    else
    end;
end;
xlabel(['height = ' int2str(h)]);
axis([0 1 0 1]);
```

Appendix D

Supplementary Material to Chapter 4: Comparison of results between a complete binary tree with 7 nodes and a complete binary tree with 7 levels

This appendix complements and supports results for Chapter 4. Since a detailed description and presentation of all the cases studied is beyond the scope of the paper, we provide and compare the numerical results for the case of a complete binary tree of height 7 and one of size 7. The table below serves as a road map to easily locate the corresponding page to each case. We note that different cases depend on the homogeneity of reaches within a network, the closeness of the network and the downstream transport of the disturbance.

Case of a single disturbance	$\rho = 1$	$\rho < 1$	$\rho > 1$
Closed network	Table D.1	Table D.3	Table D.5
Open network	Table D.2	Table D.4	Table D.6

Case of two disturbances	$\rho = 1$	$\rho < 1$	$\rho > 1$
Closed network	Table D.7	Table D.9	Table D.10
Open network	Table D.8		

Table D.1: The case of a closed homogeneous network

Cases	Complete binary tree with 7 nodes (3 levels)	Complete binary tree with 7 levels (127 nodes)
$\rho = 1$ closed No transport	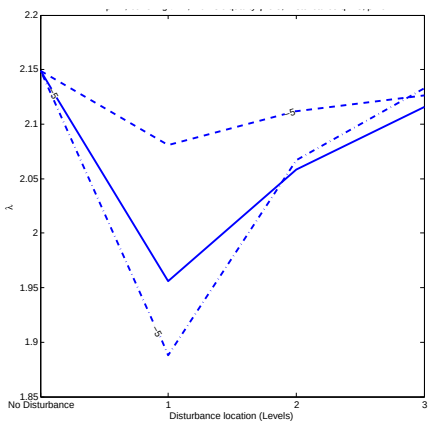	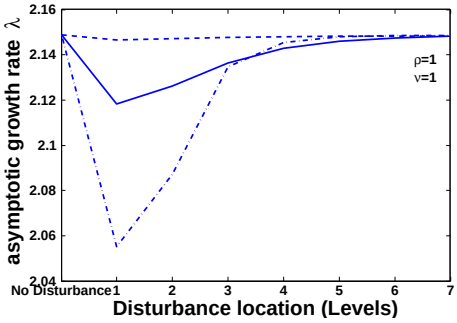
$\rho = 1$ closed Transport	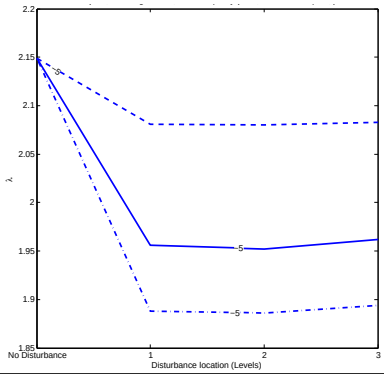	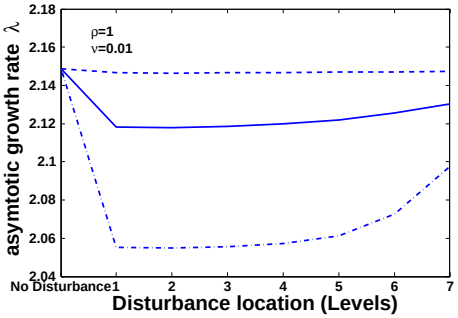
$\rho = 1$ closed Sensitivity Analysis	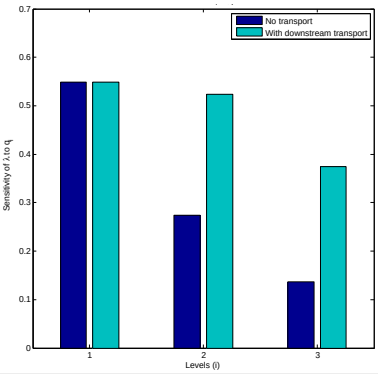	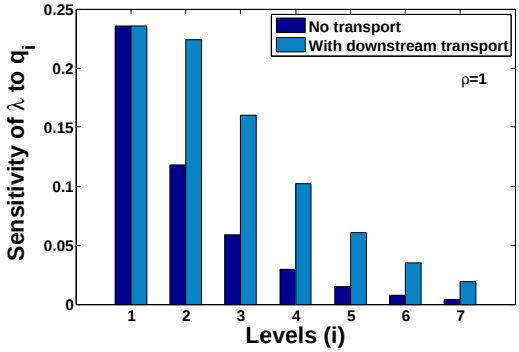

Table D.2: The case of an open homogeneous network

Cases	Complete binary tree with 7 nodes (3 levels)	Complete binary tree with 7 levels (127 nodes)
$\rho = 1$ open No transport	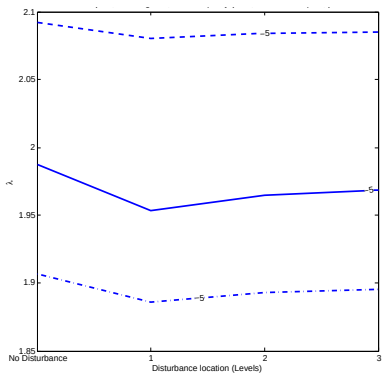	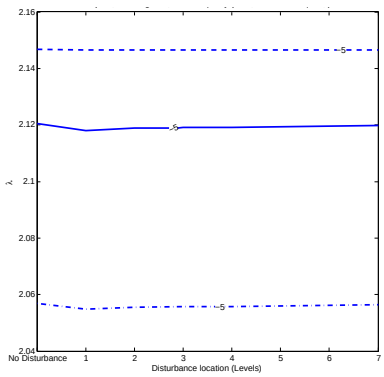
$\rho = 1$ open Transport	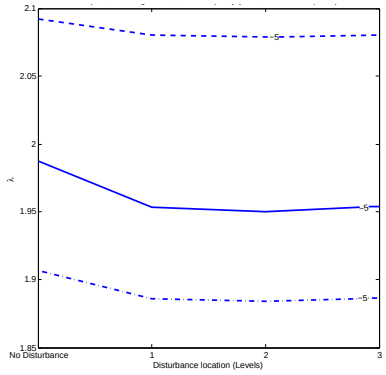	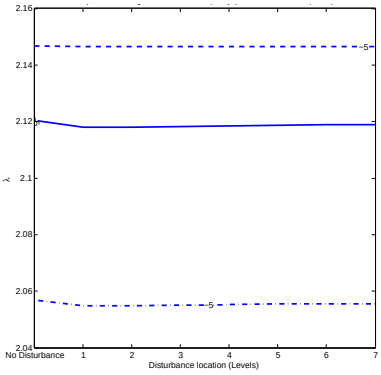
$\rho = 1$ open Sensitivity Analysis	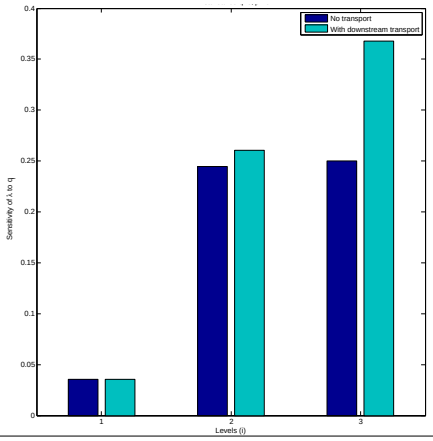	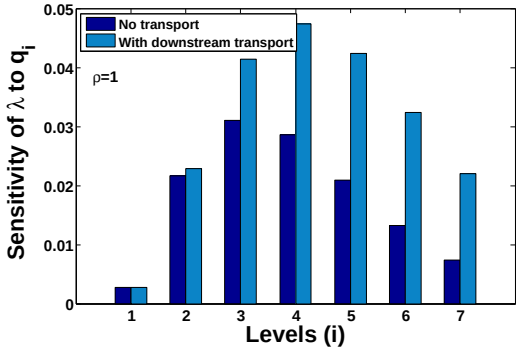

Table D.3: The case of a closed heterogeneous network ($\rho < 1$)

Cases	Complete binary tree with 7 nodes (3 levels)	Complete binary tree with 7 levels (127 nodes)
$\rho < 1$ closed No transport	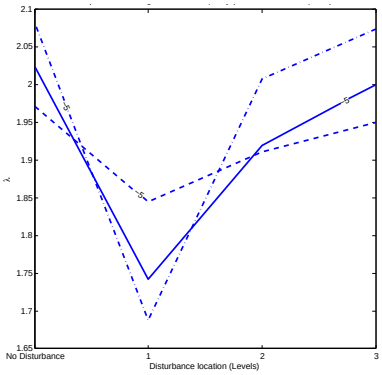	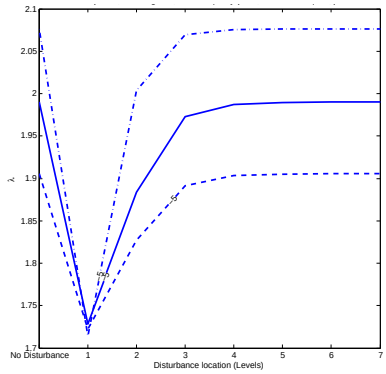
$\rho < 1$ closed Transport	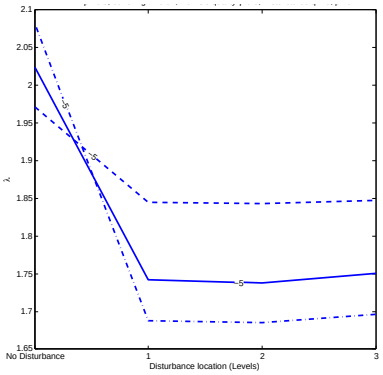	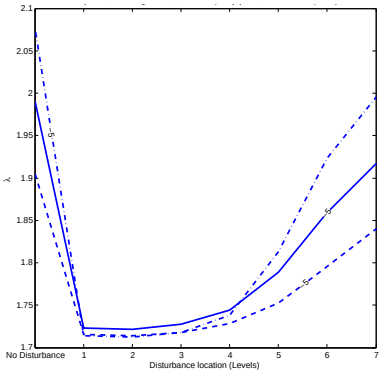
$\rho < 1$ closed Sensitivity Analysis	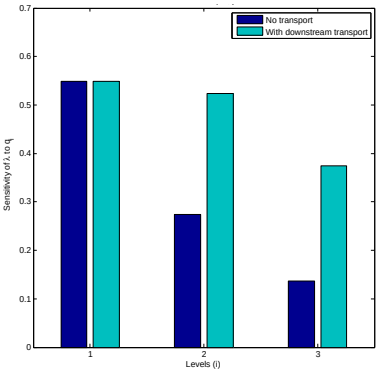	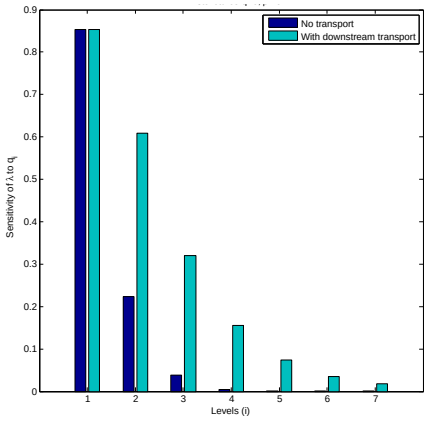

Table D.4: The case of an open heterogeneous network ($\rho < 1$)

Cases	Complete binary tree with 7 nodes (3 levels)	Complete binary tree with 7 levels (127 nodes)
$\rho < 1$ open No transport	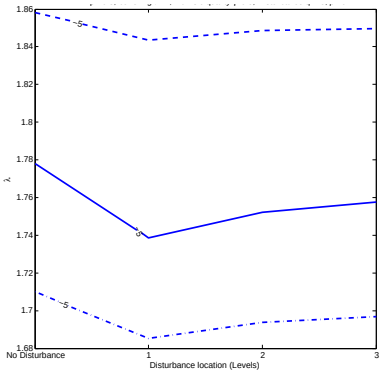	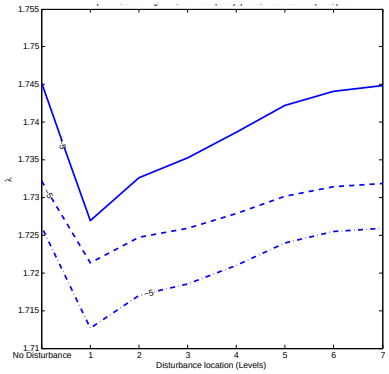
$\rho < 1$ open Transport	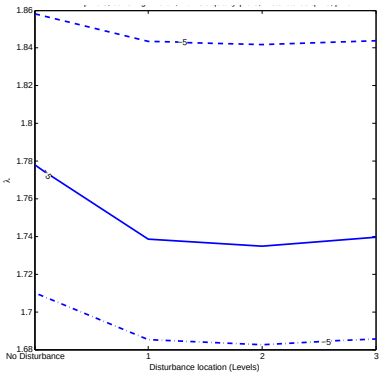	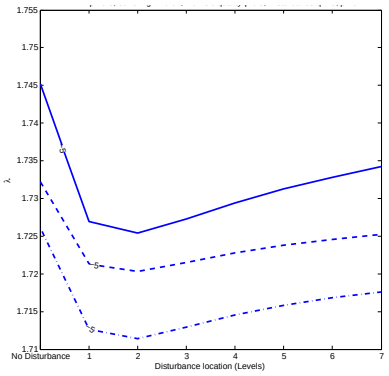
$\rho < 1$ open Sensitivity Analysis	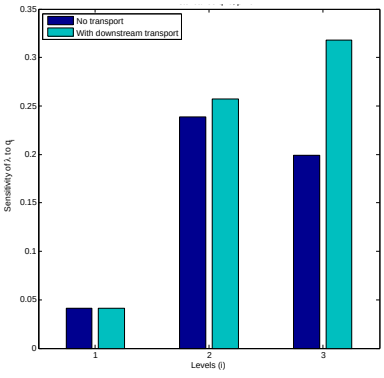	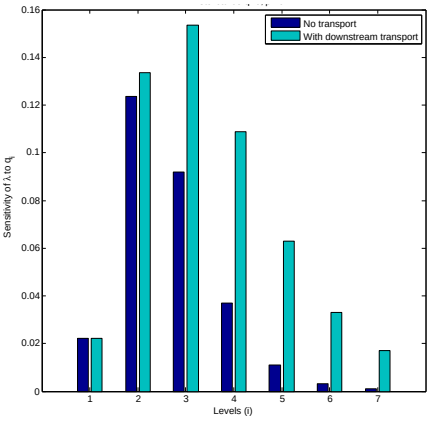

Table D.5: The case of a closed heterogeneous network ($\rho > 1$)

Cases	Complete binary tree with 7 nodes (3 levels)	Complete binary tree with 7 levels (127 nodes)
$\rho > 1$ closed No transport	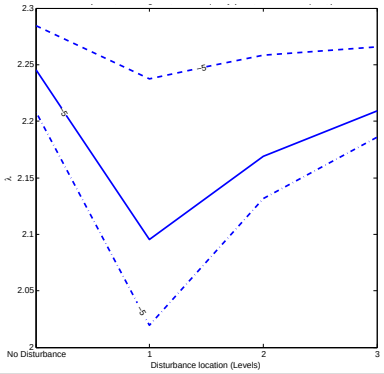	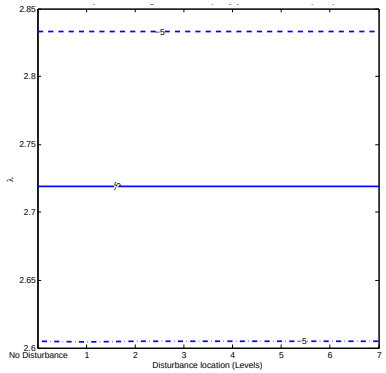
$\rho > 1$ closed Transport	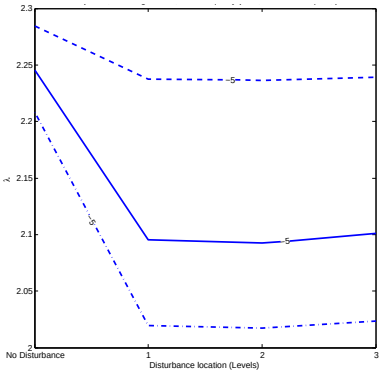	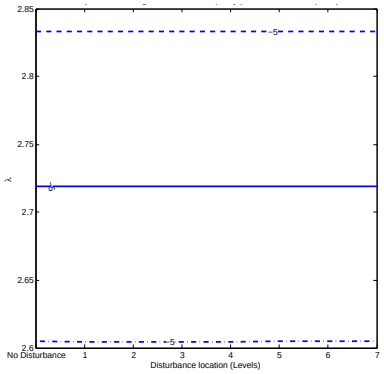
$\rho > 1$ closed Sensitivity Analysis	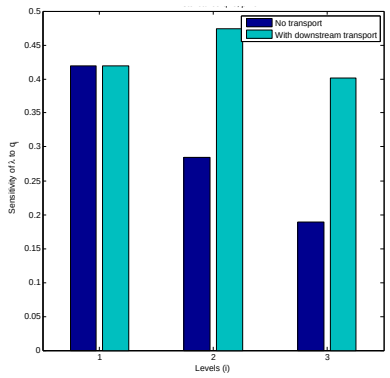	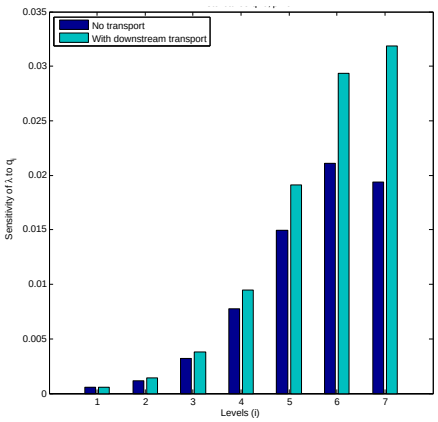

Table D.6: The case of an open heterogeneous network ($\rho > 1$)

Cases	Complete binary tree with 7 nodes (3 levels)	Complete binary tree with 7 levels (127 nodes)
$\rho > 1$ open No transport	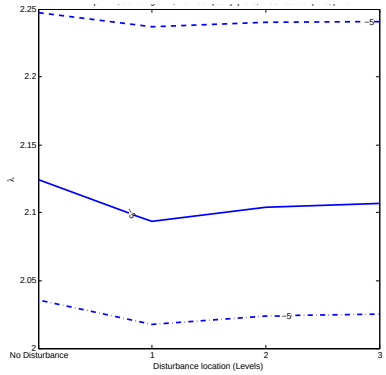	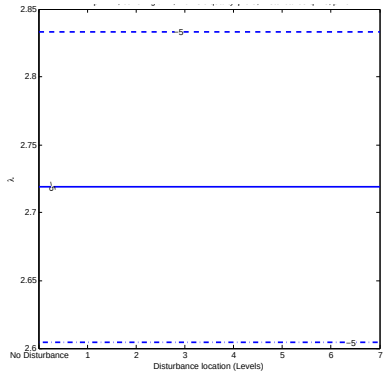
$\rho > 1$ open Transport	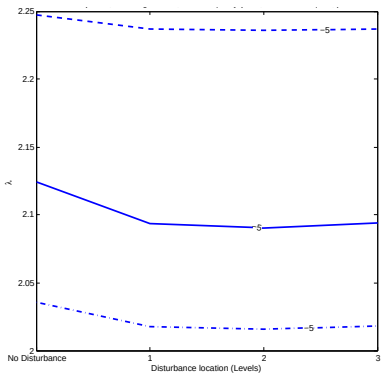	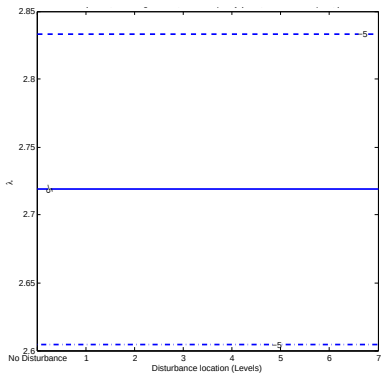
$\rho > 1$ open Sensitivity Analysis	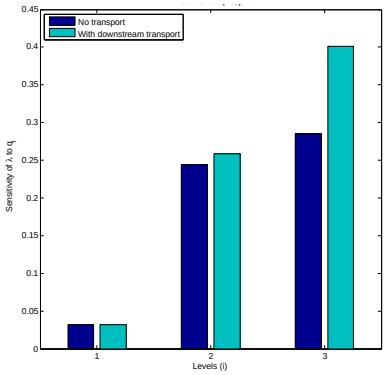	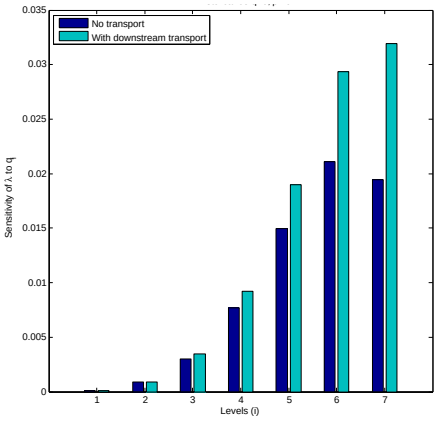

Table D.7: Matrix plots for two disturbances: the case of a closed homogeneous network

Cases	Complete binary tree with 7 nodes (3 levels)	Complete binary tree with 3 levels (15 nodes)
$\rho = 1$ closed No transport	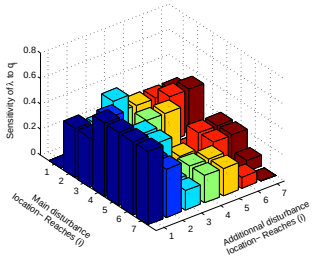	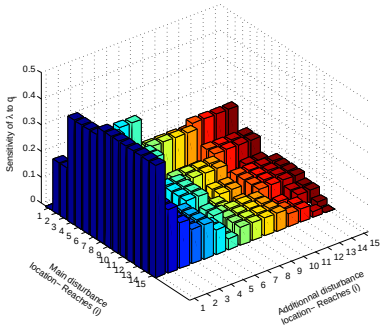
$\rho = 1$ closed Transport	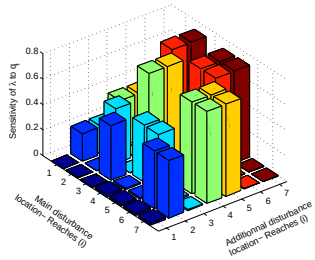	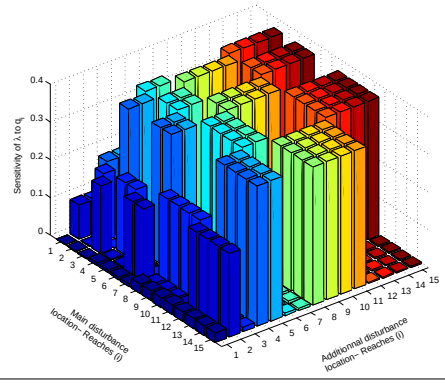

Table D.8: Matrix plots for two disturbances: the case of an open homogeneous network

Cases	Complete binary tree with 7 nodes (3 levels)	Complete binary tree with 3 levels (15 nodes)
$\rho = 1$ open No transport	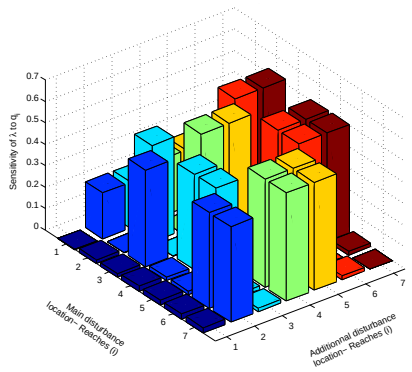	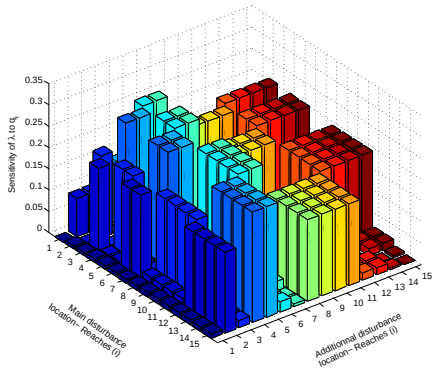
$\rho = 1$ open Transport	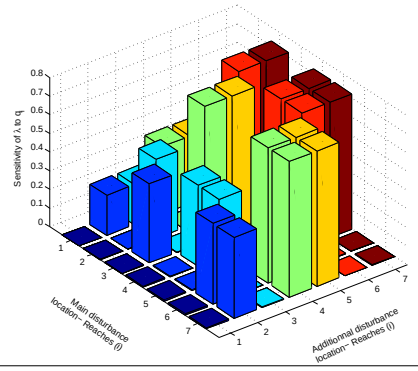	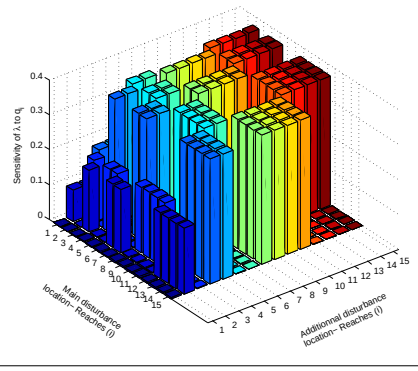

Table D.9: Matrix plots for two disturbances: the case of a closed heterogeneous network ($\rho < 1$)

Cases	Complete binary tree with 7 nodes (3 levels)	Complete binary tree with 3 levels (15 nodes)
$\rho < 1$ closed No transport	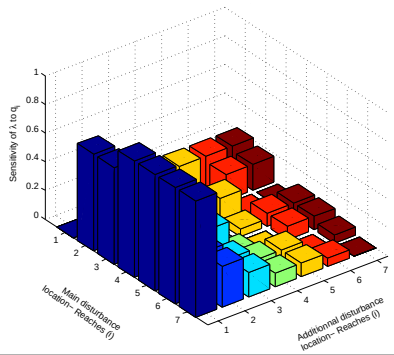	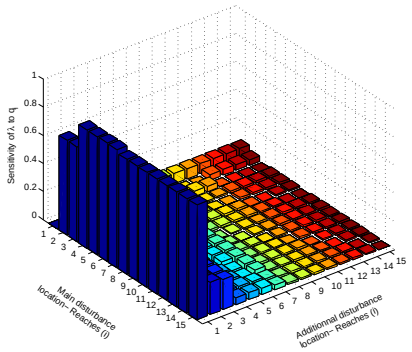
$\rho < 1$ closed Transport	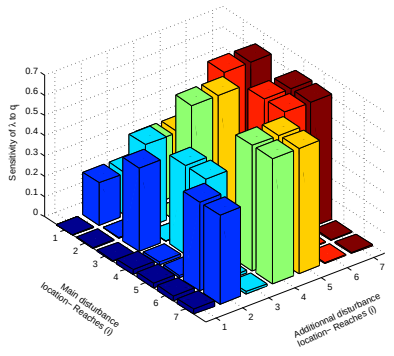	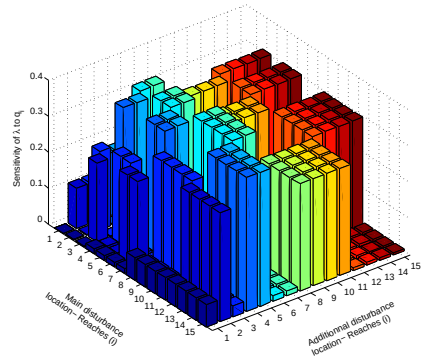

Table D.10: Matrix plots for two disturbances: the case of a closed heterogeneous network

Cases	Complete binary tree with 7 nodes (3 levels)	Complete binary tree with 3 levels (15 nodes)
$\rho > 1$ closed No transport	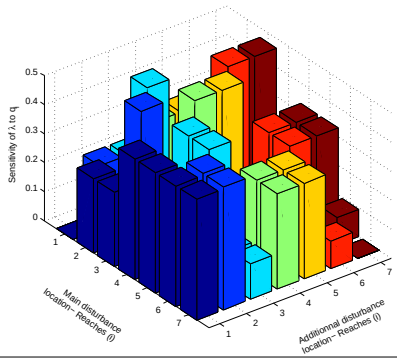	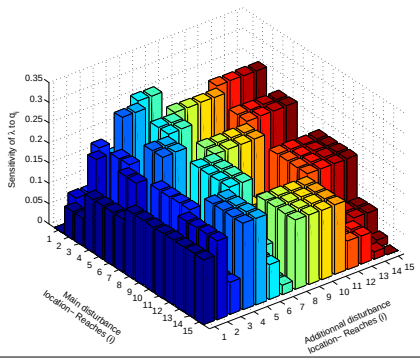
$\rho > 1$ closed Transport	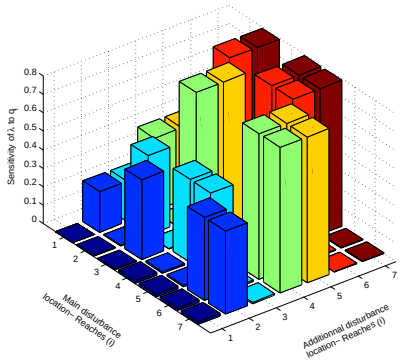	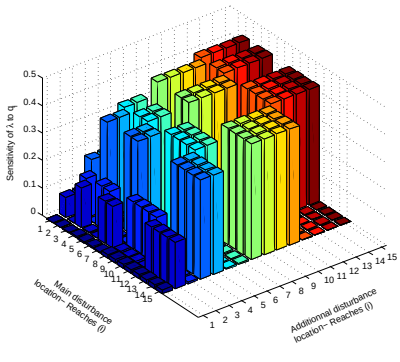

Bibliography

[1] J. Allan. *Stream ecology: Structure and function of running waters*. Chapman & Hall, New York, 1995.

[2] D. Banks, P.L. Younger, R.-T. Arnesen, E.R. Iversen, and S.B. Banks. Mine-water chemistry: the good, the bad and the ugly. *Environmental Geology*, 32(3):157–174, 1997.

[3] J.M. Calabrese and W.F. Fagan. A comparison-shopper's guide to connectivity metrics. *Front. Ecol. Environ.*, 2(10):529–536, 2004.

[4] E.H.C. Grant, W.H. Lowe, and W.F. Fagan. Living in the branches: population dynamics and ecological processes in dendritic networks. *Ecology Letters*, 10(2):165–175, 2007.

[5] H. Caswell. *Matrix population models: construction, analysis, and interpretation* . Second edition. Sinauer Associates, Sunderland, Massachusetts, USA, 2001.

[6] S. Charles, E. Billoir, C. Lopes, and A. Chaumot. Matrix population models as relevant modeling tools in ecotoxicology. In J. Devillers, editor, *Ecotoxicology Modeling, Emerging topics in Ecotoxicology: Principles, Approaches and Perspectives*, volume 2, pages 261–298. Springer, 2009.

[7] S. Charles, R. Bravo de la Parra, J.-P. Mallet, H. Persat, and P. Auger. A density dependent model describing *Salmo trutta* population dynamics in an arborescent river network. effects of dams and channelling. *Comptes Rendus de l'Académie des Sciences-Series III-Sciences de la Vie*, 321(12):979–990, 1998.

[8] S. Charles, R. Bravo de La Parra, J.-P. Mallet, H. Persat, and P. Auger. Annual spawning migrations in modelling brown trout population dynamics inside an arborescent river network. *Ecological Modelling*, 133(1):15–31, 2000.

[9] S. Charles, R. Bravo de La Parra, J.-P. Mallet, H. Persat, and P. Auger. Population dynamics modelling in an hierarchical arborescent river network: an attempt with salmo trutta. *Acta Biotheoretica*, 46(3):223–234, 1998.

[10] A. Chaumot, S. Charles, P. Flammarion, and P. Auger. Do migratory or demographic disruptions rule the population impact of pollution in spatial networks? *Theoretical Population Biology*, 64(4):473–480, 2003.

[11] A. Chaumot, S. Charles, P. Flammarion, and P. Auger. Ecotoxicology and spatial modeling in population dynamics: An illustration with brown trout. *Environmental Toxicology and Chemistry*, 22(5):958–969, 2003.

[12] A. Chaumot, S. Charles, P. Flammarion, J. Garric, and P. Auger. Using aggregation methods to assess toxicant effects on population dynamics in spatial systems. *Ecological Applications*, 12(6):1771–1784, 2002.

[13] C. A. Cobbold and F. Lutscher. Mean occupancy time: linking mechanistic movement models, population dynamics and landscape ecology to population persistence. *Journal of Mathematical Biology*, 68(3):549–579, 2013.

[14] R. Costanza, R. d'Arge, R. De Groot, S. Farber, M. Grasso, B. Hannon, K. Limburg, S. Naeem, R.V. O'Neill, J. Paruelo, et al. The value of ecosystem services: putting the issues in perspective. *Ecological Economics*, 25(1):67–72, 1998.

[15] D. Cote, D.G. Kehler, C. Bourne, and Y.F. Wiersma. A new measure of longitudinal connectivity for stream networks. *Landscape Ecology*, 24(1):101–113, 2009.

[16] T. Erős, J.D. Olden, R.S. Schick, D. Schmera, and M.-J. Fortin. Characterizing connectivity relationships in freshwaters using patch-based graphs. *Landscape Ecology*, 27(2):303–317, 2012.

[17] T. Erős, D. Schmera, and R.S. Schick. Network thinking in riverscape conservation–a graph-based approach. *Biological Conservation*, 144(1):184–192, 2011.

[18] W.F. Fagan. Connectivity, fragmentation, and extinction risk in dendritic metapopulations. *Ecology*, 83(12):3243–3249, 2002.

[19] J. Fischer and D.B. Lindenmayer. Landscape modification and habitat fragmentation: a synthesis. *Global Ecology and Biogeography*, 16(3):265–280, 2007.

[20] A.H. Fullerton, K.M. Burnett, E.A. Steel, R.L. Flitcroft, G.R. Pess, B.E. Feist, C.E. Torgersen, D.J. Miller, and B.L. Sanderson. Hydrological connectivity for riverine fish: measurement challenges and research opportunities. *Freshwater Biology*, 55(11):2215–2237, 2010.

[21] A.E. Hershey, J. Pastor, B.J. Peterson, and G.W. Kling. Stable isotopes resolve the drift paradox for baetis mayflies in an arctic river. *Ecology*, pages 2315–2325, 1993.

[22] A. Kolpas and R.M. Nisbet. Effects of demographic stochasticity on population persistence in advective media. *Bulletin of Mathematical Biology*, 72(5):1254–1270, 2010.

[23] M. Larinier. Dams and fish migration. World Commission on Dams. *FAO Fisheries Technical Paper*, 419:45–89, Toulouse, 2000.

[24] P.H. Leslie. On the use of matrices in certain population mathematics. *Biometrika*, pages 183–212, 1945.

[25] F. Lutscher, M.A. Lewis, and E. McCauley. Effects of heterogeneity on spread and persistence in rivers. *Bulletin of Mathematical Biology*, 68(8):2129–2160, 2006.

[26] F. Lutscher, E. McCauley, and M.A. Lewis. Spatial patterns and coexistence mechanisms in systems with unidirectional flow. *Theoretical Population Biology*, 71(3):267–277, 2007.

[27] F. Lutscher, R.M. Nisbet, and E. Pachepsky. Population persistence in the face of advection. *Theoretical Ecology*, 3(4):271–284, 2010.

[28] F. Lutscher, E. Pachepsky, and M.A. Lewis. The effect of dispersal patterns on stream populations. *Siam Review*, 47(4):749–772, 2005.

[29] F. Lutscher and G. Seo. The effect of temporal variability on persistence conditions in rivers. *Journal of Theoretical Biology*, 283(1):53–59, 2011.

[30] L.H. MacDonald and D. Coe. Influence of headwater streams on downstream reaches in forested areas. *Forest Science*, 53(2):148–168, 2007.

[31] U. Malvadkar, F. Scatena, and M. Leon. A comparison of connectivity metrics on watersheds and implications for water management. *River Research and Applications*, 31(2):256–267, 2015.

[32] P. McCully et al. *Rivers no more: the environmental effects of dams.* Zed Books, 1996.

[33] I. Moreno and J. Billeaud. Wastewater from Colorado Mine Reaches New Mexicos. *The Big Story, Associated Press*, 2015. Published online on 09-August-2015.

[34] E. Pachepsky, F. Lutscher, R. Nisbet, and M. Lewis. Persistence, spread and the drift paradox. *Theoretical Population Biology*, 67(1):61–73, 2005.

[35] M. Padgham and J.A. Webb. Multiple structural modifications to dendritic ecological networks produce simple responses. *Ecological Modelling*, 221(21):2537–2545, 2010.

[36] V. Pasour and S. Ellner. Computational and analytic perspectives on the drift paradox. *SIAM J. Applied Dynamical Systems*, 9(2):333–356, 2010.

[37] M. Pépino, M. A. Rodríguez, and P. Magnan. Fish dispersal in fragmented landscapes: a modeling framework for quantifying the permeability of structural barriers. *Ecological Applications*, 22(5):1435–1445, 2012.

[38] S. Postel and B. Richter. *Rivers for life: managing water for people and nature.* Island Press, Washington, DC, 2012.

[39] B. Rayfield, M.-J. Fortin, and A. Fall. Connectivity for conservation: a framework to classify network measures. *Ecology*, 92(4):847–858, 2011.

[40] Y. Samia and F. Lutscher. Persistence probabilities for stream populations. *Bulletin of Mathematical Biology*, 74(7):1629–1650, 2012.

[41] Y. Samia and F. Lutscher. Downstream flow and upstream movement determine the value of a stream reach for potadromous fish populations. *Theoretical Ecology* (Accepted pending minor changes).

[42] Y. Samia, F. Lutscher, and A. Hastings. Connectivity, passability and heterogeneity interact to determine fish population persistence in river networks. *Journal of Royal Society Interface*, 12:20150435, 2015.

[43] D.C. Speirs and W.S. Gurney. Population persistence in rivers and estuaries. *Ecology*, 82(5):1219–1237, 2001.

[44] L. Stanfield, L. Del Guidice, F. Lutscher, M. Trudeau, L. Alexander, W. Fagan, R. Fertik, R. Mackereth, J. Richardson, N. Shrestha, G. Tetreault, and M. Wipfli. A discussion paper on: Cumulative effects from alteration of headwater drainage features and the loss of ecosystem integrity or river networks. Technical report, Ontario Ministry of Natural Resources, 2014.

[45] P.D. Taylor, L. Fahrig, K. Henein, and G. Merriam. Connectivity is a vital element of landscape structure. *Oikos* 68: 571-73, 1993.

[46] O. Vasilyeva and F. Lutscher. Population dynamics in rivers: analysis of steady states. *Canadian Applied Math Quarterly*, 18(4):439–469, 2011.

[47] World Wildlife Fund. Free-flowing rivers: Economic luxury or ecological necessity? `http://www.wwf.se/source.php/1120326/Free`, 2006.